



RAPPORT

M-142 2014

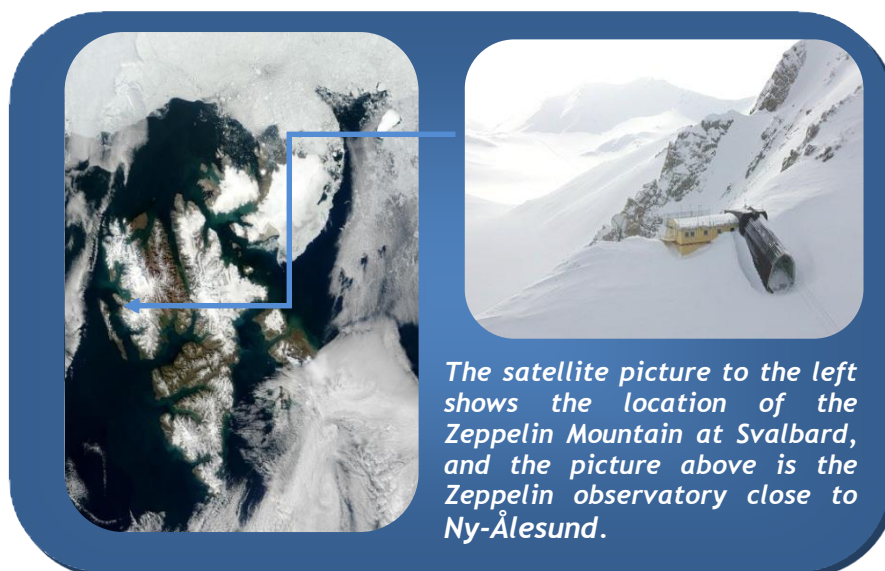
Monitoring of greenhouse gases and aerosols at Svalbard and Birkenes in 2012 - Annual report



Preface

In 1999 The Norwegian Environment Agency (the former Klif and SFT) and NILU - Norwegian Institute for Air Research signed a contract commissioning NILU to run a programme for monitoring greenhouse gases at the Zeppelin station, close to Ny-Ålesund at Svalbard. This collaborative Norwegian Environment Agency/NILU programme includes monitoring of 23 greenhouse gases at the Zeppelin observatory in the Arctic. In 2009 NILU upgraded and extended the observational activity at the Birkenes Observatory in Aust-Agder. From 2010 the Norwegian Environment Agency/NILU monitoring programme was extended to also include the new observations from Birkenes of the greenhouse gases CO₂ and CH₄ and selected aerosol observations particularly relevant for the understanding of climate change.

The unique location of the Zeppelin observatory at Svalbard together with the infrastructure of the scientific research community at Ny-Ålesund makes it ideal for monitoring the global changes of the atmosphere. There are few local sources of emissions, and the Arctic location is also important as the Arctic is a particularly vulnerable region. The observations at the Birkenes Observatory complement the Arctic site. Birkenes Observatory is located in a forest area with few local sources. However, the observatory often receives long range transported pollution from Europe and the site is ideal to analyse the contribution of long range transported greenhouse gases and aerosol properties.



In 1987 the Montreal Protocol was signed and entered into force in 1989 in order to reduce the production, use and eventually emission of the ozone-depleting substances (ODS). The amount of most ODS in the troposphere is now declining slowly and one expects to be back to pre-1980 levels around year 2050. It is crucial to follow the development of the concentration of these ozone depleting gases in order to verify that the Montreal Protocol and its amendments work as expected. Further these gases and their replacement gases are strong greenhouse gases making it even more important to follow the development of their concentrations. In December 1997 the Kyoto protocol was adopted. The target set by the Kyoto protocol is to reduce the total emissions of greenhouse gases from the industrialized countries during the period 2008 to 2012. The six most important groups of greenhouse gases included are: CO₂, CH₄, N₂O, fluorinated hydrocarbons (HFCs and PFCs) and sulphurhexafluoride (SF₆).

The following greenhouse gases are regulated through the Montreal protocol and measured at the Zeppelin Observatory: chlorofluorocarbons (CFC), hydrochlorofluorocarbons (HCFC), and halons as well as other halogenated organic gases. Further the following gases included in the Kyoto protocol are monitored; methane (CH₄), nitrous oxide (N₂O) from 2010, hydrofluorocarbons (HFC), sulphurhexafluoride (SF₆). Additionally carbon monoxide (CO) and tropospheric ozone (O₃) are a part of the programme. The amount of particles in the air above the stations is also measured. The station is hosting measurements of carbon dioxide (CO₂) performed by ITM, University of Stockholm as well, but the availability of data is limited. This activity is funded by the Swedish Environmental Protection Agency.

NILU - Norwegian Institute for Air Research is responsible for the operation and maintenance of the monitoring programme. The purpose of the programme is to:

- Provide continuous measurements of greenhouse gases in the Arctic region resulting in high quality data that can be used in trend analysis
- Provide continuous measurements of the greenhouse gases CO₂ and CH₄ at the Birkenes Observatory resulting in high quality data that can be used in trend analysis
- Provide trend analysis and interpretations of the observations from Zeppelin assess the influence regional anthropogenic emissions of greenhouse gases has on the radiative balance
- Provide information on the status and the development of the greenhouse gases with a particular focus on the gases included in the international conventions the Montreal and Kyoto protocol.
- Provide results of aerosol observations of relevance to the understanding of climate change
- Indicate sources regions with high influence on the measurements.

Observations and results from the monitoring programme are processed and used to assess the progress towards compliance with international agreements like the Kyoto and the Montreal Protocols. This report summarises the activities and results of the greenhouse gas and aerosol monitoring programme for the year 2012, and comprises a trend analysis for the period 2001-2012 including interpretation of the results.

Kjeller, April 2014

Cathrine Lund Myhre
Senior Scientist and Project Manager

Contents

Preface	1
1. Executive Summary	5
2. Introduction	9
3. The Zeppelin and Birkenes Observatories; Norwegian atmospheric supersites	12
3.1 Norwegian atmospheric supersites as part of European atmospheric research infrastructures	12
3.2 The Zeppelin Observatory	13
3.3 The Birkenes Observatory	15
4. Observations and trends of greenhouse gases at the Zeppelin Observatory in the Norwegian Arctic	17
4.1 Greenhouse gases with natural and anthropogenic sources	18
4.1.1 Observations of Methane in the period 2001-2012	18
4.1.2 Observations of Nitrous Oxide at the Zeppelin Observatory	22
4.1.3 Observations of Carbon Dioxide in the period 1988-2012	23
4.1.4 Observations of Methyl Chloride in the period 2001-2012	25
4.1.5 Observations of Methyl Bromide in the period 2001-2012	26
4.1.6 Observations of tropospheric ozone in the period 1990-2012	28
4.1.7 Observations of CO in the period 2001-2012	29
4.2 Greenhouse gases with solely anthropogenic sources	30
4.2.1 Observations of Chlorofluorocarbons (CFCs) in the period 2001-2012	31
4.2.2 Observations of Hydrochlorofluorocarbons (HCFCs) in the period 2001-2012	33
4.2.3 Observations of Hydrofluorocarbons (HFCs) in the period 2001-2012	35
4.2.4 Observations of halons in the period 2001-2012	36
4.2.5 Observations of other chlorinated hydrocarbons in the period 2001-2012	37
4.2.6 Perfluorinated compounds	40
5. Observations of CO₂ and CH₄ at the Birkenes Observatory in Aust-Agder	41
6. Analysis of CO from satellite observations to support ground based measurements	43
7. Aerosols and climate: Observations from Zeppelin and Birkenes Observatories	46
7.1 Observations of climate relevant aerosol properties: recent developments in Norway and internationally	47
7.2 Optical aerosol properties measured at Birkenes: estimating the local, instantaneous direct aerosol radiative forcing	49
7.3 Physical aerosol properties measured at Birkenes in 2010-2012	53
7.4 Observations of the total aerosol load above Ny-Ålesund and Birkenes	57
7.4.1 Measurements of the total aerosol load above Ny-Ålesund	58
7.4.2 Measurements of the total aerosol load above the Birkenes observatory	61
7.4.3 Use of aerosol data retrieved from satellites as complementary information	62
8. Transport of air to the Zeppelin Observatory	63
9. References	66
APPENDIX 1 Description of instruments, methods and trend analysis	71
APPENDIX 2 Acknowledgements	83

1. Executive Summary

This annual report describes the activities and main results of the programme “*Monitoring of greenhouse gases and aerosols at the Zeppelin Observatory, Svalbard, and Birkenes Observatory, Aust-Agder, Norway*”. This is a part of the Governmental programme for monitoring pollution in Norway. The report comprises all natural well mixed greenhouse gases, the most important anthropogenic greenhouse gases and various particle’s properties with high relevance to climate and climate change. Many of the gases also have strong ozone depleting effect.

The concentration in the atmosphere of the main greenhouse gases with high anthropogenic emissions has been increasing over the period of investigation, except for CFCs and a few halogenated gases. These gases have strong ozone depleting effect and are regulated through the successful Montreal protocol. The positive effect of this regulation on the recovery of the ozone layer is well documented. It is also a benefit for the climate. The uneven growth of the concentration of methane makes it particularly difficult to identify the sources for the growth. To better understand the causes of this increase, it is necessary to improve the monitoring program of methane both in Norway as well as in international networks.

The trends of all gases included in the programme are shown in Table 1, and the main results are commented briefly in the summary. Further details are presented in section 3 of the report.

Greenhouse gases regulated through the Kyoto protocol - Key findings from the Zeppelin and Birkenes observatories

The report includes the 6 greenhouse gases or groups of gases included in the Kyoto protocol. The key findings are:

Methane - CH₄: : In 2012 the mixing ratios of methane increased to a **new record level both at our sites at Zeppelin, Birkenes and globally**. At Zeppelin the annual mean value reached 1892 ppb after an increase of as much as 12 ppb since 2011. This is the 3rd highest yearly increase since the measurements started. The methane increase at the Zeppelin observatory from 2005 to 2012, (50 ppb, or around 2.7%) was larger than the global increase in the same period (approx. 36 ppb, or 2.0 %). Both values constitute a relatively large change compared to the evolution of the methane levels in the period from 1998-2005, when the change was close to zero both at Zeppelin and globally, after a strong increase during the 20th Century. The measurements of CH₄ at Birkenes showed an annual mean value for 2012 of 1900 ppb, which is higher than the annual values both for Zeppelin and the global mean global mean. The increase from 2011 to 2012 at Birkenes was 5 ppb.

There is yet no clear explanation for the global increase in methane that started in 2005, but a probable explanation is increased methane emissions from wetlands, both in the tropics as well as in the Arctic region. Melting permafrost, both in terrestrial regions and at the sea floor, might introduce new possible methane emission sources initiated by the temperature increase the last years. A recent research project **MOCA (Methane emission for Arctic Ocean to Atmosphere - <http://moca.nilu.no>)** is focusing on the understanding of emission of methane from ocean to atmosphere, and the impact of climate change on these emissions.

To improve our understanding of the ongoing processes an extension of the monitoring of methane is needed, to better identify and distinguish the strength of the various sources in the Arctic. Methane from various sources has different isotopic ratios of ¹³C/¹²C. Isotopic measurements of methane at Zeppelin combined with transport modeling as well as climate modeling would be a very powerful tool to distinguish between methane from various sources as wetlands, oceans and exploitation of gas fields included gas transportation. Measurements are currently included in research projects at NILU financed by The Research Council of Norway.

Table 1: Key findings; Greenhouse gases measured at Ny-Ålesund; lifetimes in years¹, global warming potential (GWP), absolute change in concentrations since 2011, concentrations in 2012, their trends per year over the period 2001-2012, and relevance to the Montreal and Kyoto Protocols. All concentrations are mixing ratios in pptv, except for methane and carbon monoxide (ppbv) and carbon dioxide (ppmv).

Compound	Formula	Life-time	GWP ²	Change last year	2012	Trend / Year	Montreal or Kyoto Prot.	Comments on sources for the halocarbons
Methane	CH ₄	12 ³	25	12.6	1892	+4.4	K	
Carbon monoxide	CO	Months		5.3	121	-1.1		
Carbondioxide⁴	CO ₂		1	2.3	394.8	+2.1	K	
Chlorofluorocarbons								
CFC-11*	CCl ₃ F	45	4750	-1.7	237	-2.08	M phased out	foam blowing, aerosol propellant
CFC-12*	CF ₂ Cl ₂	100	10900	-3.8	528	-1.8	M phased out	temperature control
CFC-113*	CF ₂ CICFCI ₂	640	6130	-0.7	73.9	-0.67	M phased out	solvent, electronics industry
CFC-115*	CF ₃ CF ₂ Cl	1020	7370	0.0	8.42	+0.02	M phased out	temperature control, aerosol propellant
Hydrochlorofluorocarbons								
HCFC-22	CHClF ₂	11.9	1810	5.6	232	+6.9	M freeze	temperature control, foam
HCFC-141b	C ₂ H ₃ FCI ₂	9.2	725	1.2	24.2	+0.58	M freeze	foam blowing, solvent
HCFC-142b*	CH ₃ CF ₂ Cl	17.2	2310	0.3	23.0	+0.85	M freeze	foam blowing
Hydrofluorocarbons								
HFC-125	CHF ₂ CF ₃	28.2	3500	1.6	12.5	+0.91	K	temperature control
HFC-134a	CH ₂ FCF ₃	13.4	1430	5.0	73.4	+4.70	K	temperature control, foam, solvent, aerosol propellant
HFC-152a	CH ₃ CHF ₂	1.5	124	0.3	10.4	+0.74	K	foam blowing
Halons								
H-1211*	CBrClF ₂	16	1890	-0.1	4.1	-0.03	M phased out	fire extinguishing
H-1301	CBrF ₃	65	7140	0.03	3.4	+0.03	M phased out	fire extinguishing
Halogenated compounds								
Methylchloride	CH ₃ Cl	1.0	13	4.5	513	-0.2		natural emissions (algae)
Methylbromide	CH ₃ Br	0.8	5	-0.2	6.9	-0.19	M freeze	agriculture, natural emissions (algae)
Dichloromethane	CH ₂ Cl ₂	0.38	8.7	3.6	44.9	+1.2		solvent
Chloroform	CHCl ₃	0.5	30	0.2	12.1	+0.10		solvent, natural emissions
Methylchloroform	CH ₃ CCl ₃	5	146	-1.1	5.4	-2.87	M phased out	solvent
Trichloroethylene	CHClCCl ₂			-0.04	0.51	-0.01		solvent
Perchloroethylene	CCl ₂ CCl ₂			-0.07	2.7	-0.16		solvent
Sulphurhexafluoride*	SF ₆	3200	22800	0.3	7.8	+0.26	K	Mg-production, electronics

CO₂ reached new record levels in 2012 both globally and at the Zeppelin Observatory. The global value was 393.1 according to WMO (2013) and the preliminary analysis of the Zeppelin measurements indicates a mixing ratio of 394.8 ppm. The annual growth rates were slightly higher than the last years, above 2 ppm per year both globally and at Zeppelin. The CO₂ measurements at Birkenes showed an annual mean value of 397.2 ppm.

Nitrous Oxide -N₂O: The global mean level of N₂O has increased from around 270 ppb prior to industrialization and up to an average global mean of 325.1 ppb in 2012 (WMO, 2013) which is new record level after an increase of 0.9 ppb since 2011. The annual mean for 2011 at Zeppelin was 324.2 ppb at Zeppelin, coincidentally the same as the global mean. In 2012 measurements were lacking due to instrument problems part of the year, and it was not possible to get a comparable annual mean. The recent Assessment of the ozone depletion (WMO, 2011) suggests that current emissions of N₂O are presently the most significant substance that depletes ozone with consequences for the ozone layer.

Hydrofluorocarbons - HFCs: These gases replace the strongly ozone depleting substances CFC's, and are relatively new gases emitted to the atmosphere. They are all of solely anthropogenic origin. The mixing ratios

* The measurements of these components have higher uncertainty. See Appendix I for more details.

¹ From Scientific Assessment of Ozone Depletion: 2010 (WMO, 2011b) and the 4th Assessment Report of the IPCC

²GWP (Global warming potential) 100 year time period, CO₂ = 1

³ The lifetime for CH₄ includes feedbacks of indirect effects on the lifetime. The lifetime is close to 9 year without adjustments.

⁴ Measurements of CO₂ is performed by Stockholm University until 2011, from 2012 NILU has own measurements.

of HFC-125, HFC-134a, HFC-152a have increased by as much as 522%, 253% and 267% respectively since 2001 at the Zeppelin observatory. However, their concentrations are still very low, thus the total radiative forcing of these gases since the start of their emissions around 1970 and up to 2011 is only about 0.016 W m^{-2} . For comparison: The forcing of a typical 2 ppm annual increase in CO_2 is around 0.03 W m^{-2} . Thus the contribution from these manmade gases to the global warming is small today, but given the observed extremely rapid increase in the use and atmospheric concentrations, it is crucial to follow the development of these gases in the future.

The perfluorinated compound - SF_6 : The only perfluorinated compound measured at Zeppelin is Sulphurhexafluoride, SF_6 . This is an extremely potent greenhouse gas, but the concentration is still low. However, measurements show that the concentration has increased as much as 57% since 2001.

Greenhouse gases regulated through the Montreal protocol - Key findings

All gases regulated through the Montreal protocol are substances depleting the ozone layer. In addition they are all greenhouse gases. The amount of most of the ozone-depleting substances (ODS) in the troposphere is now declining slowly globally and is expected to be back to pre-1980 levels around the year 2050. The gases included in the monitoring programme at Zeppelin are the man-made greenhouse gases called chlorofluorocarbons (CFCs), the hydrogen chlorofluorocarbons (HCFCs), which are CFC substitutes, and halons.

CFCs: In total the development of the CFC gases measured at the global background site Zeppelin give reason for optimism. The mixing ratio of the observed CFCs, **CFC-11, CFC-12 and CFC-113 are declining**. The mixing ratios of these gases are now at a lower level than in 2001 when measurements started at Zeppelin, and are reduced with approx. 8.6%, 3.5% and 9.3% respectively since the start. **CFC-115 seems to have stabilised and was in 2012 at the same level as in 2010 and 2011.**

HCFCs: The CFC substitutes **HCFC-22, HCFC-141b and HCFC-142b have a strong increase in the levels measured at Zeppelin from 2001-2012**. HCFC-22 used for temperature control and foam blowing had the largest growth rate. This is the most abundant substance of the HCFCs and its mixing ratio at Zeppelin increased by a rate of 6.9 ppt/year which is almost 4% per year, and the increase is as much as a 45% since 2001, and the change is accelerating. HCFC-142b had the strongest relative increase with more than 58% since 2001.

Halons: Halons are the Bromine containing halocarbons. The levels of the two gases monitored have been relatively stable over the observation period at Zeppelin. The recent results indicate that there was a maximum in 2004 for halon-1211 at Zeppelin, and a small decline after that. Since 2001 this compound is reduced with approx. 6.5%. According to the last Ozone Assessment (WMO, 2011) the total stratospheric Bromine concentration is no longer increasing and Bromine from halons stopped increasing during the period 2005-2008.

Methylchloride and Methylbromide are also reduced as a direct result of the Montreal protocol.

Greenhouse gases not regulated through the protocols - Key findings

The monitoring programme also includes five greenhouse gases not regulated through any of the two protocols.

Chlorinated greenhouse gases: The following five chlorinated gases are measured at the Zeppelin Observatory: methylchloride (CH_3Cl), dichloromethane (CH_2Cl_2), chloroform (CHCl_3), trichloromethane ($\text{CHCl}_2\text{CCl}_3$), perchloroethylene (C_2Cl_4). Three of these gases have increased the last years and a considerable increase in chloroform is evident at Zeppelin from 2006-2012, and since 2008 the component has increased with approx. 17%. The reason for this is not clear. **Dichloromethane shows an increase of as much as 44% since 2001.** The main use of this compound is as an active ingredient in paint removers.

Long range transport of pollutions; aerosols and reactive gases - Key findings

Aerosols are small particles in the atmosphere. Major sources of anthropogenic aerosols are combustion of fossil fuel, coal and biomass including waste from agriculture and forest fires. Aerosols can have a cooling or warming effect depending on the chemical composition and location. Globally the cooling effect dominates, and has offset the warming of the greenhouse gases since the year 1750 considerably. However, the magnitude is connected with significant uncertainty, causing large uncertainty in the climate sensitive to the doubling of CO_2 . The uncertainty with respect to the effects of aerosols on the radiative balance and climate is one of the main reasons for the large range in global temperature projected in the IPCC's scenarios. Measuring a wide range of aerosol variables is therefore crucial for improved understanding of global warming, and effective mitigation strategies.

Climate effect of BC: A recent assessment quantifies the radiative forcing of BC to a best estimate of $+0.71 \text{ W/m}^2$, which implies a potential to mitigate climate change by regulating BC emissions. It needs to be pointed out that this best estimate is highly uncertain, and that different observation types of atmospheric

aerosol absorption imply diverging numbers on BC radiative forcing. The assessment of $+0.71 \text{ W/m}^2$ is based on indirect observations by ground-based remote sensing with good spatial coverage, but unknown accuracy. Ground-in situ observations with less spatial coverage, but known accuracy, constrain the BC radiative forcing to $+0.24 \text{ W/m}^2$. If the lower number for the BC radiative forcing was true, the potential for mitigating climate change by regulating BC emissions would be greatly reduced.

Zeppelin Observatory: Observations of the total amount of aerosol particles in the atmosphere above Ny-Ålesund (aerosol optical depth) show increased concentration levels during springtime compared to the rest of the year. This phenomenon, called Arctic haze, is due to transport of pollution from lower latitudes (mainly Europe and Russia) during winter/spring. In 2012 this aerosol optical depth was slightly lower compared to previous years. A typical dominance of fine mode, submicron aerosols, is seen. In 2012, there were also shorter episodes with elevated levels of particles later than springtime, but no contributions from volcanic emission (as seen in 2008, 2009 and 2011). The 11-year time-series of total aerosol column did not show a significant trend. To improve the knowledge about the different types of aerosols and their effects in the Arctic atmosphere, extension of the aerosol observations at Zeppelin with measurements of the aerosol absorption properties will be very useful, and total column measurements during polar night are needed to fill in the gap of aerosol climatology during polar winter. Unfortunately, we lack accesses to comprehensive measurement program of aerosols at Zeppelin, as is available at Birkenes.

Birkenes Observatory: Since it's re-opening as EMEP supersite and WMO GAW station, Birkenes Observatory has now collected 3 full years of high quality data on atmospheric aerosol microphysical and optical properties in addition to the existing long time series on aerosol chemical properties collected within EMEP. Together, these datasets give a consolidated and comprehensive picture of the direct aerosol climate effect, which acts by direct interaction of aerosol particles and atmospheric radiation. Parameters addressing the indirect aerosol climate effect, which acts by modifying cloud reflectivity and life time, are now also measured at Birkenes, but not included in this governmental monitoring programme. Aerosol properties at Birkenes are determined by long-range transport of air from continental Europe with its sources of pollution and Arctic air, as well as regional sources like biogenic particle formation and regional pollution events. These two regional sources show distinct and opposite annual cycles. Being controlled by photochemical reactions, biogenic particle formation peaks in summer, whereas regional pollution events occur most often in winter. Occurrence of regional pollution events is associated with a higher fraction of absorbing aerosol particles. This causes the direct aerosol climate effect to be less cooling in winter than in summer. Over a snow-covered surface, the winter direct aerosol climate forcing at Birkenes may even be positive, i.e. warming. For Birkenes, the observations of the total amount of aerosol particles in the atmosphere above Birkenes show lower levels in 2012 than in 2009-2011.

Reactive gases: Tropospheric ozone and CO have elevated levels in polluted regions like central Europe. They are suitable indicators for long range transport of pollution from the continents to Svalbard, and CO is also a proper tracer for transport of emissions from biomass burning and other fire events. There were fewer episodes with elevated levels of CO at Zeppelin in 2011 but back to normal in 2012. In general, there has been a reduction in the CO concentration at Zeppelin in the period 2003-2012 of approx. 10%. The reason for this is not yet understood.

The crucial link to monitoring networks and European atmospheric research infrastructures

A key point in the analysis and understanding of atmospheric variables are quality assured and harmonised measurements within Europe, as well as on larger geographical scale. NILU acts as the Chemical Coordinating Centre for EMEP⁵ and coordinates the atmospheric monitoring work under the Convention on Long-Range Transboundary Air Pollution (under United Nations Economic Commission for Europe). There are mutual benefits and close links between selected infrastructure programs in EU and EMEP. In particular NILU is involved in ACTRIS (Aerosols, Clouds, and Trace gases Research InfraStructure Network, (<http://www.actris.net/>)) and InGOS (Integrated non-CO₂ greenhouse gases observing system). NILU is also involved in ICOS (Integrated Carbon Observation System), but without any funding or financial support. Birkenes and Zeppelin will become ICOS sites if national funding is established. This is important for the understanding of carbon cycle and GHG in Europe, and our contribution is essential to include the Arctic region in these networks. The infrastructure projects are improving the national monitoring program significantly with respect to quality, giving access to more data, and processed products combining data across Europe. The projects are focusing on both long-lived and short-lived climate forcers. International collaboration and harmonisation of these types of observations are required for processes understanding and satisfactory quality of measurement to assess trends. It is important to underline that participation in these projects is crucial for the quality and development of the national monitoring programmes. Harmonised measurement on international level is a prerequisite for the assessment and understanding of atmospheric change.

⁵ EMEP: European Monitoring and Evaluation Programme: <http://www.emep.int/>

2. Introduction

The greenhouse effect is a naturally occurring process in the atmosphere caused by trace gases, especially water vapour (H₂O), carbon dioxide (CO₂), methane (CH₄) and nitrous oxide (N₂O) that naturally occur in the atmosphere. The content of the last three gases in the atmosphere are closely related to emissions from main sources, whilst the water content varies mainly with temperature. Without these gases, the global mean temperature would have been much lower. These gases absorb infrared radiation and thereby trap energy emitted by the Earth. Due to this energy trapping the global mean temperature is approximately 13.7°C, more than 30 degrees higher than it would have been without these gases present (IPCC, 2007). This is the natural greenhouse effect. The enhanced greenhouse effect refers to the additional effect of the greenhouse gases from human activities. In the industrial era, after 1750, the concentration of greenhouse gases in the atmosphere has increased significantly. The global atmospheric mean mixing ratios of CO₂ has increased by 39% (from 280 ppm as a pre-industrial concentration to 393.1 ± 0.1 ppm in 2012) and methane has increased by as much as 170% from 700 ppb to 1819 ± 1 ppb in 2012) according to WMO (WMO, 2013). 2012 showed new record levels of both these gases. The overall changes in the concentrations of the greenhouse gases are the main cause of the global mean temperature rise of 0.74°C over the last century reported by IPCC (2007). Depending on the various emission scenarios used and natural feedback mechanisms, the temperature is predicted to increase with 1.1-6.4°C approaching the year 2100, according to IPCC (2007).

Radiative forcing⁶ is a tool to estimate the relative climate impacts of various components inducing atmospheric radiative changes. Global-average radiative forcing estimates from the 4th IPCC assessment report are shown in Figure 1 (IPCC, 2007). Revised updates of this was published in January 2014 in the new IPCC report.

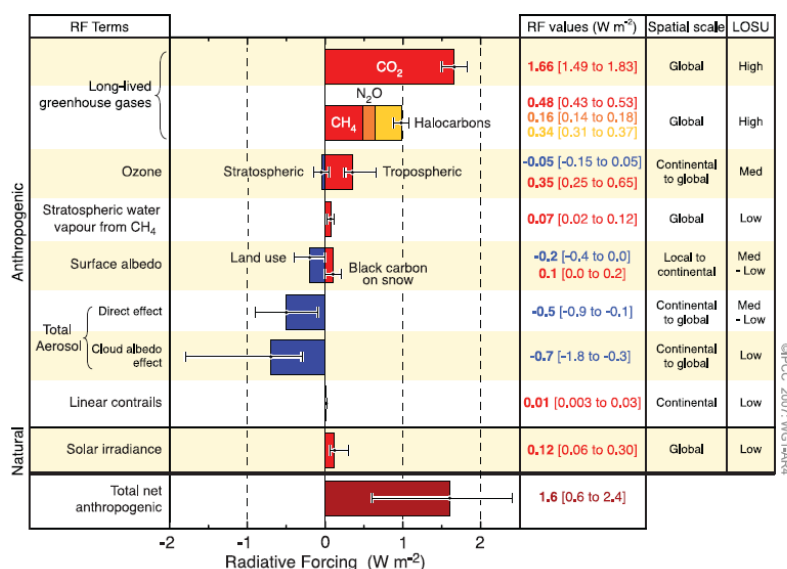


Figure 1: Global-average radiative forcing (RF) estimates for important anthropogenic agents and mechanisms together with the typical spatial scale of the forcing and the assessed level of scientific understanding (LOSU).

The most important greenhouse gas emitted from anthropogenic activities is CO₂ with a radiative forcing of 1.66 W m⁻² given in the 4th IPCC report (IPCC, 2007). This is an increase of 0.2 W m⁻² since the IPCC report from 2001. CH₄ and N₂O are other components with strong forcings of 0.48 W m⁻² and 0.16 W m⁻² respectively. It is worth noting that even the change in CO₂ radiative forcing since 2001 is stronger than the total forcing of e.g. N₂O since 1750, emphasising the importance of CO₂.

The joint group of halocarbons is also a significant contributor to the radiative forcing. Halocarbons include a wide range of components. The most important ones are the ozone depleting gases regulated through the Montreal protocol. This includes the CFCs, the HCFCs, chlorocarbons, bromocarbons and halons. Other gases are the HFC (fluorinated halocarbons), PFCs (per fluorinated halocarbons), and SF₆. These fluorinated gases are regulated through the Kyoto protocol. The total forcing of the halocarbons is 0.337 Wm⁻², the concentration of CFC-12 seems to have reached its peak value. The trend for CFC-12, to lower concentrations, gives reason for

⁶ Radiative forcing is a measure of the influence a factor has in altering the balance of incoming and outgoing energy in the Earth-atmosphere. It is an index of the importance of the factor as a potential climate change mechanism. It is expressed in Wm⁻² and positive radiative forcing tends to warm the surface. A negative forcing tends to cool the surface.

optimism for this substance. Observations of the halocarbons and methane are central activities at the Zeppelin observatory. Most of the halocarbons have now a negative trend in the development of the atmospheric mixing ratios.

The diagram below shows the relative contribution (in percent) of the long-lived greenhouse gases and ozone to the anthropogenic greenhouse warming since pre-industrial times (1750). The numbers are based on the radiative forcing estimates in the IPCC report from 2007. The diagram shows that CO₂ has contributed to 55% of the changes in the radiative balance while methane has contributed 16% since pre-industrial times. The halocarbons have contributed 11% to the direct radiative forcing of all long-lived greenhouse gases.

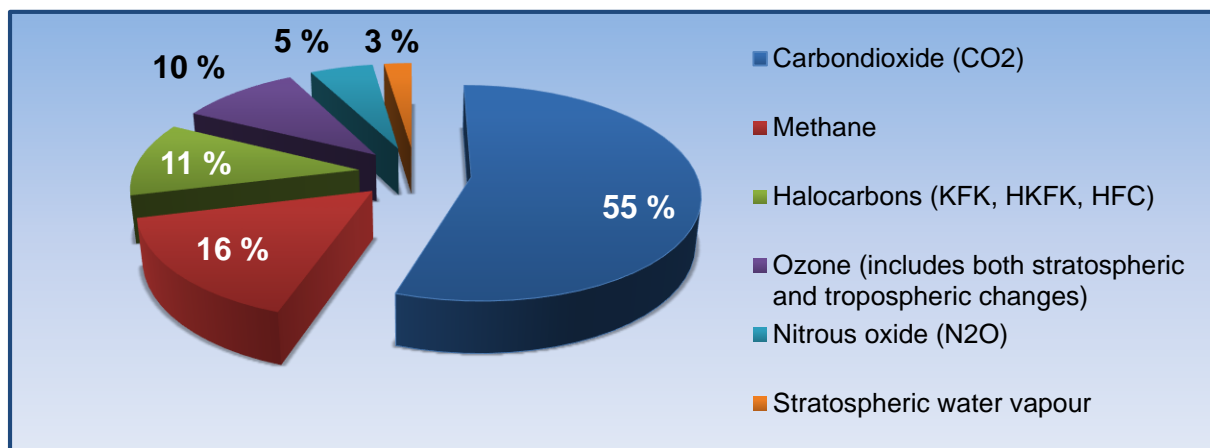


Figure 2: The relative contribution in percent of the long-lived greenhouse gases and ozone to the anthropogenic warming since pre-industrial times (1750). The numbers are based on the radiative forcing estimates in the IPCC report from 2007.

According to the IPCC report from 2007 (IPCC, 2007), a large source of uncertainty in climate predictions is caused by insufficient understanding of the atmospheric aerosol processes and historic evolution.

There are two dominant pathways for atmospheric aerosols to influence climate, both exerting a cooling effect in most cases. On one hand, aerosol scatter incoming solar radiation back into space, preventing it from reaching the ground and warm the surface. This is the so-called direct aerosol climate effect. Additionally, aerosols are activated to cloud particles. Increasing the number of aerosols will in turn increase the cloud particles and also the reflectivity and lifetime of the cloud, again with a cooling effect. This is called indirect aerosol climate effect. Both effects are quantified by negative aerosol radiative forcing in

Figure 1 leading to cooling of the surface. The negative aerosol radiative forcing partially offsets the positive, warming radiative forcing by greenhouse gases. In this way the aerosols mask the warming of the greenhouse gases, the magnitude is still uncertain.

The main objective of NILU's monitoring programme is to observe, analyse and interpret the changes in the atmospheric concentrations of the gases included in the Montreal protocol and the Kyoto protocol. An overview of all gases observed together with their trends, lifetime and GWP is given in Table 1 in the Summary. Furthermore, the programme shall provide relevant information about aerosols observations important for increased understanding of climate change.

The international collaboration regarding the protection of the ozone layer leading to the Montreal protocol started with the Vienna convention in 1985. Two years later the Montreal protocol was signed and for the first time there was an international agreement forcing the participating countries to reduce and phase out anthropogenic substances. Halocarbons and their relation to the Montreal protocol are indicated in Table 1. 197 countries have ratified the protocol and most of the countries have also ratified the later amendments to the protocol. The Montreal protocol has goals and strategies for all of the ozone depleting substances and the protocol is a part of the UN environmental program UNEP. According to the last ozone assessment report from WMO (WMO, 2011) the total combined abundance of anthropogenic ozone-depleting gases in the troposphere has continued to decrease from the peak value observed in the 1992-1994 time period. However, the decrease is slower than previous projected due to slower decrease in CFC-11 and CFC12, and also larger increase in HCFC than anticipated. The reduction is around 28% relative to the peak value. In the stratosphere, the peak is later, around 200-2002, and the reduction since then is close to 10% (WMO, 2011).

The target set by the Kyoto protocol was to reduce the total emissions of greenhouse gases from the industrialized countries during the period 2008 to 2012. The four most important greenhouse gases and two groups of gases are included: CO₂, CH₄, N₂O, SF₆ (sulphurhexafluoride), hydrofluorocarbons (HFCs) and perfluorocarbons (PFCs). The emissions are calculated as annual mean values during the period 2008-2012. The gases are considered jointly and weighted in accordance with their global warming potentials as given by IPCC (2007) and shown in Table 1 .

A Norwegian introduction to the Montreal and Kyoto protocol can be found at “Miljøstatus Norge” (<http://www.miljostatus.no>). The English link to the Montreal protocol is http://ozone.unep.org/Ratification_status/montreal_protocol.shtml whereas the Kyoto protocol can be found at http://unfccc.int/essential_background/kyoto_protocol/items/1678.php.

3. The Zeppelin and Birkenes Observatories; Norwegian atmospheric supersites



Figure 3: Location of NILU's atmospheric supersites measuring greenhouse gases and aerosol properties.

There are considerable future challenges connected with the understanding of atmospheric change, and the effects of this. This includes the evolution and assessments of long-lived greenhouse gases (LLGHG) as well as the understanding of short-lived climate forces (SLCF) with near time forcing. SLCF includes aerosols and tropospheric ozone in particular, and related gases as CO, NO_x, methane and volatile organic compounds (VOC). Furthermore, also the interaction between aerosols and clouds is largely unknown. Norway has a national interest and particular responsibility to develop harmonized and high quality observation infrastructures in the northern region including the Sub-arctic and Arctic areas. Long-range transport of air pollution from the central-European continent is occurring, and of high relevance. There is also transport from the North-American continent, China and other Asian regions (Stohl, 2006) detected at Zeppelin. Furthermore, the industrial development in the Arctic regions, increasing the oil, gas, and ship activities, will influence the levels of both GHGs and aerosols in this vulnerable region. Moreover, possible emission from the huge reservoirs of methane in the Arctic region is crucial to follow over long time. These are typical emissions from regions with thawing of permafrost, changes in wetlands and thaw lakes, and methane hydrates at the sea floor. All are sensitive to global warming, with strong positive feedbacks.

The measurement activities at the Zeppelin and Birkenes Observatories contribute to a number of global, regional and national monitoring networks and are atmospheric supersites observatories included in atmospheric research infrastructures as described in 3.1.

- EMEP (European Monitoring and Evaluation Programme under "UN Economic Commission for Europe")
- AGAGE (Advanced Global Atmospheric Gases Experiment)
- Global Atmospheric Watch (GAW under WMO)
- Network for detection of atmospheric change (NDAC under UNEP and WMO)
- Arctic Monitoring and Assessment Programme (AMAP)

Most data are public available through the international database hosted at NILU: <http://ebas.nilu.no>.

3.1 Norwegian atmospheric supersites as part of European atmospheric research infrastructures

A key point in the analysis and understanding of atmospheric variables are quality assured and harmonised measurements within Europe, as well as on larger geographical scale. NILU acts as the Chemical Coordinating Centre for EMEP⁷ and coordinates the atmospheric monitoring work under the Convention on Long-Range Transboundary Air Pollution (under United Nations Economic Commission for Europe). This is a scientifically based and policy driven programme with high relevance for the institute's involvement in, and relation to, international research infrastructure projects and ESFRI (European Strategy Forum on Research Infrastructures) research infrastructures. There are mutual benefits and close links between selected infrastructure programs in EU and

⁷ EMEP: European Monitoring and Evaluation Programme: <http://www.emep.int/>

EMEP. In particular NILU is involved in ACTRIS (Aerosols, Clouds, and Trace gases Research InfraStructure Network, www.actris.net) and InGOS (Integrated non-CO₂ greenhouse gases observing system). NILU is also involved in ICOS (Integrated Carbon Observation System). Birkenes and Zeppelin will become ICOS sites if national funding is established, but unfortunately the Norwegian Research Council decided in October 2013 that they didn't support the development of this infrastructure.

The importance of these projects is high for the development of optimised observational infrastructures (both with respect to equipments, analysis and cost) to meet the future needs for studying atmospheric compositional change. The projects are focusing on both long-lived and short-lived climate forcers. International collaboration and harmonisation of these types of observations are crucial for processes understating and satisfactory quality to assess trends. The map in Figure 4 shows the sites include in the research infrastructure project ACTRIS (www.actris.net). This project started 1. April 2011 and NILU is involved in many parts of the project.

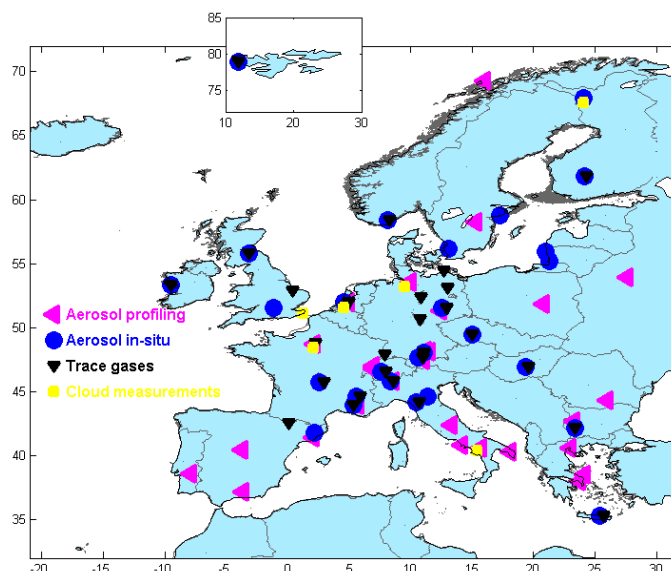


Figure 4: The map shows sites in ACTRIS and the distribution of various types atmospheric measurements.

3.2 The Zeppelin Observatory

The monitoring observatory is located in the Arctic on the Zeppelin Mountain, close to Ny-Ålesund at Svalbard. At 79° north, 11°East the station is placed in an undisturbed arctic environment, away from major pollution sources. Situated 474 meters a.s.l and most of the time above the inversion layer, there is minimal influence from local pollution sources in the nearby small community of Ny-Ålesund.

The unique location of the station makes it an ideal platform for the monitoring of global atmospheric change and long-range transport of pollution. The main goals of NILU's research activities at the Zeppelin station are:

- Studies of climate related matters and stratospheric ozone
- Exploration of atmospheric long-range transport of pollutants. This includes greenhouse gases, ozone, persistent organic pollutants, aerosols and others.
- Characterization of the arctic atmosphere and studies of atmospheric processes and changes

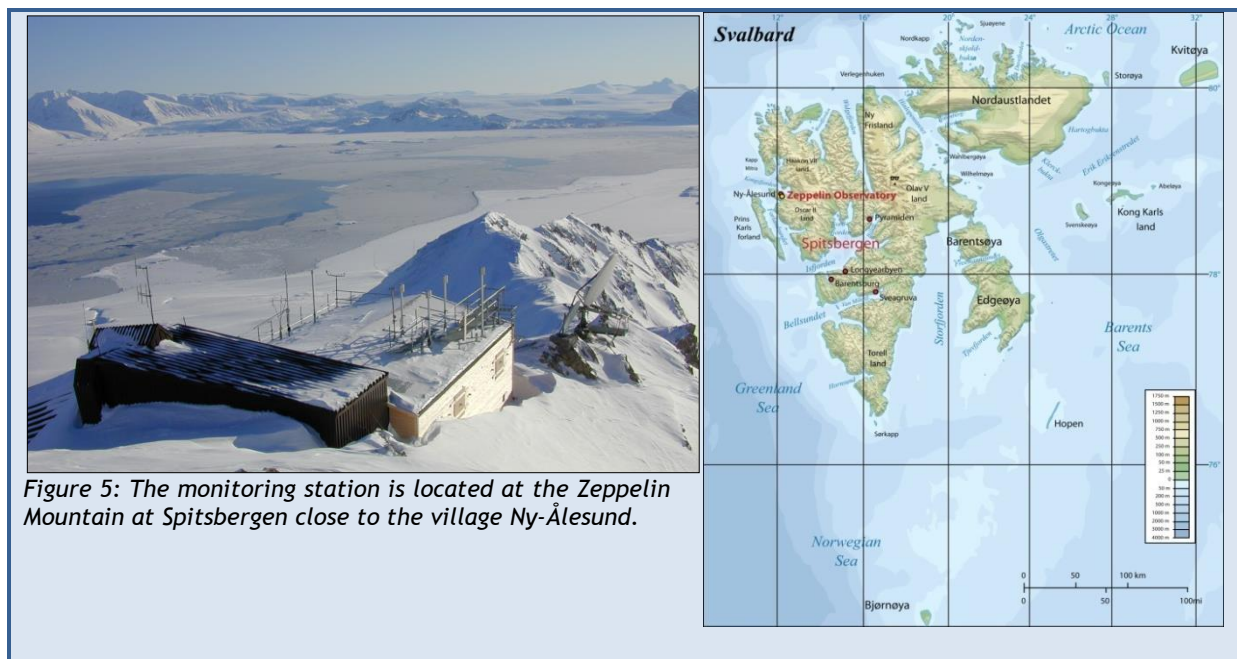


Figure 5: The monitoring station is located at the Zeppelin Mountain at Spitsbergen close to the village Ny-Ålesund.

The Zeppelin station is owned and maintained by the Norwegian Polar Institute. NILU is coordinating the scientific activities at the station. The station was built in 1989-1990. After 10 years of use, the old building was removed to give place to a new modern station that was opened in May 2000. The building contains several separate laboratories, some for permanent use by NILU and Stockholm University, others intended for short-term use like measurement campaigns and visiting scientists. A permanent data communication line permits on-line contact with the station for data reading and instrument control.

NILU performs measurements of more than 30 greenhouse gases including CO₂, halogenated greenhouse gases, methane, N₂O, SF₆, and carbon monoxide. In Appendix I there are more details about sampling techniques and frequency of observations. CO₂, CH₄ and CO are now measured sampled with 45 s resolution, aggregated to 1 h mean. This high sampling frequency gives valuable data for the examination of episodes caused by long-range transport of pollutants as well as a good basis for the study of trends and global atmospheric change. Close cooperation with AGAGE-partners on the halocarbon instrument and audits on the methane and CO-instruments performed by EMPA (see <http://www.empa.ch>) on the behalf of GAW/WMO results in show data of high quality.

The amount of particles in the air is monitored by a Precision-Filter-Radiometer (PFR) sun photometer. This instrument gives the aerosol optical depth (AOD). AOD is a measure of the aerosols attenuation of solar radiation in the total atmospheric column.

The instrumentation measuring aerosol microphysical and optical properties, which is operated by Stockholm University and has been the same since the opening of the station in 1991, has been modernized with the aim of meeting operation guidelines and quality standards set out by the European Supersites for Atmospheric Aerosol Research⁸ (EUSAAR) network.

The station at Zeppelin Mountain is also used for a wide range of other measurements, which are not reported here. This includes daily measurements of sulphur and nitrogen compounds (SO₂, SO₄²⁻, (NO₃⁻ + HNO₃) and (NH₄⁺ + NH₃), main compounds in precipitation (performed in Ny-Ålesund), total gaseous mercury, particulate heavy metals, persistent organic pollutants (HCB, HCH, PCB, DDT, PAH etc.) in air, as well as tropospheric ozone. Zeppelin observatory is also widely used in campaigns as during the International Polar Year.

At the Zeppelin station carbon dioxide (CO₂) is also measured by Stockholm University (SU) (Institute of Applied Environmental Research, ITM). SU maintain an infrared CO₂ instrument measuring CO₂ continuously. The instrument has been in operations since 1989, which this ensure a long time series of CO₂. This complements the measurement performed by NILU, and is very valuable. The continuous data are enhanced by the weekly flask sampling programme in co-operation with NOAA CMDL. Analysis of the flask samples provide CH₄, CO, H₂, N₂O and SF₆ data for the Zeppelin station in addition to CO₂.

⁸ EUSAAR: European Supersites for Atmospheric Aerosol Research <http://www.eusaar.net>

3.3 The Birkenes Observatory

Birkenes is located in Southern-Norway at 58° 23'N, 8° 15'E, 190 m a.s.l. Birkenes atmospheric observatory in Aust-Agder fills a central position in the Norwegian climate monitoring programme since it represents Norway's South also downwind from Europe receiving long range transported air pollution. The observatory has been in operation since 1971 and is one of the longest-running sites in Europe, and it is one of the core EMEP sites. In 2009, the aerosol observation programme at Birkenes Atmospheric Observatory received a major upgrade along with the upgrade of the general station infrastructure. The observatory was moved a few hundred meters and considerably upgraded in 2009 now measuring CO₂ and CH₄ with a Picarro instrument and a comprehensive aerosol program. The old station was situated in a hollow with limited line of sight to the oncoming flow. Since summer 2009, the observations are housed in a container assembly on the top of a hill a, with free line of sight to the oncoming flow in all directions (see Figure 6). The land use in the close vicinity of the site is characterized by 65% forest, 10% meadow, 15% freshwater lakes, and 10% agricultural areas (low intensity). This relocation improved the regional representativeness of the station significantly. The observation programme concerning atmospheric aerosol parameters was augmented by measurements of coarse mode particle size distribution, spectral particle scattering coefficient, and aerosol optical depth. It now meets ACTRIS and GAW standards, and comprises now almost all observations considered by the GAW aerosol scientific advisory group as relevant for aerosol climate effect assessments. This upgrade is also an important improvement of the Norwegian observation programme of climate forcing agents, which so far was more focussed on the Polar Regions. Accurate observations of climate relevant aerosol properties are a prerequisite for better climate predictions for this region.

In 2012, a cloud condensation nucleus counter (CCNC) has been taken into operation at Birkenes. A CCNC measures the number of aerosol particles able to act as nucleus for liquid-phase cloud drops as a function of water vapor supersaturation. This is a key parameter in constraining the indirect aerosol climate effect, i.e. the aerosol effect on cloud lifetime and reflectivity ("colour"). Birkenes is so far the first and only site in continental Norway including this observation. In addition, the instrumentation for measuring the aerosol absorption coefficient has been upgraded from single wavelength to three wavelength operation. Old and new instrument will be operated in parallel for at least a year to ensure a continuous time series.

All electrical and data infrastructure is new and upgrade with Near-Real-Time measurements controlled at NILU. Data from Birkenes (e.g. daily measurements SO₂, SO₄²⁻, NO₃⁻ + HNO₃ and NH₄⁺ + NH₃, main compounds in precipitation, mercury and other heavy metals, persistent organic pollutants, tropospheric ozone) have been essential for the study of long-range transport and deposition of air pollution to Scandinavia. The monitoring at this site, together with other central European regional sites, has provided the necessary background for establishing international binding agreements for targeting emission reductions, c.f. the convention for long-range transboundary air pollutions (CLTRAP) and the protocols hereunder. Personnel is visiting the observatory on a daily basis, and engineers from NILU are present at the station regularly (approximately once per month).

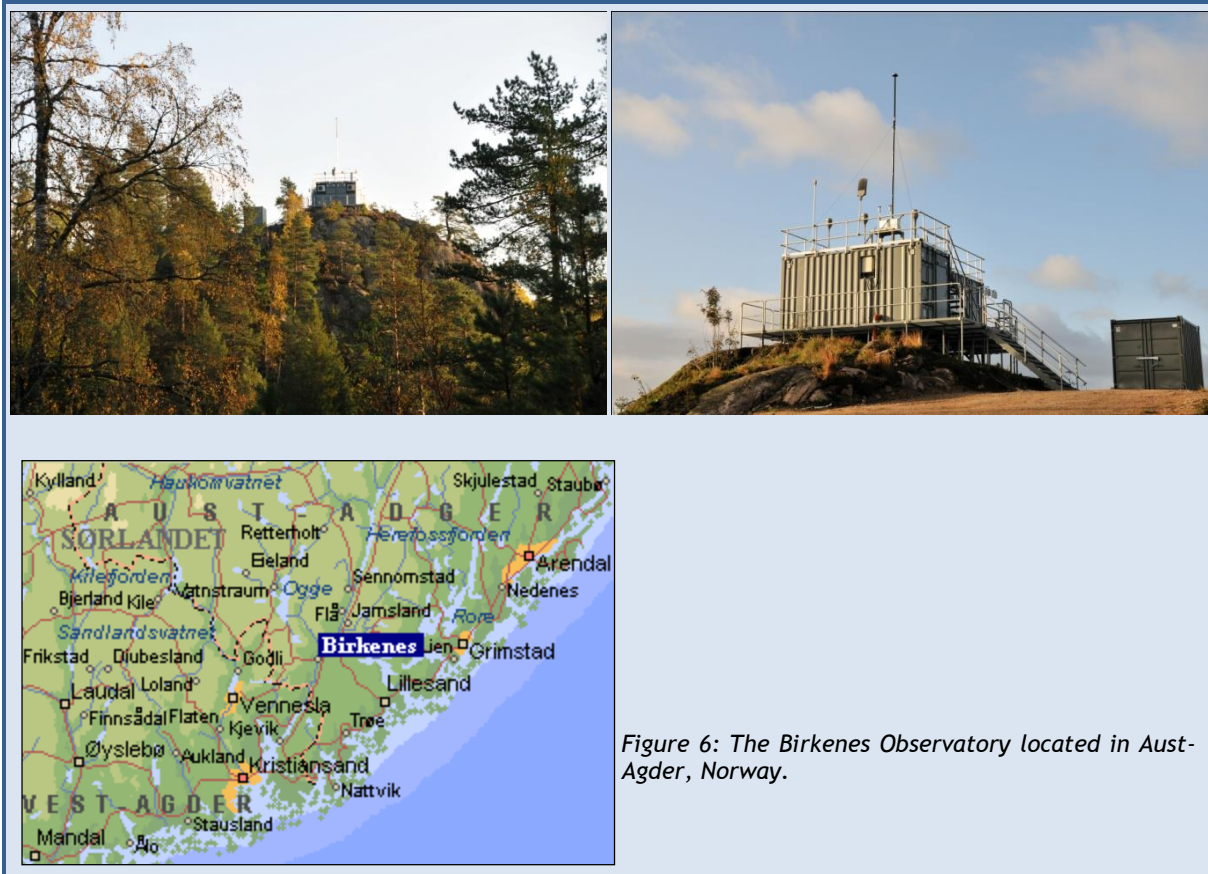


Figure 6: The Birkenes Observatory located in Aust-Agder, Norway.

4. Observations and trends of greenhouse gases at the Zeppelin Observatory in the Norwegian Arctic

NILU measures 23 greenhouse gases at the Zeppelin observatory at Svalbard. The results from the measurements, analysis and interpretations are presented in this chapter. Also observations of CO₂, which are performed by the Stockholm University - Department of Applied Environmental Science (ITM), are included in the report.

Table 2 presents the main results and annual mean values since the beginning of the observation period in 2001. Also trend per year and change (acceleration) in the trend for each component is given. The change in trend (acceleration in the trend) show how the growth rate has changed the last few years⁹.

Table 2: Yearly average concentration levels of greenhouse gases measured at the Zeppelin station for the years 2001-2012. All concentrations are in ppt_v, except for methane and carbon monoxide (ppb_v) and CO₂ (ppm_v). The trends are calculated from observations for the period 2001-2012.

Compound	Formula	2001	2012	Trend / year (1 σ) ^c	Change in trend (1 σ) ^c
Methane	CH ₄	1851	1892	+4.4 (0.09)	+0.44 (0.06)
Carbon monoxide	CO		121	-1.1 (0.08)	-0.21 (0.05)
Carbon dioxide^b	CO ₂	370.9	394.8	+2.1 ^b (0.02)	-0.04** (0.01)
Chlorofluorocarbons					
CFC-11 ^a	CFC1 ₃	259	237	-2.08 (0.007)	-0.03 (0.005)
CFC-12 ^a	CF ₂ Cl ₂	547	528	-1.8 (0.02)	-0.48 (0.01)
CFC-113 ^a	CF ₂ ClCFCl ₂	81.5	73.9	-0.67 (0.003)	-0.004 (0.002)
CFC-115 ^a	CF ₃ CF ₂ Cl	8.23	8.42	+0.02 (0.001)	-0.005 (0.0005)
Hydrochlorofluorocarbons					
HCFC-22	CHF ₂ Cl	160	232	+6.9 (0.01)	0.21 (0.006)
HCFC-141b	CH ₃ CFCl ₂	16.6	24.2	+0.58 (0.002)	-0.01 (0.001)
HCFC-142b ^a	CH ₃ CF ₂ Cl	14.5	23.0	+0.85 (0.001)	+0.005 (0.0009)
Hydrofluorocarbons					
HFC-125	CHF ₂ CF ₃	2.0	12.5	+0.91 (0.001)	+0.12 (0.0009)
HFC-134a	CH ₂ FCF ₃	20.8	73.4	+4.70 (0.004)	+0.05 (0.002)
HFC-152a	CH ₃ CHF ₂	2.8	10.4	+0.74 (0.002)	-0.05 (0.001)
Halons					
H-1211 ^a	CF ₂ ClBr	4.4	4.1	- 0.03 (0.0002)	-0.015 (0.0001)
H-1301	CF ₃ Br	3.0	3.4	+ 0.03 (0.0005)	-0.005 (0.0003)
Halogenated compounds					
Methyl Chloride	CH ₃ Cl	505	513	-0.2 (0.09)	-0.92 (0.06)
Methyl Bromide	CH ₃ Br	8.9	6.9	-0.19 (0.003)	-0.05 (0.002)
Dichloromethane	CH ₂ Cl ₂	31.0	44.9	+1.2 (0.01)	+ 0.22 (0.0008)
Chloroform	CHCl ₃	10.8	12.1	+0.10 (0.003)	+0.07 (0.002)
Methylchloroform	CH ₃ CCl ₃	38.3	5.4	-2.87 (0.002)	+0.48 (0.002)
Trichloroethylene	CHClCCl ₂	0.7	0.51	-0.01 (0.003)	+0.02 (0.002)
Perchloroethylene	CCl ₂ CCl ₂	4.6	2.7	-0.16 (0.007)	+0.06 (0.004)
Sulphurhexafluoride ^a	SF ₆	4.96	7.80	+0.26 (0.0005)	+0.01 (0.0004)

^aThe measurements of these components are not within the required precision of AGAGE. See Appendix I for more details.

^bMeasurements of Carbon dioxide are performed by Stockholm University, Department of Applied Environmental Science (ITM).

^c Standard errors from model fit to the data (see appendix A)

⁹ As the time series still are short and the seasonal and annual variations are large for many of the components, there are considerable uncertainties connected with the results.

Greenhouse gases have numerous sources both anthropogenic and natural. Trends and future changes in concentrations are determined by their sources and the sinks, and in section 4.1 **Error! Reference source not found.** are observations and trends of the monitored greenhouse gases with both natural and anthropogenic sources presented in more detail. In section 4.2 **Error! Reference source not found.** are the detailed results of the gases with purely anthropogenic sources presented. These gases are not only greenhouse gases but also a considerable source of chlorine and bromine in the stratosphere, and are thus responsible for the ozone depletion and the ozone hole discovered in 1984. The ozone depleting gases are controlled and regulated through the successful Montreal protocol. Section 3 describes the Zeppelin observatory at Svalbard where the measurements take place and the importance of the unique location. Zeppelin observatory is a unique site for observations of changes in the background level of atmospheric components. All peak concentrations of the measured gases are significantly lower at Ny-Ålesund than at other sites at the Northern hemisphere, due to the stations remote location. A description of the instrumental and theoretical methods applied is included in Appendix I.

4.1 Greenhouse gases with natural and anthropogenic sources

All gases presented in this section (methane, carbon dioxide, methyl chloride, methyl bromide, carbon monoxide and tropospheric ozone) have both natural and anthropogenic sources. This makes it complex to interpret the observed changes as the sources and sinks are numerous. Moreover, several of these gases are produced in the atmosphere from chemical precursor gases and often dependant on the solar intensity.

4.1.1 Observations of Methane in the period 2001-2012

Methane (CH₄) is the second most important greenhouse gas from human activity after CO₂ with a radiative forcing of 0.48 W m⁻² since 1750 and up to 2005 (Forster et al., 2007). In addition to be a dominating greenhouse gas, methane also plays central role for the atmospheric chemistry. The atmospheric lifetime of methane is approx. 9 years and about 12 years when indirect effects are included (Forster et al., 2007).

The average CH₄ concentration in the atmosphere is determined by a balance between emission from the various sources at the earth's surface and reaction and removal by free hydroxyl radicals (OH) in the troposphere. In the atmosphere, methane is destroyed by reaction with OH giving water vapour and CO₂. A small fraction is also removed by surface deposition. Since the reaction with OH also represents a significant loss path for the oxidant OH, additional CH₄ emission will suppress OH and thereby increase the CH₄ lifetime, implying further increases in atmospheric CH₄ concentrations (Isaksen and Hov, 1987; Prather et al., 2001). This positive chemical feedback is estimated to be significant in the current atmosphere with a feedback factor of about 1.4¹⁰ (Prather et al., 2001). The OH radical has a crucial role in the tropospheric chemistry by reactions with many emitted components and is responsible for the cleaning of the atmosphere (like removal of CO, hydrocarbons, HFCs, and others). A stratospheric impact of CH₄ is due to the fact that CH₄ contributes to water vapor buildup in this part of the atmosphere, influencing and reducing the stratospheric ozone amount.

The atmospheric mixing ratio of methane was, after a strong increase during the 20th century, relatively stable over the period 1998-2006. The global average change was close to zero for this period according to IPCC (Forster et al, 2007), and also at Zeppelin site for the short period 2001-2004. 2003 was an exception globally and at Zeppelin; a annual mean of 1856 ppb at Zeppelin was obtained, considerable higher than the other years up till then. This seems to have been caused by increased precipitation in the tropical regions leading to increased methane emissions from wetland areas and a global rise in the concentration. Recently an increase in the methane levels is evident from both our observations, both at Zeppelin and Birkenes and observations at other sites (Rigby et al., 2008; WMO, 2013).

Figure 7 depict the observations of methane at Zeppelin since the start in 2001.

¹⁰ This means that with current atmospheric chemical distribution a 10 % increase in emission of methane, the atmospheric composition increases will reach 14 %.

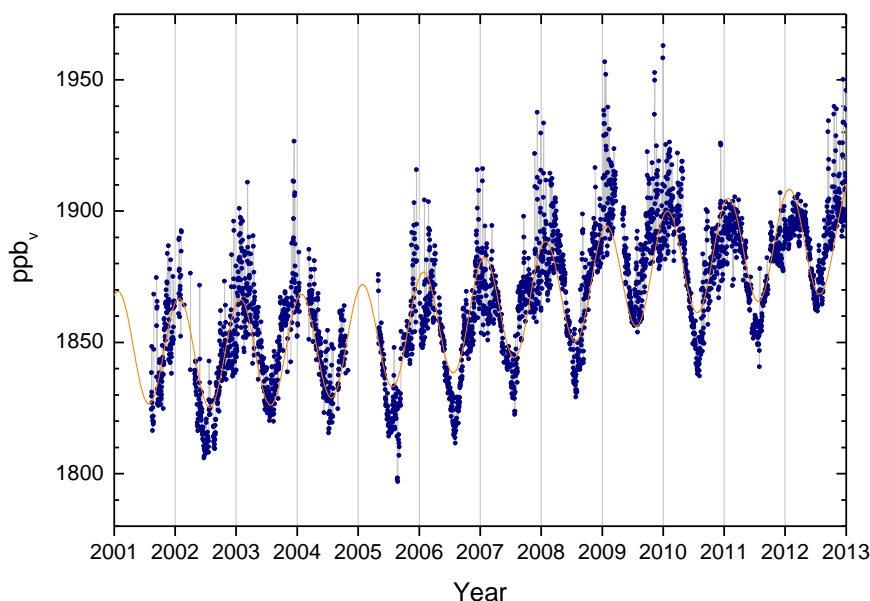


Figure 7: Observations of daily averaged methane mixing ratio for the period 2001-2012 at the Zeppelin observatory. Blue dots: daily mean observations, orange solid line: modelled background methane mixing ratio.

During 2012 the methane data series from Zeppelin has been revised as part of the EU project InGOS (see section 3.1 and Appendix I). All original measurement signals have been processed with new improved software to recalculate every single measurement over the last 12 years as a part of harmonized quality assurance procedures. As can be seen from the figure there has been an increase in the concentrations of methane observed at Zeppelin the last years. The pronounced increase started in November/December 2005 and continued throughout the years 2007 - 2009, and is particularly evident in the late summer-winter 2007, and summer-autumn 2009. The year 2012 showed new record globally, and at Zeppelin (see Figure 8). The measurements show very special characteristics in 2010 and 2011 at Zeppelin. As can be seen there is remarkable lower variability in the daily mean in 2011 with fewer episodes than the typical situation previous years, and also after summer/autumn 2012. This characteristic is also partly evident for CO, displayed in Figure 18 at page 29. The reason for this is under analysis, and part of intensive research at NILU. A conclusion is still not possible to draw. An analysis of the general transport pattern of air to Zeppelin for 2011 year does not seem to differ from the normal situation (see e.g. "Figure 46: The percentage of polluted and clean air arriving at Zeppelin in the period 2001-2012 from the various sectors." at page 64). Additionally, a more detailed preliminary study for the full period 2001 to 2012, reveals no indication of any change in atmospheric transport nor any transport anomaly in 2011. This is true for both short- and long-range transport and analysis if change in local sources at Svalbard is also studied. We also operated two different instruments in parallel parts of 2012 with satisfactory results (see page 81). There have also been other changes and improvements at the station during this period (see the Appendix I, particularly section. *Methane and nitrous oxide*), but these seem not to explain the change in the variability. Rather, the preliminary results indicate that there is a change in the CH₄ sources in the Arctic region in 2010-2012, but this need more investigations. Among the hypothesis is if a significant anomaly in soil water volume in Northern Europe and Western Siberia in this period could have reduced emissions of CH₄ from wetlands as we know that wetland is an important source for CH₄ at Zeppelin. Also changes in gas leaks and pipe lines from oil and gas installations need to be investigated. Isotopic measurements included on short term in an ongoing research project (*GAME: Causes and effects of Global and Arctic changes in the MEthane budget*¹¹) might improve the knowledge about this.

To retrieve the annual trend in the methane for the entire period the observations have been fitted by an empirical equation. The modelled methane values are shown as the orange solid line in Figure 7. Only the observations during periods with clean air arriving at Zeppelin are used in the model, thus the model represents the background level of methane at the site (this is described in Appendix I, page 81). Chapter 8 and Figure 47 visualise the daily mean methane observations when clean air is arriving, compared to daily mean when air from the polluted sections is arriving. At Zeppelin, the average annual growth rate is +4.4 ppb_v per year for the period 2001-2012. This corresponds to an increase of 0.18% per year.

¹¹ GAME started 1. March 2011 and is a project is funded by the Research Council of Norway under the program NORKLIMA. It is lead by NILU and Cicero is a partner. Isotopic measurements of CH₄ for summer 2012-end 2013. The project ends 30.06.2014.

The increase in the methane levels the last years is visualized in Figure 8 showing the CH₄ annual mean mixing ratio for the period 2001-2012. The annual means are based on a combination of the observed methane values and the modelled background values; during periods with lacking observations, we have used the modelled background mixing ratios in the calculation of the annual mean.

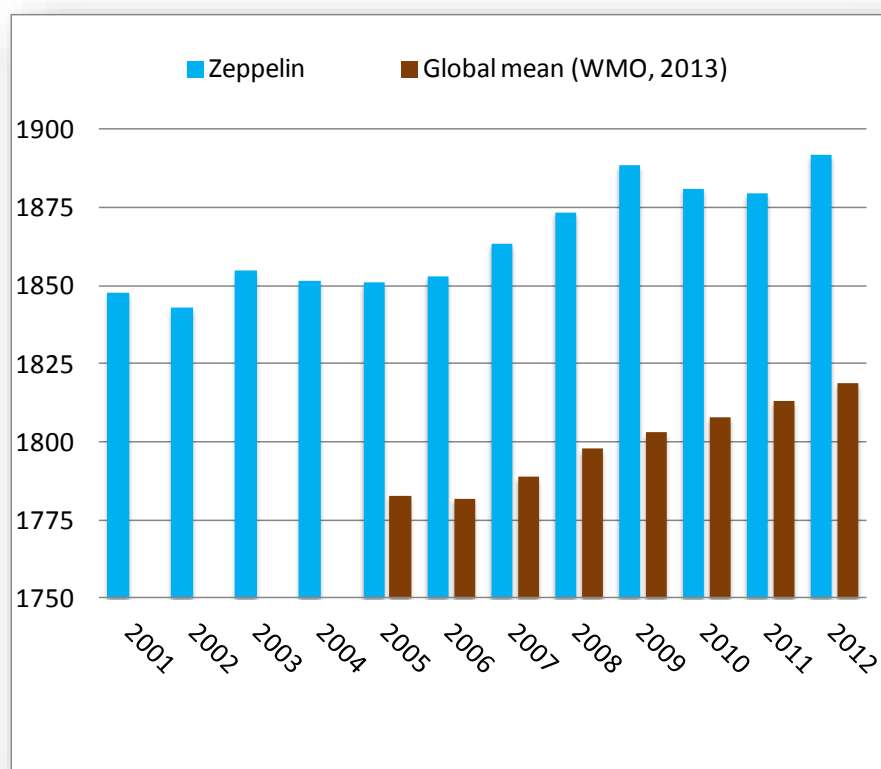


Figure 8: Development of the annual mean mixing ratio of methane in ppb measured at the Zeppelin Observatory (blue bars) for the period 2001-2012 compared to global mean provided by WMO as red bars (WMO, 2013).

This diagram clearly illustrates the increase in the concentrations of methane at Zeppelin during 2005-2009, a small decrease in 2010 and 2011, and then a new record level in 2012. The increase since 2011 was relatively large, as much as 12.2 ppb. The reduction from 2010-2011 is probably mainly due to reduced variability and fewer episodes as described above.

The annual mean mixing ratio for 2012 was 1892 ppb while the level was 1880 ppb_v in 2011. The increase since 2005 at Zeppelin is 50.7 ppb (approx. 2.2 %) which is considered as relatively large compared to the development of the methane mixing ratio in the period from 1999-2005 both at Svalbard and globally. It is also larger than the global mean increase since 2005, which is 36 ppb (WMO, 2009; 2011a, 2013). The global mean shows an increase since 2006, and the last 4 years of ca 5-6 ppb per year, while larger fluctuations are evident at Zeppelin. This is explained by the distribution of the sources; there are more sources at the northern hemisphere, and thus larger interannual variations. For comparison, during 1980s when the methane mixing ratio showed a large increase, the annual global mean change was around 15 ppb_v per year.

The main sources of methane include boreal and tropical wetlands, rice paddies, and emission from ruminant animals, biomass burning, and fossil fuels extraction and combustion. Further, methane is the principal component of natural gas and e.g. leakage from pipelines; off-shore and on-shore installations are a known source of atmospheric methane. The distribution between natural and anthropogenic sources is approximately 40% natural sources, and 60% of the sources are direct a result of anthropogenic emissions. Of natural sources there is a large unknown potential methane source at the ocean floor, so called methane hydrates. Other sources include mud volcanoes which are connected with deep geological faults. Further, a large unknown amount of methane is bounded in the permafrost layer in Siberia and North America and this might be released if the permafrost layer melts as a feedback to climate change. According to a paper in Nature (Schuur and Abbot, 2011), there is a high risk of permafrost thaw and substantial release of both CO₂ and CH₄. They estimated a release of 30-63 billion tonnes carbon from Arctic soil before the year 2040 as response to a predicted Arctic temperature increase and scenario with 7.5°C by the year 2100. This is 1.7-5.2 times larger than previous

estimates. They assume that most of the carbon release will be as CO₂, and less than 3% will be emitted as CH₄. However, because CH₄ has higher global warming potential (25 compared to CO₂), almost half of the climate effect will be caused by CH₄. According to the IPCC report from 2007 (Alley et al., 2007) the temperature of the top of the permafrost layer has generally increased by up to 3°C since 1980s.

The recent observed increase in the atmospheric methane concentrations has led to enhanced focus and intensified research to improve the understanding of the methane sources and changes particularly in responses to global and regional temperature increase. Currently the observed increase the last years is not explained or understood. The high level observed in 2003 was a global feature, and is still not fully understood. It is essential to find out if the increase since 2005 is due to large point emissions or if it is caused by newly initiated processes releasing methane to the atmosphere like e.g. the thawing of the permafrost layer. Recent and ongoing scientific discussions point in the direction of increased emissions from wetlands located both in the tropical region and in the Arctic region.

One valuable method to study various methane sources is to exploit isotopic measurements. Many arctic methane sources have different isotopic ratios of $\delta^{13}\text{C}$. Combined with model studies of air transport to Zeppelin it is possible to improve the quantification of emission from wetlands, gas from fossil fuel, and emission from methane hydrates at the sea floor. This has been done in selected periods during 2008 and 2009 at Zeppelin and the results are described in Fischer et al. (2011). The study shows that the dominant Arctic summer CH₄ source in 2008 and 2009 was from wetlands. During winter time fossil gas emissions emitted at lower latitudes dominated the CH₄ input. The results presented in Fisher et al. (2011) are in agreements with the findings of Bousquet et al. (2011). They have used models to study global source attribution to the changes in atmospheric methane for 2006-2008. Their conclusions were that in 2007 tropical wetland contributed with 2/3 to the global increase, but with a significant contribution also from wetlands at high latitudes boreal regions. Submarine emissions along the West Spitsbergen slope was found to have negligible CH₄ input to the atmosphere in summer, despite the fact that it was possible to identify methane bubbles in the sea from the sea floor. Gas hydrates at the sea floor are widespread in thick sediments in this area between Spitsbergen and Greenland. If the sea bottom warms, this might initiate further emissions from this source. This is the core of the large new research project *MOCA - Methane Emissions from the Arctic Ocean to the Atmosphere: Present and Future Climate Effects*¹², started at NILU October 2013.

Wetland CH₄ emissions respond rapidly to warming. In particular, Arctic and boreal wetlands are likely to respond immediately to sustained heat waves and increases in precipitation. Fire CH₄ is also more likely with elevated temperatures. There is a strong need for more regular CH₄ isotopic measurements in the high Arctic. High effort should be put on the issue to understand the increase in the CH₄ concentrations as the consequence might be severe.

¹² <http://moca.nilu.no/>

4.1.2 Observations of Nitrous Oxide at the Zeppelin Observatory

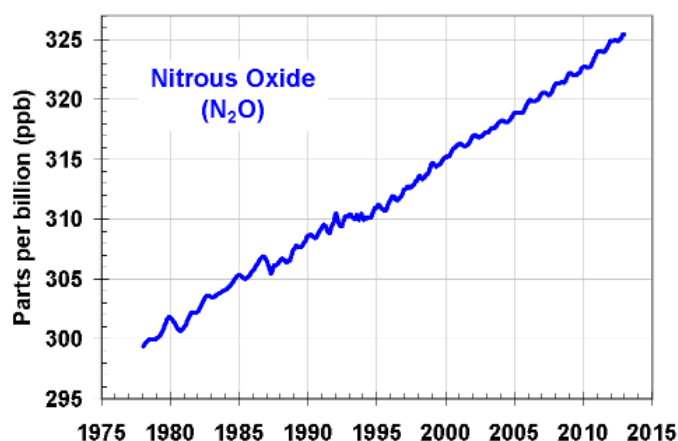


Figure 9: Global average abundances of, nitrous oxide from the NOAA global air sampling network are plotted since the beginning of 1979-2012. <http://www.esrl.noaa.gov/gmd/aggi/>

Nitrous Oxide (N_2O) is a greenhouse gas with both natural and anthropogenic sources. The sources include oceans, tropical forests, soil, biomass burning, cultivated soil and use of fertilizer, and various industrial processes. There are large uncertainties in the major soil, agricultural, combustion and oceanic sources of N_2O and also frozen peat soils in Arctic tundra is reports as a potential significant source (Repo et al., 2009). N_2O has a lifetime of approx. 114 years and the GWP is 310 (Forster et al., 2007). Thus N_2O is an important greenhouse gas with a radiative forcing of 0.16 W m^{-2} since 1750 contributing around 5-6 % to the overall long lived greenhouse gas forcing over the industrial era. The gas is regulated through the Kyoto protocol. Additionally, N_2O is also the major source of the ozone-depleting nitric oxide (NO) and nitrogen dioxide (NO_2) in the stratosphere thus the component is also influencing the stratospheric ozone

layer. The recent Assessment of the ozone depletion (WMO, 2011) suggests that current emissions of N_2O are presently the most significant substance that depletes ozone.

N_2O has increased from around 270 ppb prior to industrialization and up to an average global mean of 325.1 ppb in 2012 (WMO, 2013). The, mean annual absolute increase during last 10 years was 0.78 ppb/year (WMO, 2012a). Figure 9 is taken from NOAA and shows the average global development of N_2O since 1978. The NOAA observations are based on flask samples with mostly weekly sampling or lower time resolution. There are few continuous observations of N_2O , and particularly in the Arctic region. In 2009 NILU installed a new instrument at Zeppelin measuring N_2O with high time resolution; 15 minutes. The instrument was in full operation in April 2010 and the results for 2010 -2012 are presented in Figure 10.

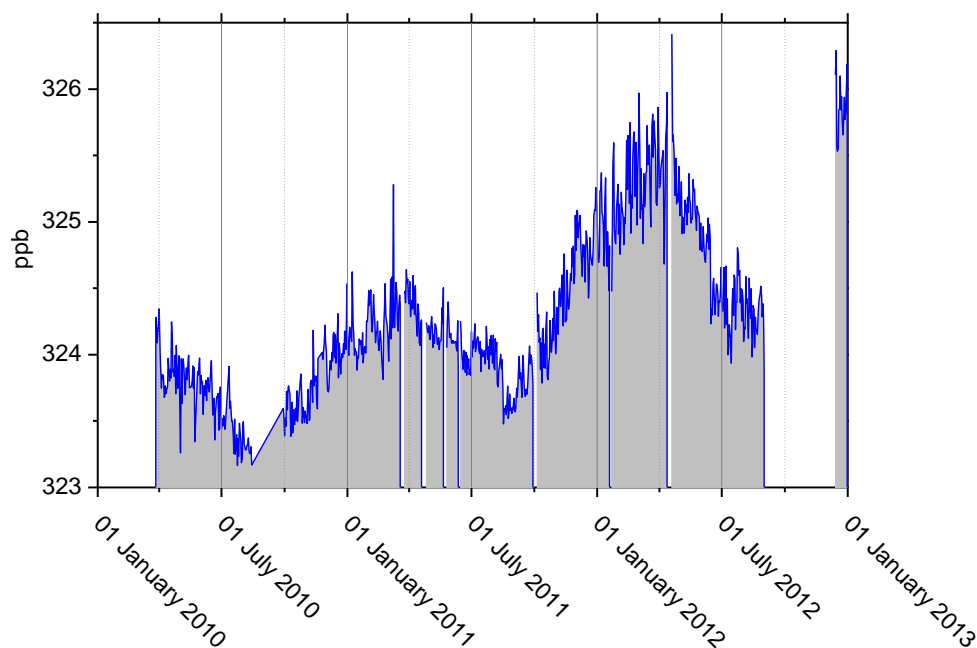


Figure 10: Measurements of N_2O at the Zeppelin Observatory for 2010-2012.

According to WMO 2013 the global mean value for 2012 was 325.1 with an increase of 0.9 ppb since 2011. Annual mean for Zeppelin in 2012 was 324.9 with a standard deviation of 0.4 ppb, slightly lower, but note that we miss measurements from the autumn due to instrumental problems.

4.1.3 Observations of Carbon Dioxide in the period 1988-2012

CO₂ is the most important greenhouse gases with a radiative forcing of 1.66 W m⁻² since 1750 and an increase in the forcing of as much as 0.2 W m⁻² since the IPCC report from 2001 (Forster et al., 2007). CO₂ is the end product in the atmosphere of the oxidation of all main organic compounds and has shown an increase of as much as 45 % since the pre industrial time (WMO, 2013). This is mainly due to emissions from combustion of fossil fuels and land use change. CO₂ emissions from fossil fuel combustions and cement production increased by 2.1% in 2012, with a total of 9.7±0.5 GtC emitted to the atmosphere, 58% above 1990 emissions (the Kyoto Protocol reference year) (<http://www.globalcarbonproject.org>).

NILU started CO₂ measurements at the Zeppelin Observatory in 2012. The atmospheric CO₂ concentration measured at Zeppelin Observatory for the period 1988-2012 is presented in Figure 11. Prior to 2012, ITM University of Stockholm provides all data and we acknowledge the effort they are doing in monitoring CO₂ at the site. Note that these data are preliminary and have not undergone full quality assurance.

The results show a continued increase since the start of the observations and in Figure 12 is the development of the annual mean concentrations measured at Zeppelin observatory for the period 1988-2012 shown.

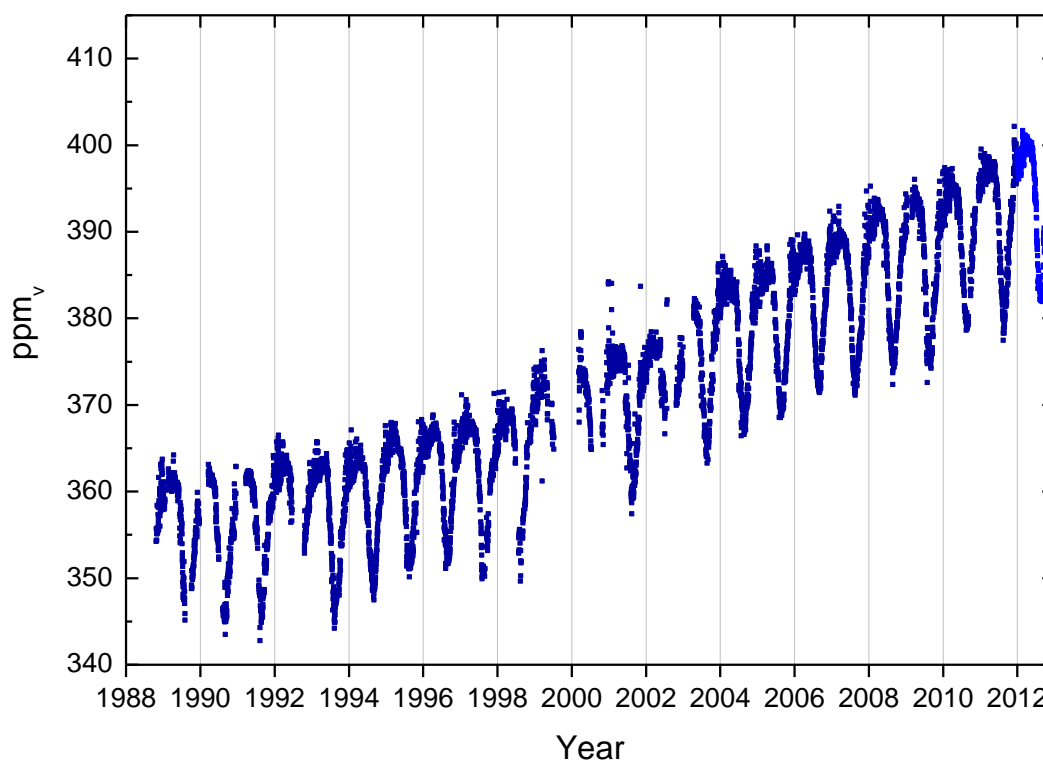


Figure 11: The CO₂ concentration in ppm measured at Zeppelin Observatory for the period 2001-2012. The change in color indicates the change from the GC instrument to cavity ring-down spectroscopy (CRDS, Picarro).

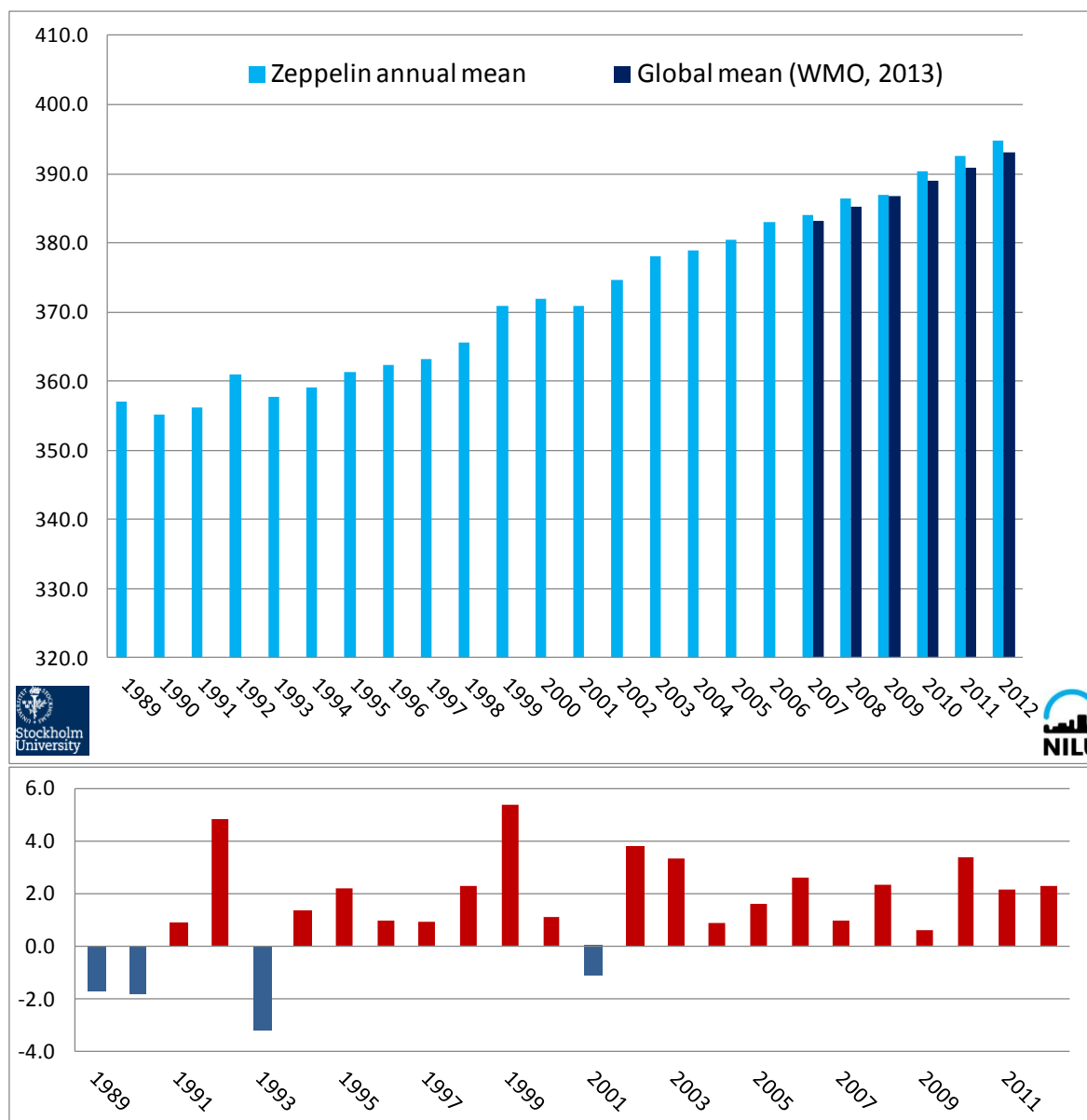


Figure 12: Upper panel: Development of the annual mean mixing ratio of CO₂ measured at Zeppelin observatory for the period 1988-2012. The light blue bars are the results from Zeppelin, and the dark blue bars show the global annual mean for 2007-2012 (WMO, 2013). Lower panel: Yearly change in ppb at Zeppelin.

The results show that 2012 is a new record year for the annual mixing ratio of CO₂ at Zeppelin, and the increase is larger than the global mean increase with an increase at Zeppelin of 2.3 ppb slightly higher than the year before and also the global mean increase of 2.1 ppb. (WMO, 2013). Also the global mean increase is higher than from 2010 to 2011; 1.9 ppb. ITM University of Stockholm have not completed their analysis of the observations, thus the mean values for the last years are preliminary. The main reason why the CO₂ level is higher at Zeppelin than globally is that in general the CO₂ emissions is lower in the Southern hemisphere, and the global mixing takes a certain time.

By use of the method described in Appendix I we have estimated the annual trend, also given in Table 2. The trend for the period 2001-2012 is -2.1 ppb per year.

4.1.4 Observations of Methyl Chloride in the period 2001-2012

Methyl chloride (CH_3Cl) is the most abundant chlorine containing organic gas in the atmosphere, and it contributes approx. 16% to the total Chlorine from the long lived gases in the troposphere (WMO, 2011). The main sources of Methyl Chloride in the atmosphere are natural, and dominating source is thought to be emissions from warm coastal land, particularly from tropical islands are shown to be a significant source but also algae in the ocean, and biomass burning. Several of these sources are expected to vary with global temperature change. Due to the dominating natural sources, this compound is not regulated through any of the Montreal or Kyoto protocols, but is an important natural source of Chlorine to the stratosphere. The degradation of the compound is dependent on solar intensity. To reach the stratosphere, the lifetime in general needs to be in the order of 2-4 years to have significant chlorine contribution, but this is also dependant on the source strength and their regional distribution. Methyl Chloride has relatively high mixing ratios, and contributes to the stratospheric Chlorine burden. With respect to the warming potential this substance is 16 times stronger than CO_2 per kg gas emitted.

The results of the observation of this substance for the period 2001-2012 are shown in Figure 13.

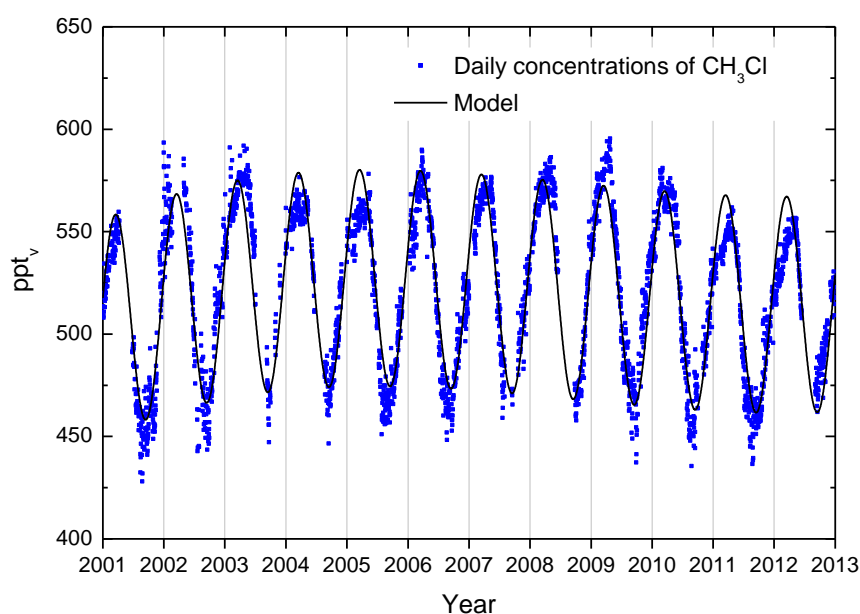


Figure 13: Observations of methyl chloride, CH_3Cl , for the period 2001-2012 at the Zeppelin observatory. Dots: daily averaged concentrations from the observations, solid line: modelled background mixing ratio.

The lifetime of the compound is only 1 year resulting in large seasonal fluctuations as shown in the Figure and rapid response to changes in sources. There is a decrease the last years, but this seems to have stopped in 2012.

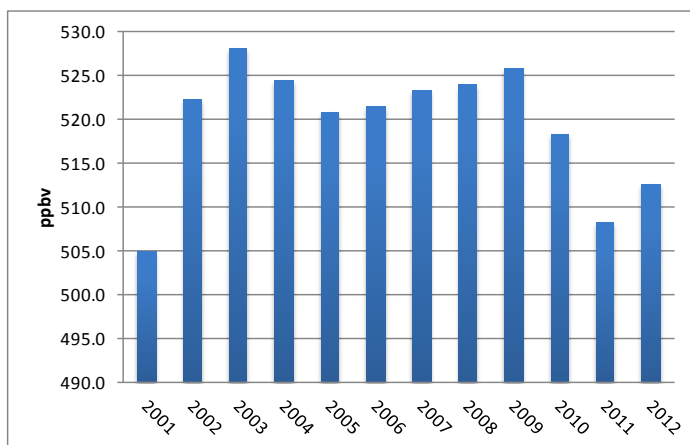


Figure 14: Development of the annual means methyl chloride measured at the Zeppelin Observatory for the period 2001-2011.

By use of the model described in Appendix I we have calculated the annual trend, and the change in the trend is also given in Table 2. The trend for the period 2001-2012 is -0.23 ppt per year, and the change in the trend is -0.9.

The annual means of methyl chloride for the period 2001-2012 is presented in Figure 14. The period 2002-2009 was relatively stable, but since 2009 there is a decrease of as much as 18 ppt (approx. 3.5%) in 2011. From 2011 to 2012 there is an increase of 4.88 ppt. The reason for this is not understood, and a closer study of sources variation for this compound is recommended, also by WMO (WMO, 2011) as sources are also related to atmospheric temperature change and ocean.

4.1.5 Observations of Methyl Bromide in the period 2001-2012

The sources of Methyl Bromide (CH_3Br) are both from natural and anthropogenic activities. The natural sources such as the ocean, plants, and soil, can also be a sink for this substance. Additionally there are also significant anthropogenic sources; it is used in a broad spectrum of pesticides in the control of pest insects, nematodes, weeds, pathogens, and rodents. Biomass burning is also a source and it is also used in agriculture primarily for soil fumigation, as well as for commodity and quarantine treatment, and structural fumigation. While methyl bromide is a natural substance, the additional methyl bromide added to the atmosphere by humans contributes to the man made thinning of the ozone layer. Total organic bromine from halons and methyl bromide peaked in 1998 and has declined since. The tropospheric abundance of bromine is decreasing, and the stratospheric abundance is no longer increasing (WMO, 2011). The observed decrease in stratospheric Bromine was solely a result of declines observed for methyl bromide. Bromine (Br) from halons continues to increase, but at slower rates in recent years, see section 4.2.4 on page 36.

The results of the daily averaged observations of this compound for the period 2001-2012 are shown in Figure 15.

A relatively large change is evident after the year 2007, a reduction of approx. 22% since the start of our measurements at Zeppelin. Methyl bromide is a greenhouse gas with a lifetime of 0.8 years and it is 5 times stronger than CO_2 , if the amount emitted of both gases were equal. The short life time explains the large annual and seasonal variations of this compound.

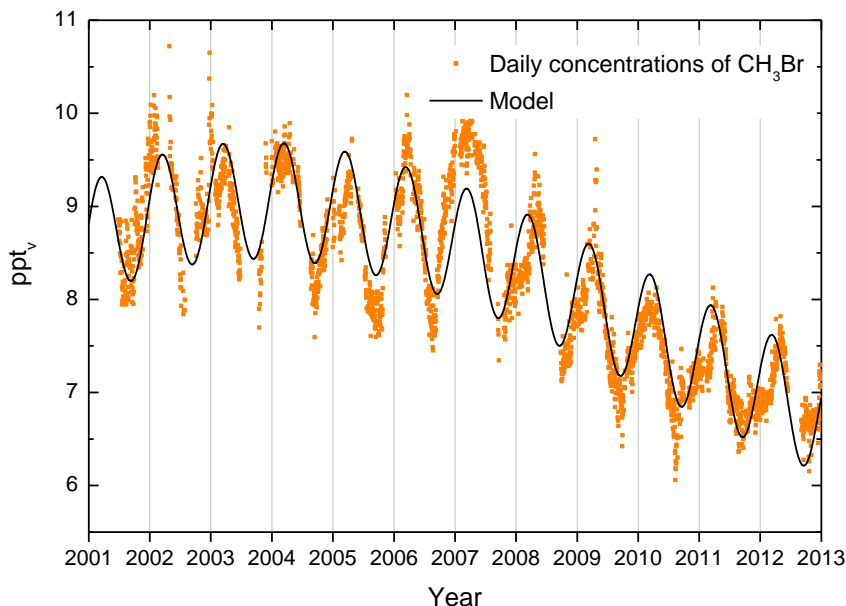


Figure 15: Observations of methyl bromide, CH₃Br, for the period 2001-2012 at the Zeppelin observatory. Dots: daily averages mixing ratios from the observations, solid line: modelled background mixing ratio.

We have calculated the annual trend by use of the model described in Appendix I. The trend and change in the trend is given in Table 2. For the period 2001-2012 there is a reduction in the mixing ratio of -0.19 ppt per year, with relaxation in the trend of -0.05. However, note that the observed changes are small (approx. 1.6 ppt since 2007) and the time period relatively short thus the seasonal and annual variations of the trends are uncertain.

The development of the annual means for the period 2001-2012 is presented in Figure 16, clearly illustrating the decrease the last years. In general atmospheric amounts of methyl bromide have declined since the beginning in 1999 when industrial production was reduced as a result of the Montreal protocol. The global mean mixing ratio was 7.3-7.5 ppt in 2008, slightly lower than at Zeppelin and also the annual mean reduction is slower than at Zeppelin, 0.14 ppt/year (WMO, 2011). The differences are explained by slower inter hemispheric mixing. The recent reduction is explained by considerable reduction in the use of this compound; in 2008 the use was 73% lower than the peak year in late 1990s (WMO, 2011).

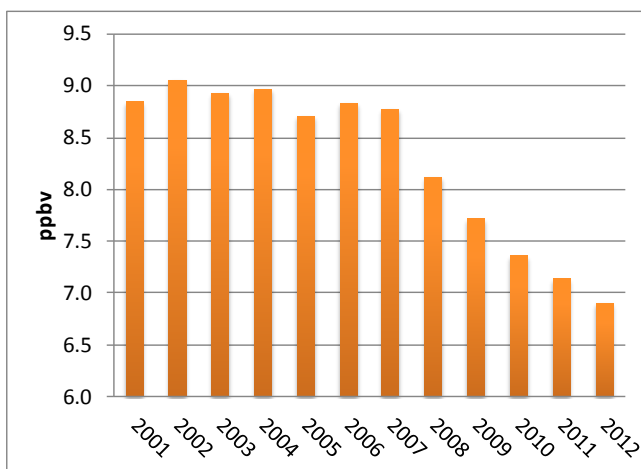


Figure 16: Development of the annual means of Methyl Bromide measured at the Zeppelin Observatory for the period 2001-2012.

4.1.6 Observations of tropospheric ozone in the period 1990-2012

Tropospheric ozone, which is the ozone in the lower part of the atmosphere, is a natural constituent of the atmosphere and plays a vital role in many atmospheric processes. It is also a short-lived greenhouse gas with a radiative forcing of $+0.35 \text{ W m}^{-2}$ (IPCC, 2007) due to man made changes in the concentrations since 1750. This is 10% of the overall global radiative forcing since 1750 making this component as the third most influencing greenhouse gas (see Figure 1 on page 9). Tropospheric ozone is a central short-lived climate forcer (SLCF) receiving enhanced focus the last years in both research and monitoring internationally. In a recent report UNEP¹³ advocates for SLCF mitigation strategies to complement CO₂ reductions. In addition to ozone, SLCF includes aerosols, black carbon (in aerosols) and sometime also direct or indirect effects of methane. Ozone is not emitted directly to the atmosphere, but it is rather produced from precursor gases; the formation of ozone is due to a large number of photochemical reactions taking place in the atmosphere and depends on the temperature, humidity and solar radiation as well as the primary emissions of nitrogen oxides, CO and volatile organic compounds. Anthropogenic emissions of VOC and nitrogen oxides have increased the photochemical formation of ozone in the troposphere. Until the end of the 1960s the problem was basically believed to be one of the big cities and their immediate surroundings. In the 1970s, however, it was found that the problem of photochemical oxidant formation is much more widespread. The ongoing monitoring of ozone at rural sites throughout Europe shows that episodes of high concentrations of ground-level ozone occur over most parts of the continent every summer. Future observations and understanding of precursor gases is targeted both by EMEP and the EU infrastructure project ACTRIS (see section 3.1). As there are no direct anthropogenic sources for ozone; the component is not regulated by the Kyoto protocol.

The 1999 Gothenburg Protocol is designed for a joint abatement of acidification, eutrophication and ground-level ozone. The critical levels defined by ECE for protection of vegetation are $150 \mu\text{g}/\text{m}^3$ for hourly mean, $60 \mu\text{g}/\text{m}^3$ for eight-hour mean and $50 \mu\text{g}/\text{m}^3$ for seven-hour mean (9 a.m. - 4 p.m.) averaged over the growing season (April-September).

The important greenhouse gas ozone is included in the KLIF program “Monitoring of long-range transboundary air pollution” and analysis of this is presented in Aas, et al., (2013), only brief overview is presented here. The observed ozone mixing ratios at the Zeppelin Observatory for the period 1990-2012 are shown in Figure 17.

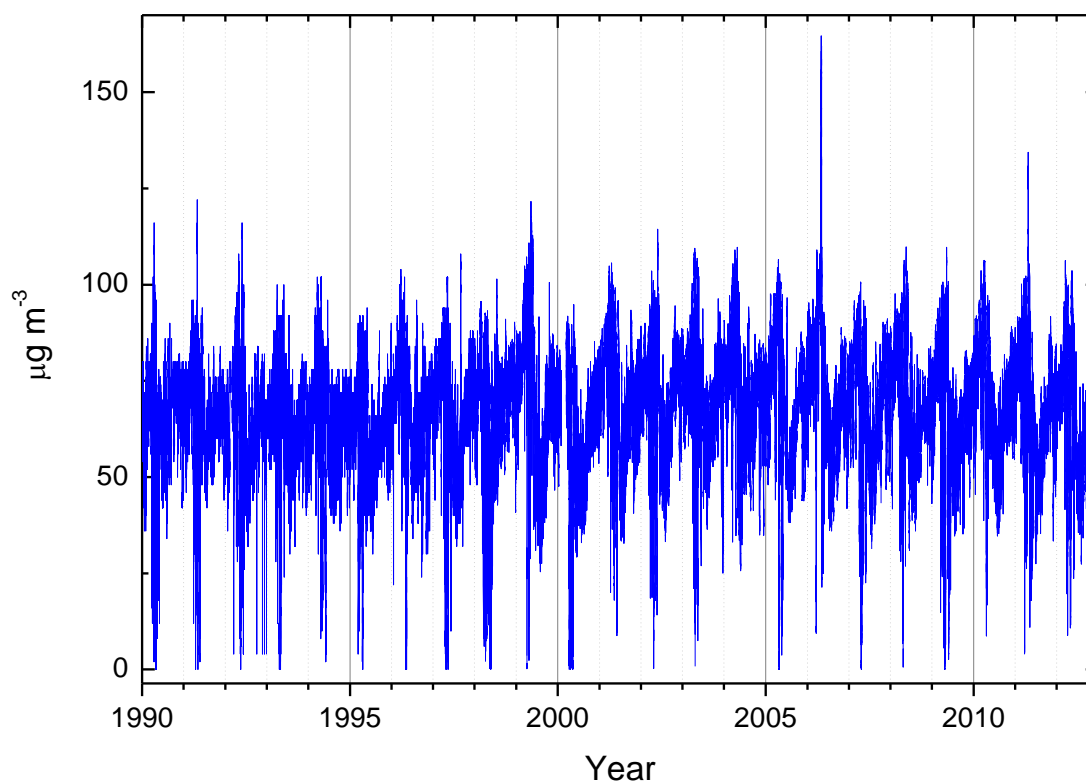


Figure 17: Observations of ozone in the troposphere for the period 1990-2012 at the Zeppelin observatory. Blue line: hourly average concentrations.

¹³ http://www.unep.org/dewa/Portals/67/pdf/Black_Carbon.pdf

There are large seasonal variations due to relatively short lifetime and the dependency on solar radiation and interactions with precursor gases. In 2006 there was an extreme episode with transport of pollution into the Arctic region and ozone levels as high as $-160 \mu\text{g m}^{-3}$. This was above all critical levels. In 2011 there have been few strong episodes, and the maximum ozone level observed was $134 \mu\text{g m}^{-3}$ at 25^h of April 2011 during night time. Analysis of the air transport to the Zeppelin Observatory this day shows that the air arrived from Poland and Eastern-Europe.

4.1.7 Observations of CO in the period 2001-2012

Carbon monoxide (CO) is not considered as a direct greenhouse gas, mostly because it does not absorb terrestrial thermal IR energy strongly enough. However, CO is able to modulate the level of methane and production tropospheric ozone, which are both very important climate components. CO is closely linked to the cycles of methane and ozone and, like methane; CO plays a key role in the control of the OH radical. CO is also emitted from biomass burning.

The observed CO mixing ratio for the period September 2001-2012 is shown in Figure 18.

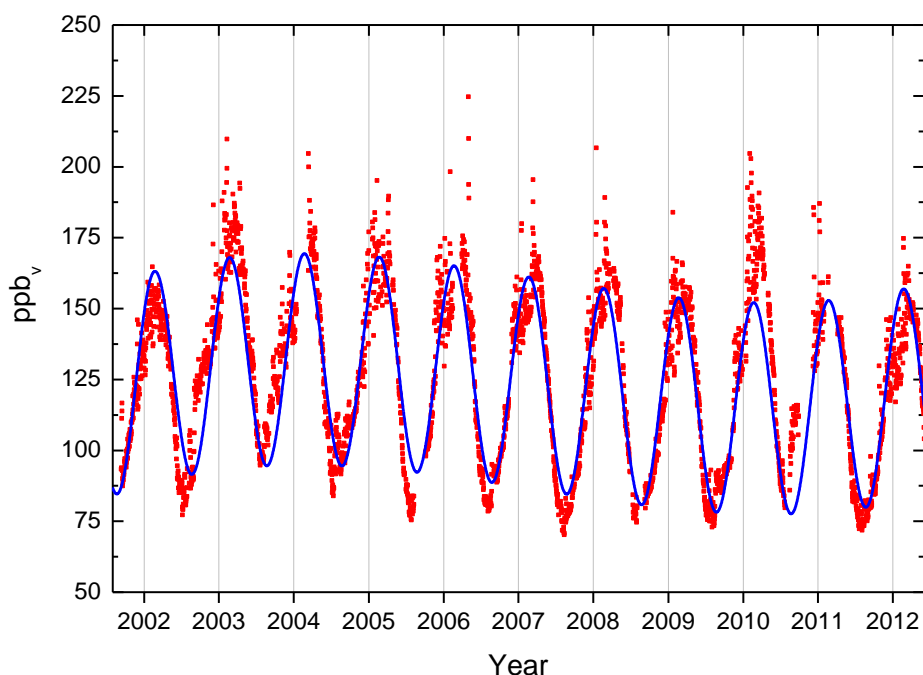


Figure 18: Observations of carbon monoxide (CO) from September 2001 to 31.12.2012 at the Zeppelin observatory. Red dots: daily averaged observed mixing ratios. The solid line is the modelled background mixing ratio.

The concentrations of CO show characteristic seasonal variations with large amplitudes in the Northern Hemisphere and small ones in the Southern Hemisphere. This seasonal cycle is driven by variations in OH concentration as a sink, emission by industries and biomass burning, and transportation on a large scale.

As for methane, the CO measurements for 2011 had lower variability and fewer episodes than most other years. The reasons for this are not clear, but it seems to be related to sources, and this was also evident for CH₄. In 2012 the measurements and variability was back to normal.

We calculated a trend at Zeppelin of -1.1 ppb per year for the period 2001-2012. The maximum daily average value in 2012 was observed on the 23th February and was 175 ppb. The maximum value is caused by transport of pollution from North West Russia as illustrated to the right in the figure.

CO is central to monitor as the sources of CO are numerous and complex and the level of this compound is important for the ozone and methane chemistry and levels in the atmosphere. The global levels of CO were increasing until the mid-1980s. Thereafter the levels have declined with an averaged global growth rate -0.9 ppb/year for the period from 1992 to 2001. The variability of the growth rates is large. High positive growth rates and subsequent high negative growth rates were observed at northern latitudes and southern low latitudes from 1997 to 1999.

The development of the annual means for the period 2001-2012 is presented in Figure 19, clearly illustrating a maximum in the year of 2003, and a decrease from 2003-2009.

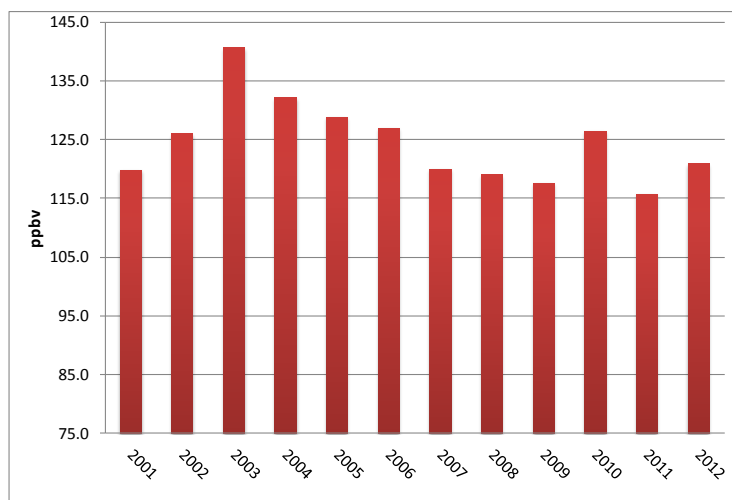


Figure 19: Development of the annual means of CO measured at the Zeppelin Observatory for the period 2001-2012.

In general the CO concentrations measured at Zeppelin show a decrease during the period 2003 to 2009, and 2011 has the lowest annual mean over the period investigated, 116 ppb. For 2010 a small increase is evident as well as in 2012.

The highest mixing ratio of CO ever observed at Zeppelin; is 217.2 ppb on the 2nd of May 2006. This peak values were due to transport of polluted air from lower latitudes; urban pollution (e.g. combustion of fossil fuel). CO is an excellent tracer for transport of smoke from fires (biomass burning, agricultural- or forest fires). The compound is very valuable in the interpretation of other variables at Zeppelin. Atmospheric CO sources are oxidation of various organic gases (volatile organic compounds, VOC) from sources as fossil fuel, biomass

burning, and also oxidation of methane is important. Additionally emissions from plants and ocean are important sources.

At NILU we wanted to study the influence of biomass burning on our measurements, both aerosols and greenhouse gases at Birkenes and Zeppelin more. This study combines satellite and ground based observations and is performed in a project funded by Norwegian Space Centre and the results so far are described in section 6.

4.2 Greenhouse gases with solely anthropogenic sources

All the gases presented in this chapter have solely anthropogenic sources. These are purely man-made greenhouse gases and are called CFCs, HCFCs, HFCs PFCs, SF₆ and halons and most of the gases did not exist in the atmosphere before the 20th century. All these gases except for SF₆ are halogenated hydrocarbons. Although the gases have much lower concentration levels than most of the natural gases mentioned in the previous section, they are strong infrared absorbers, many of them with extremely long atmospheric lifetimes resulting in high global warming potentials; see Table 1 on page 6. Together as a group, the gases contribute to around 11% to the overall global radiative forcing since 1750 (IPCC 2007).

Some of these gases are ozone depleting, and consequently regulated through the Montreal protocol. Additional chlorine and bromine from CFCs, HCFCs and halons added to the atmosphere contributes to the thinning of the ozone layer, allowing increased UV radiation to reach the earth's surface, with potential impact not only to human health and the environment, but to agricultural crops as well. In 1987 the Montreal Protocol was signed in order to reduce the production and use of these ozone-depleting substances (ODS) and the amount of ODS in the troposphere reached a maximum around 1995. The amount of most of the ODS in the troposphere is now declining slowly and one expects to be back to pre-1980 levels around year 2050. In the stratosphere the peak is reached somewhat later, around the year 2000, and observations until 2004 confirm that the level of stratospheric chlorine has not continued to increase (WMO, 2011).

The CFCs, consisting primarily of CFC-11, -12, and -113, accounted for -62% of total tropospheric Chlorine in 2004 and accounted for a decline of 9 ppt Chlorine from 2003-2004 (or nearly half of the total Chlorine decline in the troposphere over this period) (WMO, 2007).

There are two generations of substitutes for the CFCs, the main group of the ozone depleting substances. The first generation substitutes is now included in the Montreal protocol as they also influence the ozone layer. This comprises the components called HCFCs listed in Table 1 and Table 2. The second-generation substitutes, the HFCs, are included in the Kyoto protocol. The situation now is that the CFCs have started to decline, while their substitutes are increasing, and many of them have a steep increase.

4.2.1 Observations of Chlorofluorocarbons (CFCs) in the period 2001-2012

This section includes the results of the observations of the CFCs: CFC-11, CFC-12, CFC-113, CFC-115. These are the main ozone depleting gases, and the anthropogenic emissions started around 1930s and were restricted in the first Montreal protocol.

Figure 20 shows the daily averaged observed mixing ratios of these four CFCs. The current instrumentation is not in accordance with recommendations and criteria of AGAGE for measurements of CFCs and there are larger uncertainties in the observations of these compounds, see also Appendix I. As a result also the trends are connected with larger uncertainties. From September 2010 we have new and improved instrumentation installed at Zeppelin providing more accurate observations of these compounds. The higher precisions are clearly visualised in Figure 20.

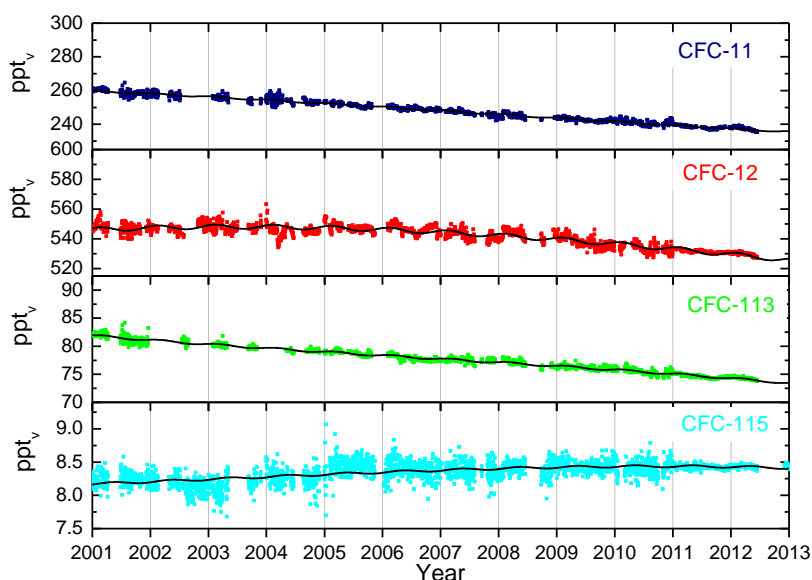


Figure 20: Daily averaged mixing ratios of the monitored CFCs: CFC-11 (dark blue), CFC-12 (red), CFC-113 (green) and CFC-115 (light blue) for the period 2001-2012 at the Zeppelin observatory. The solid lines are modelled background mixing ratio.

The main sources of these compounds were foam blowing, aerosol propellant, temperature control (refrigerators), solvent, and electronics industry. The highest production of the observed CFCs was around 1985 and maximum emissions were around 1987. The life times of the compounds is long as given in Table 1, and also the GWP due to the life time and strong infrared absorption properties is very high.

We have used the model described in Appendix I in the calculation of the annual trends, and changes in the trends. The trends per year for the substances CFC-11, CFC12 and CFC-113 are now all negative given in Table 2, and the changes in the trends are also negative indicating acceleration in the decline¹⁴. For the compound CFC-115 the trend is still slightly positive, +0.02 ppt/year, but the change in trend is negative and thus we expect the trend for to be negative in few years. In total the development of the CFC levels at the global background site Zeppelin is now very promising.

According to WMO (WMO, 2011) the global mean mixing ratios of CFC-11 are decreasing with approximately 2.0 ppt +/-0.01 ppt and CFC-113 are decreasing by approximately 0.7 ppt from 2007-2008. This is relatively close to our results at Zeppelin for CFC-113 for the period 2001-2012 (-0.7 ppt/yr for 2001-2011), and also for CFC-11 (2.1 ppt/year). The global mean reduction for CFC-12 was -2.2 ppt/year for 2007-2008. For Zeppelin there was a downward trend of 1.8 ppt/year over the period 2001-2012.

¹⁴ The current instrumentation is not in accordance with recommendations and criteria of AGAGE for measurements of the CFCs and there are larger uncertainties in the observations of this compound, see also Appendix I.

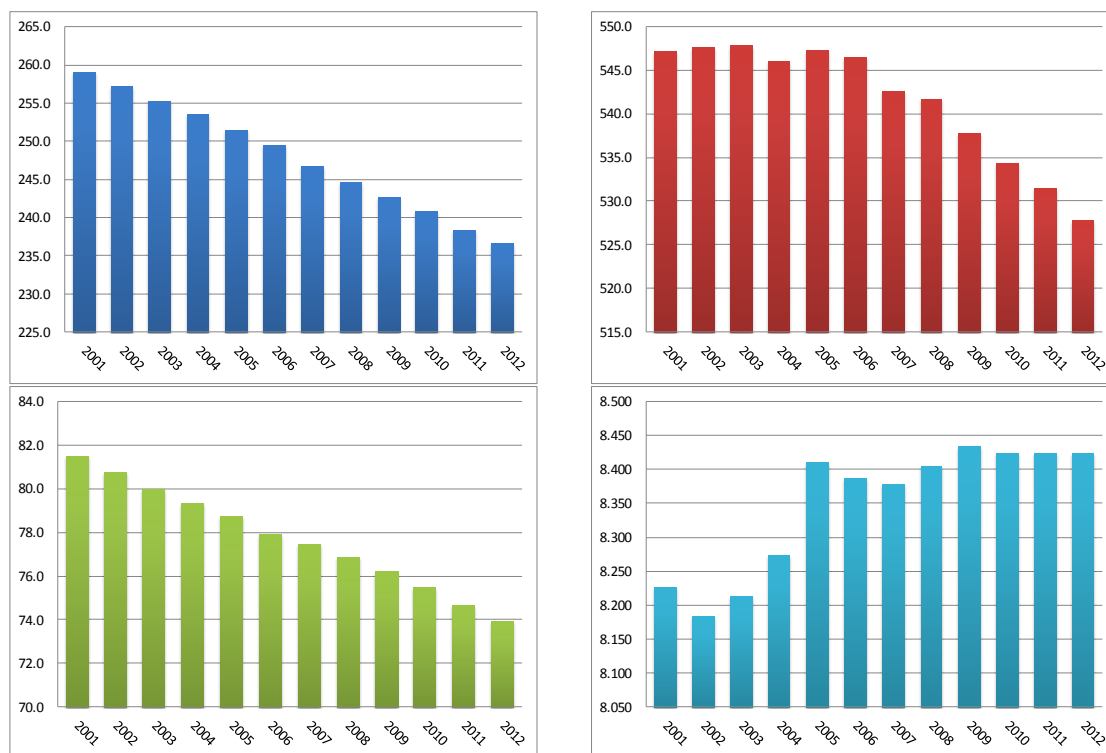


Figure 21: Development of the annual means all the observed CFCs at the Zeppelin Observatory for the period 2001-2012. Upper left panel: CFC-11, upper right panel: CFC-12, lower left panel: CFC-113, lower right panel: CFC-115. See Appendix I for data quality and uncertainty.

The development of the annual means for all the observed CFCs is shown in Figure 21. As described in Appendix I there is now a new instrument at Zeppelin giving improved and more accurate observations of CFCs. The old and new observations are harmonised as described in the appendix. CFC-12 (the red diagram) is the gas with the highest GWP of the CFCs, 10600, and the second highest of all gases observed at Zeppelin. This means that the warming potential of 1 kg emitted CFC-12 gas has 10600 times stronger warming effect than 1 kg emitted CO₂ gas. The global averaged atmospheric mixing ratio of CFC-12 has been decreasing at a rate of 0.5% over the year 2004-2008 (WMO, 2011). This fits well with our observations as illustrated in Figure 21 as CFC-12 has the maximum in 2003-2004. There is a clear reduction the last years of -19.5 ppt since the maximum year 2005.

4.2.2 Observations of Hydrochlorofluorocarbons (HCFCs) in the period 2001-2012

This section includes the observations of the following components: HCFC-22, HCFC-141b and HCFC-142b. These are all first generation replacement gases for the CFCs and their lifetimes are rather long. This means that they have potentially strong warming effects, depending on their concentrations and absorption properties; their GWPs are high (see Table 1). The compound HCFC-142b has the highest GWP, and the warming potential is 2400 times stronger than CO₂, per kg gas emitted. These gases do also contain chlorine, and thus are contributing to the depletion of the ozone layer. The HCFCs accounted for 7.5% of the total tropospheric chlorine in 2004 versus 6% of the total in 2004 (WMO, 2011).

The daily averaged observations of these gases are shown in Figure 22 for the period 2001-2012¹⁴. As a result also the trends are connected with larger uncertainties. From September 2010 we have new and improved instrumentation installed at Zeppelin providing better measurements of these compounds with considerable higher precision.

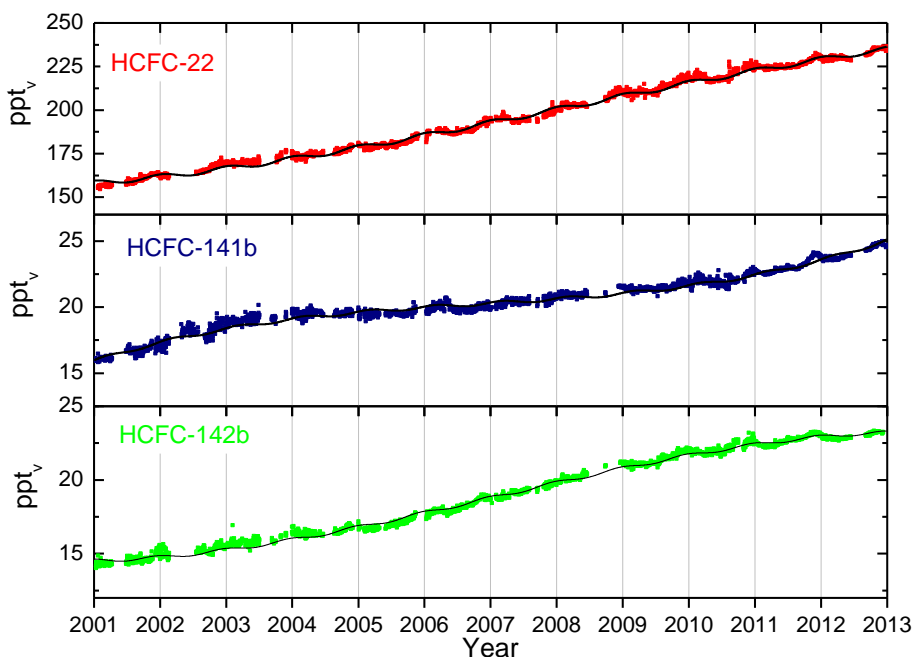


Figure 22: Daily average mixing ratios of the monitored HCFCs: HCFC-22 (red), HCFC-141b (dark blue) HCFC-142b¹⁴ (green) for the period 2001-2012 at the Zeppelin observatory. The solid lines are modelled background mixing ratio.

The trends per year for the compounds HCFC-22, HCFC-141b and HCFC-142b are all positive, and HCFC-22 has the largest change as given in Table 2. HCFC-22 is the most abundant of the HCFCs and is currently increasing at a rate of 6.9 ppt/year over the period 2001-2012. In comparison, the global mean increase for 2007-2008 was approx. 8 ppt according to WMO, (WMO, 2011). Our result for Zeppelin showed an increase of 8.5 ppt for 2007-2008, in close agreement with the annual mean. The mixing ratios of HCFC-141b and HCFC-142b have increased by 0.6 ppt/yr and 0.8 ppt/year, respectively over the same period.

It is worth mentioning that the changes in trends close to zero for HCFC-22 and HCFC-141b, indicating that the yearly increases in the concentrations is stable. The rates of increase for three of these HCFC substances are stronger than or comparable to the scenarios projected in the Ozone Assessment 2006 (WMO, 2011).

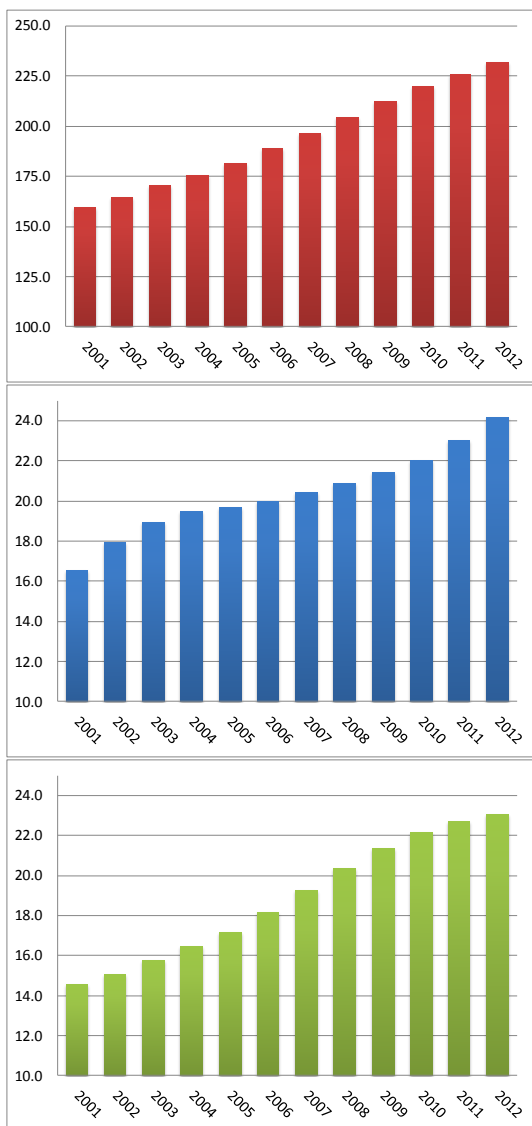


Figure 23 shows the annual means for the full period for the three compounds, clearly illustrating the development; a considerable increase. The main sources of these gases are temperature control (refrigerants), foam blowing and solvents, as for the CFCs, which they suppose to replace. All these gases are regulated through the Montreal protocol as they all contain Chlorine. The use of the gases is now frozen, but they are not completely phased out. With lifetimes in the order of 10-20 years it is central to monitor the levels in the future as they have an influence both on the ozone layer, and are strong climate gases.

Figure 23: Development of the annual means the observed HCFCs at the Zeppelin Observatory for the period 2001-2012. Red: HCFC-22, Blue: HCFC-141b, and green: HCFC-142b.

4.2.3 Observations of Hydrofluorocarbons (HFCs) in the period 2001-2012

The substances called HFCs are the so called second generation replacements of CFCs, which means that they are considered as better alternatives to the CFCs with respect to the ozone layer than HCFCs. This sub-section includes the following components: HFC-125, HFC-134a, HFC-152a with lifetimes in the order of 1.5-29 years. These substances do not contain chlorine thus they do not have a direct influence on the ozone layer, but they are infrared absorbers and contribute to the global warming.

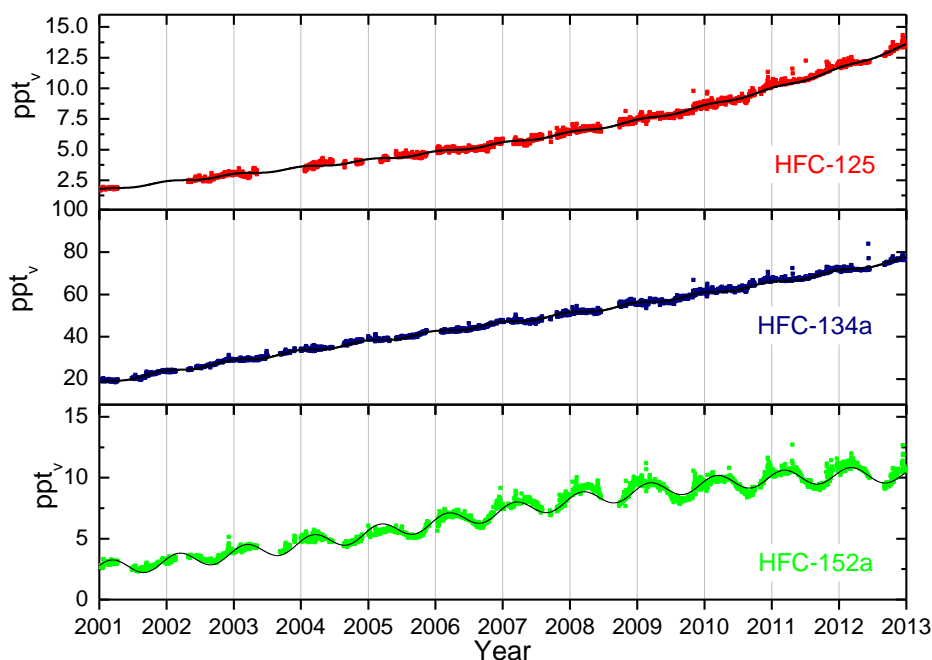


Figure 24: Daily average concentrations of the monitored HFCs: HFC-125 (red), HFC-134a (dark blue), HFC-152a (green) for the period 2001-2012 at the Zeppelin observatory. The solid lines are modelled background mixing ratio.

HFC-152a has the shortest lifetime and is mainly destroyed in the lowest part of the atmosphere by photolysis and reactions with OH. The seasonal cycle in the observed mixing ratios of these substances is caused by the variation in the incoming solar radiation and is clearly visible in the time series shown in Figure 24 for HFC-152a.

Even if these compounds are better alternatives for the protection of the ozone layer as they do not contain chlorine or bromine, they are still problematic as they are highly potent greenhouse gases. 1 kg of the gas HFC-125 is as much as 3400 times more powerful greenhouse gas than CO₂. However, still their mixing ratios are rather low, but the background mixing ratios are increasing steeply as our results show. This is also clearly illustrated in Figure 25 showing the development of the annual means. The gases are continuously increasing at a constant rate per year as earlier.

The three main HFCs are HFC-23 (measured at Zeppelin from 2010, but not a part of the national monitoring program), HFC-134a and HFC-152a. HFC-134a is the most widely used refrigerant (temperature control), and also in air conditioners in cars. Since 1990, when it was almost undetectable in the atmosphere, concentrations of HFC-134a have risen massively. For the period 2001-2011 we find an annual increase per year of 4.6 ppt, which leaves this compound as the one with the second highest change per year of the all the halocarbons measured at Zeppelin. The mixing ratios of HFC-125, HFC-134a and HFC-152a have increased by as much as 522%, 253% and 267% respectively since 2001. This is a rapid average increase in the interval from ~20-45 % per year. The last ozone Assessment report (WMO, 2011) does not include these compounds as they are not affecting the ozone layer directly.

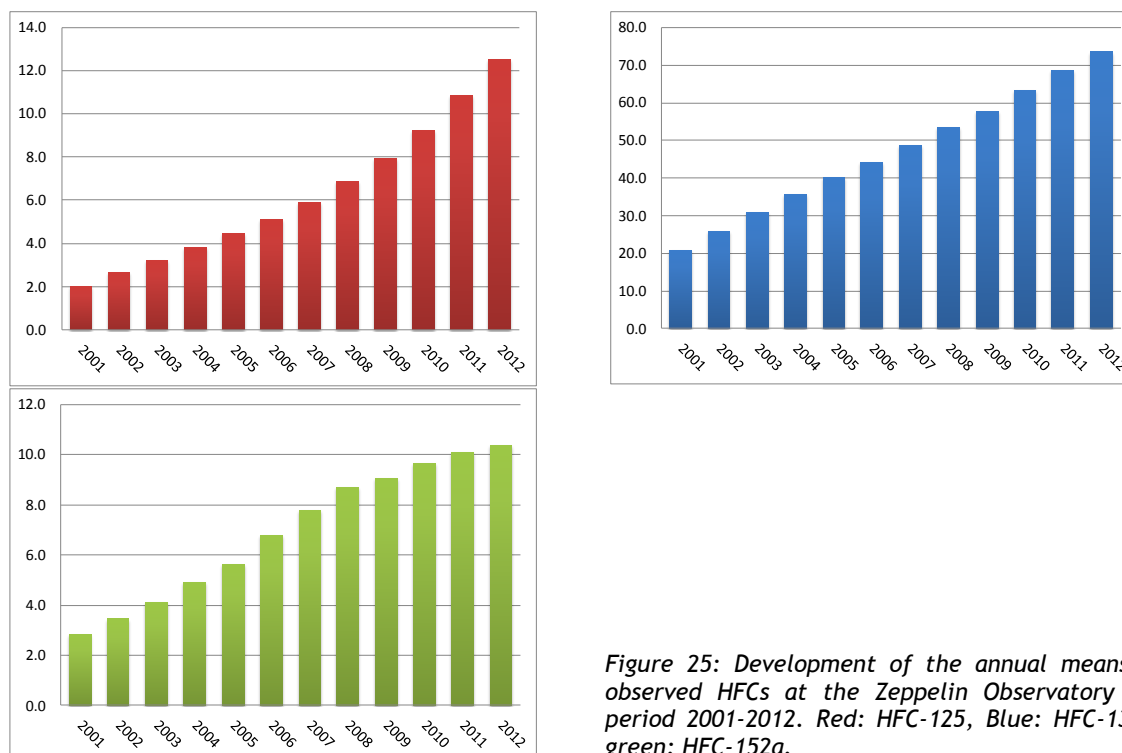


Figure 25: Development of the annual means of the observed HFCs at the Zeppelin Observatory for the period 2001-2012. Red: HFC-125, Blue: HFC-134a, and green: HFC-152a.

Due to the large increase in these compounds, it is relevant to calculate the radiative forcing of these observed changes. Based on the assumption that these changes are homogeneous distributed and the same at all locations (constant geographical distribution) we find that the total radiative forcing for these three gases since the start of the emissions is 0.016 W m^{-2} (using the forcing efficiency from Forster et al., 2007). Thus the contribution from the recent man made emissions of these gases is still considered as small. This is explained by the (still) low mixing ratios of the compounds. It is important to follow the development of these gases in the future due to the rapid annual growth.

4.2.4 Observations of halons in the period 2001-2012

Halons include the following components: H-1301, H-1211. These greenhouse gases contain bromine, also contributing to the depletion of the ozone layer. Actually, bromine is even more effective in destroying ozone than chlorine. The halons are regulated through the Montreal protocol, and are now phased out. The main source of these substances was fire extinguishers. Figure 26 presents the daily average concentrations of the monitored halons at Zeppelin¹⁴.

By use of the model described in Appendix I we have calculated the annual trends, and changes in trends, given in Table 2. The trends for the period 2001-2012 shows a small increase for both substances in total, with a very small reduction in the rates indicating that the trend is expected to be lower the next years (if there are no abrupt changes in sources and sinks).

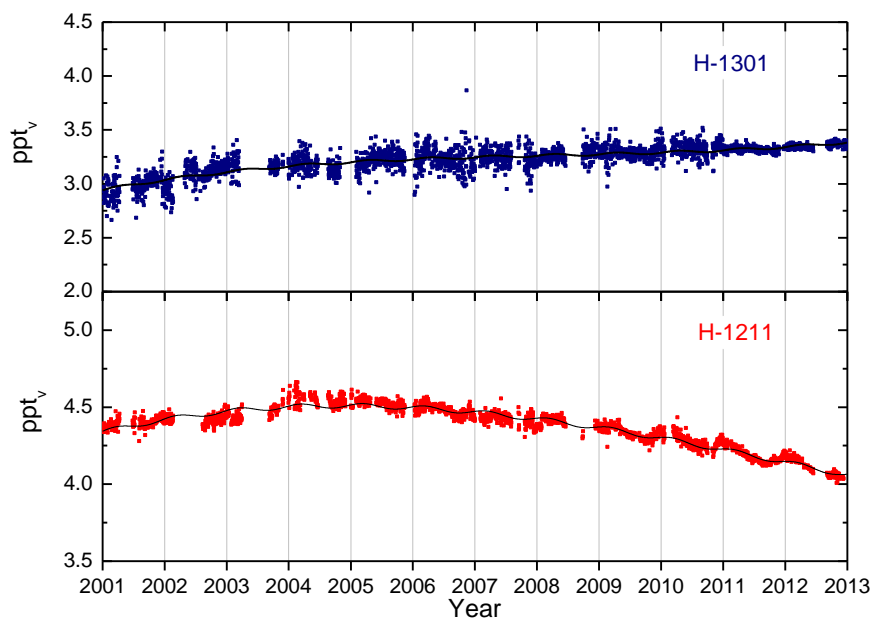


Figure 26: Daily average concentrations of the monitored halons: H-1301 (blue in the upper panel) and H-1211⁵ (Red in the lower panel) for the period 2001-2012 at the Zeppelin observatory. The solid lines are modelled background mixing ratio.

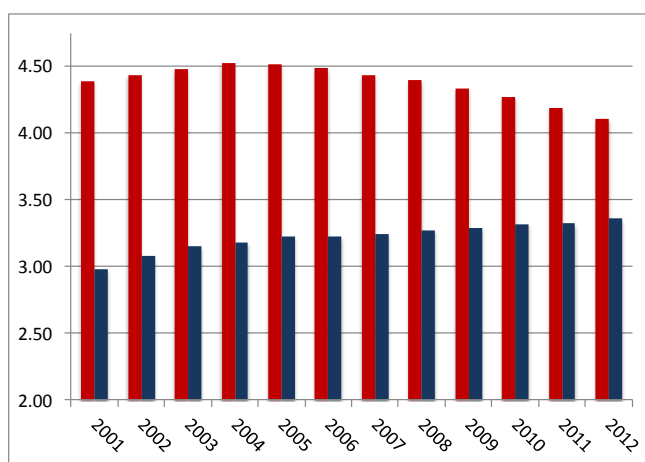


Figure 27: Development of the annual means the observed Halons at the Zeppelin Observatory for the period 2001-2012. Blue: Halon-1301, Red: H-1211.

The development of the annual means are shown in the Figure to the left, and the mixing ratios are relatively stable over the measured period explained by low emissions and relatively long lifetimes (11 years for H-1211 and 65 years for H-1301). However, a clear reduction is evident in Halon-1211, with the shortest lifetime. According to the last Ozone Assessment (WMO, 2011) the total stratospheric Bromine concentration is no longer increasing and Bromine from halons stopped increasing during the period 2005-2008. H-1211 decreased for the first time in this period, while H-1301 continued to increase, but at a slower rate than previously. The global atmospheric decrease in H-1211 was ~ 0.04 ppt in average in 2007-2008 and for H-1301 the increase was around ~ 1.2 ppt (WMO, 2011). Our observations of H-1301 in the Arctic region showed approximately no change from 2007-2008, but a decrease for H-1211 since 2004, also in 2007-2008.

4.2.5 Observations of other chlorinated hydrocarbons in the period 2001-2012

This section includes observations of the components: trichloromethane (also called methyl chloroform, CH_3CCl_3), dichloromethane (CH_2Cl_2), chloroform (CHCl_3), trichloroethylen (CHClCCl_2), perchloroethylene (CCl_2CCl_2). The main sources of all these substances are solvents. Note that Chloroform also has natural sources and the largest single source being in offshore seawater. The daily averaged concentrations are shown in Figure 28.

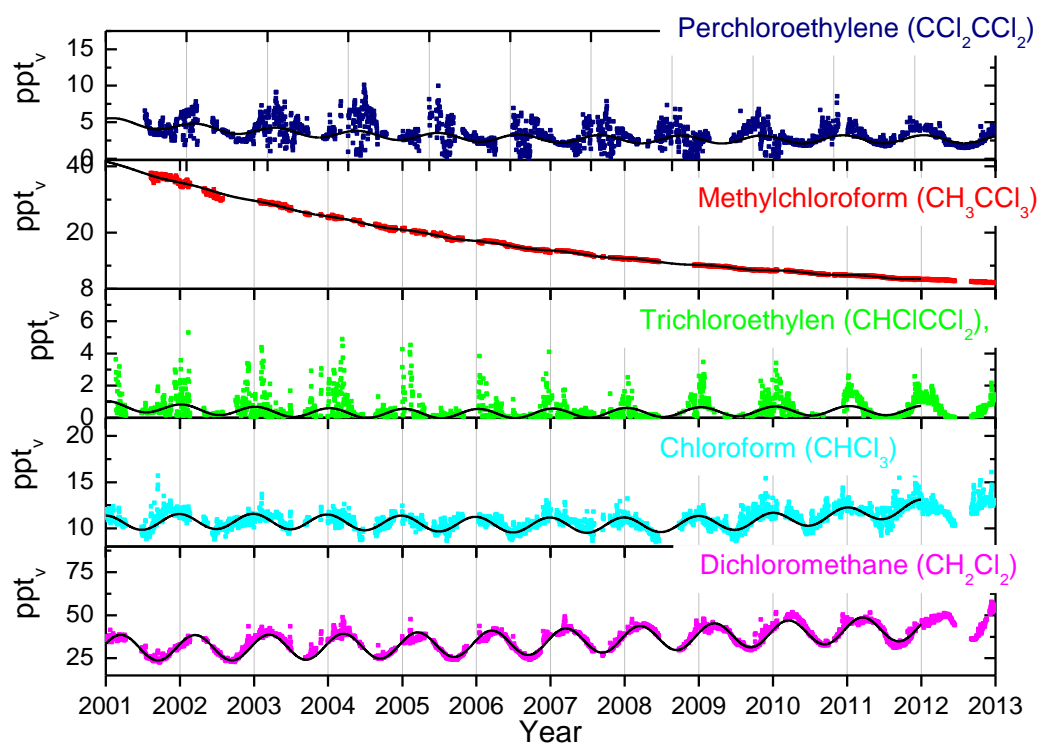


Figure 28: Daily average concentrations chlorinated hydrocarbons: From the upper panel: perchloroethylene (dark blue) methylchloroform (red), trichloroethylen (green), chloroform (light blue) and dichloromethane (pink) for the period 2001-2012 at the Zeppelin observatory. The solid lines are the modelled background mixing ratio.

Methylchloroform (CH_3CCl_3) has continued to decrease, and accounted only for 1% of the total tropospheric Chlorine in 2008, a reduction from a mean contribution of 10% in the 1980s (WMO, 2011). Globally averaged surface mixing ratios were around 10.5 ppt in 2008 (WMO, 2011) versus 22 ppt in 2004 (WMO, 2007). Our measurements at Zeppelin show that the component has further decreased to low levels, 6.5 ppt, a reduction of 83% since 2001.



It is worth noting the recent increase in trichloroethylene (green), chloroform (blue). A considerable increase in chloroform is evident at Zeppelin the last years (16% since 2008), and also at other sites (e.g. Mauna Loa at Hawaii and Barrow in Alaska). This is not expected and the reason for this is not yet clear. Large seasonal variations are observed for this component as the lifetime is only 1 year (see Figure 28).

The concentration of trichloroethylene is very low, and uncertainties and missing data might explain at least part of the variations.

Figure 29: Annual means of the chlorinated hydrocarbons. From upper panel: perchloroethylene (grey), trichloromethane (red), trichloroethylene (green), chloroform (blue) and dichloromethane (violet) for the period 2001-2012.

4.2.6 Perfluorinated compounds

The only perfluorinated compound measured at Zeppelin is sulphurhexafluoride, SF₆. This is an extremely strong greenhouse gas emitted to the atmosphere mainly from the production of magnesium and electronics industry. The atmospheric lifetime of this compound is as much as 3200 years, and the global warming potential is 22200, which means that the emission of 1 kg of this gas has a warming potential which is 22200 times stronger than 1 kg emitted CO₂.

The other perfluorinated compounds are also very powerful greenhouse gases thus NILU has extended the monitoring with Carbon tetrafluoride (CF₄) and hexafluoroethane (C₂F₆) from 2010, as we have new and improved instrumentation installed at Zeppelin. However, these compounds are not a part of the national monitoring programme.

The current instrumentation is not the best suited for measurements of SF₆ thus there are larger uncertainties for this compound's mixing ratios than for most of the other compounds reported.¹⁴ The daily averaged concentration of SF₆ is presented in Figure 30. The compound is increasing with a rate of 0.26 ppt/year, and has increased by more than 50% since the start of our measurements in 2001. Note that the variations through the year are not due to seasonal variations, but rather to instrumental adjustments, and also the improvement with the new instrumentation in 2010.

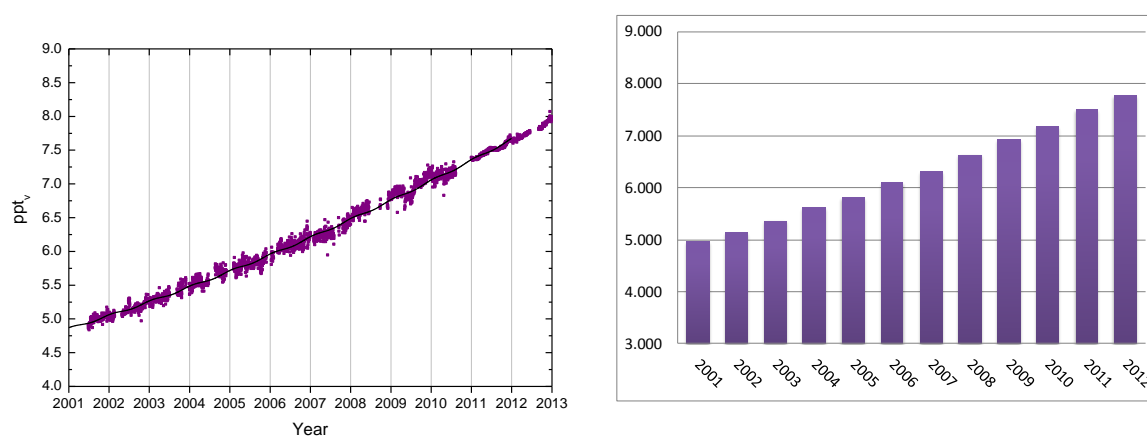


Figure 30: Daily average concentrations of SF₆ for the period 2001-2012¹⁴ to the left, and the development of the annual mean concentrations in the right panel.

5. Observations of CO₂ and CH₄ at the Birkenes Observatory in Aust-Agder

In 2009 NILU upgraded and extended the observational activity at the Birkenes Observatory in Aust-Agder. Until 2009 the only Norwegian site measuring long-lived greenhouse gases (LLGHG) greenhouse gases was Zeppelin, but from mid May 2009 there are also continues measurements of CO₂ and CH₄ at Birkenes. The results from the start and including 2012 are presented below.

The upper panel shows the daily (black line) and hourly (grey line) variations in CO₂. It is clear that the variations are largest during the summer months. In this period, there is a clear diurnal variation with high values during the night and lower values during daytime. This is mainly due to changes between plant photosynthesis and respiration, but also the meteorological situation during summer contributes to larger variations in the compound. In the lower panel is the CH₄ measurements shown. The diurnal variation for this compound is smaller, but the variations are still largest during summer and early autumn. In addition to the diurnal variations, there are also episodes with higher levels of both components due to transport of pollution from various regions. In general, there are high levels when the meteorological situation results in transport from Central Europe.

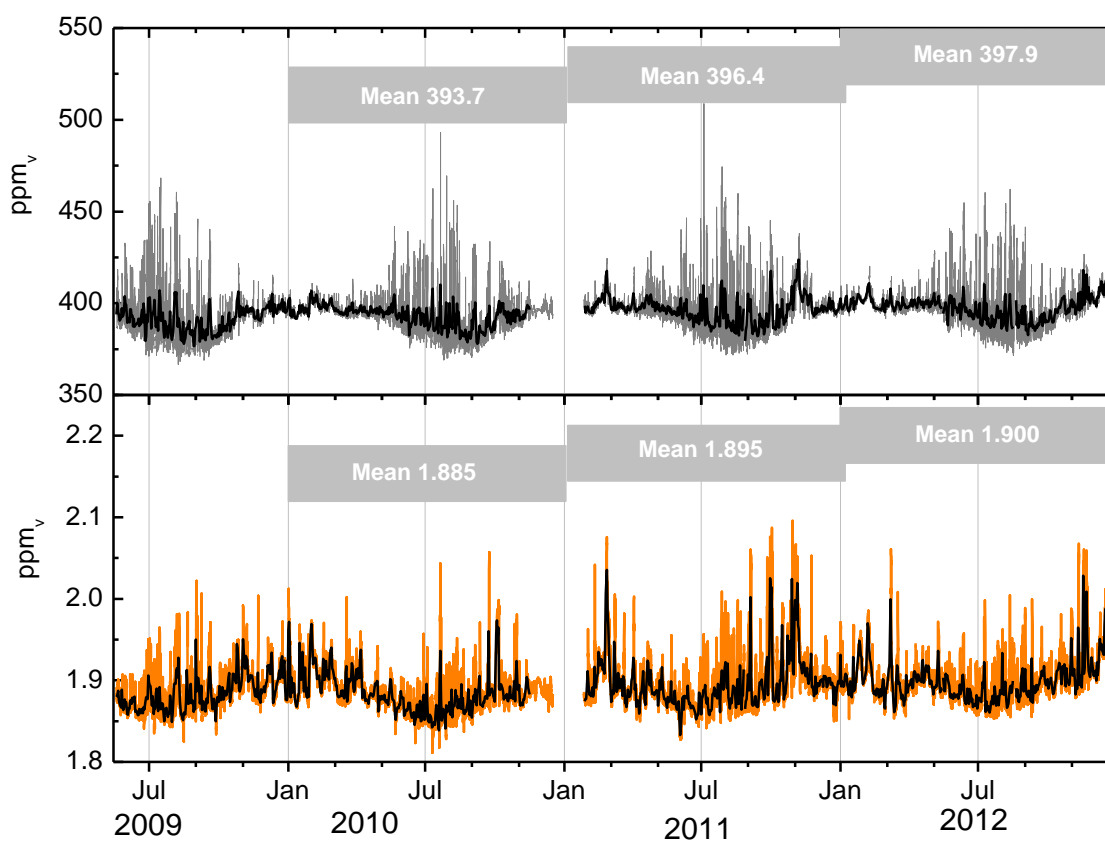


Figure 31: Greenhouse gas measurements at Birkenes Observatory from 19. May 2009 to 31. December 2012. Upper panel: CO₂ measurements, grey line: hourly mean, black line: daily mean. Lower panel: CH₄ from Birkenes, orange line: hourly mean, black line: daily mean. The grey shaded areas show the annual mean for the years 2010 to 2012, for both components.

Generally, the largest variability in CO₂ measurements are during summer and particularly warm periods, however the maximum daily mean value for CO₂ was 418 ppm during night and morning 17. November. The maximum value of CH₄ was on the same day, as high as 2.028 ppm. The highest monthly mean values are during autumn and winter months for both components.

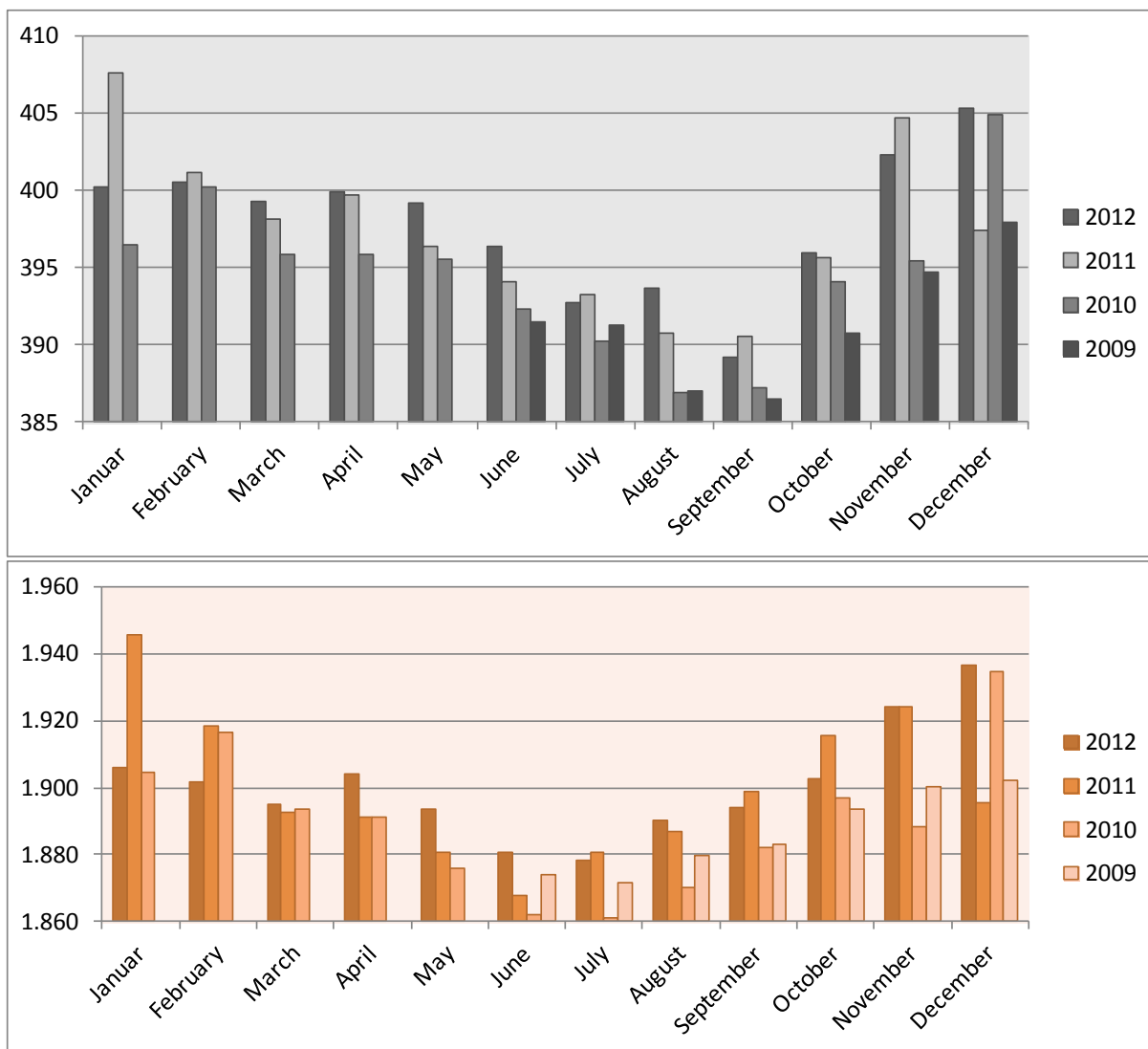


Figure 32: Monthly mean variations for CO₂ (upper panel) and CH₄ (lower panel) at Birkenes Observatory for the periode June 2009- December 2012.

Figure 32 shows the monthly mean variations for both CO₂ and CH₄ at Birkenes. There is a clear minimum in the summer months and a maximum in the fall/winter as expected, and winter 2012 is the period with highest values, together with January 2011, which was the highest monthly mean for both components.

6. Analysis of CO from satellite observations to support ground based measurements

CO (carbon monoxide) is a component of particular importance as tracer for biomass burning, and knowledge of this compound is important for the understanding of sources and levels of both aerosols (see chapter 7) and gases like CH₄ and CO₂. Ground based monitoring of CO is lacking in the mainland of Norway; it is only available at Svalbard, far from fire sources and industrial pollution. Based on a project financed by The Norwegian Space Centre (Norsk Romsenter (NRS), <http://www.romsenter.no/>) we are now in a position where we can support the national monitoring of greenhouse gases and aerosols by exploring and utilize satellite observations of CO for 2012. Based on the outcome of the NRS funded project *SatMonAir (2012)*, a new project named SatMonAir II started in January 2013 and lasted to December 2013, and NRS is highly acknowledged for their support.

The goal of the work in SatMonAir II and towards the national monitoring is twofold; set up and maintain an alert system to detect fires and monitor possible influence on the observations in near real time, and secondly, support the analysis of aerosols (particularly the absorbing aerosol) and CO₂ and CH₄ monitored at the Zeppelin and Birkenes Observatories.

Results from the work in work package 2 of SatMonAir II (*Carbon Monoxide (CO) in Scandinavia and Polar regions: The use of satellite data as supplement for national monitoring program and EMEP*) are included in the current report.

Monthly means and orbit/swat data from CO products from the MOPITT (*Measurements of Pollution in the Troposphere*) and SCIAMACHY satellites are explored in detail for 2003-2012, currently with focus on 2012. The availability of data in time and space does in some cases not cover the region or the years of interest, and while investigating the available products in detail, we discovered that the routines for searching, online plotting and download of data are not straight forward. Not all the EO CO products available online on the web for visualization and download are well suited for our purpose. Our conclusion in SatMonAir II is that the MOPITT monthly mean CO product is suitable for the work on studying the long term trends in CO, and thus this product will be used in further trend analyses. MOPITT swat data and gridded daily mean products will be used as supplementary products for monitoring of in situ NRT data for detecting episodes of long transport into Zeppelin and Birkenes Observatories (see below).

An example of the use of the MOPITT gridded monthly mean is shown in Figure 33. The satellite CO product shows good agreement with the in situ data, but due to poor data coverage in space and time for the Arctic areas, we only recommend to use satellite products as a supplement for ground based in situ monitoring.

Our conclusion in SatMonAir II is that the MOPITT monthly mean CO product is a suitable product to try to use to look at long-term trends in CO.

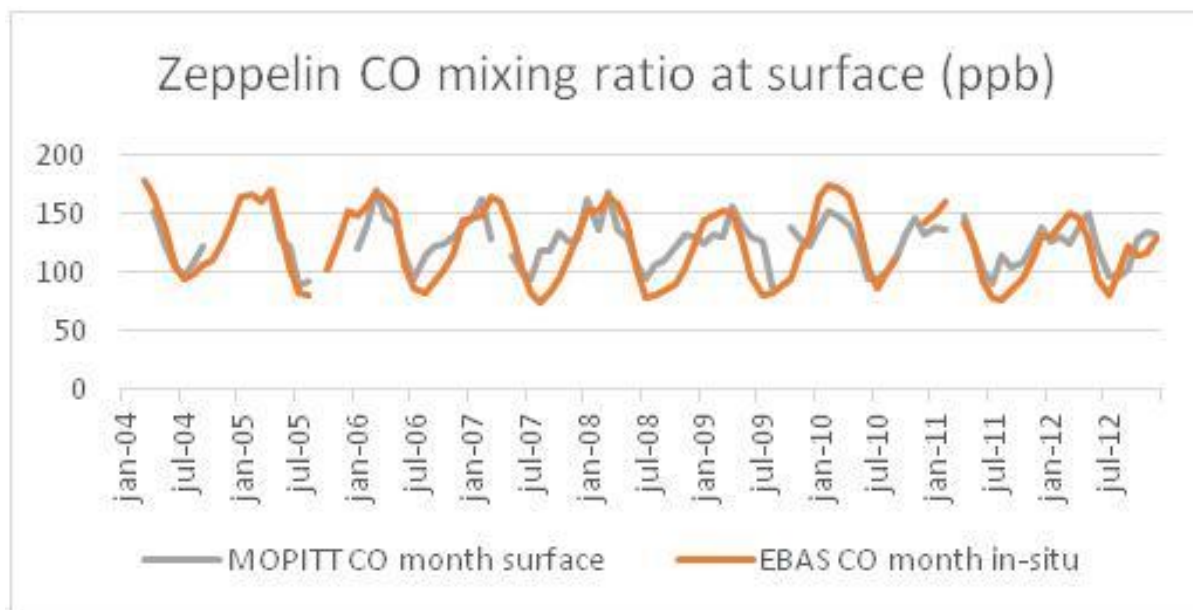


Figure 33: Time series of CO from in-situ measurements at Zeppelin Observatory (orange line) overloaded the MOPITT monthly mean surface product from LARC NASA (grey line).

In SatMonAir (2012) shown in the report from last year, we set up and demonstrated a tool for monitoring the number and geographical distribution of fires in the Eastern Europe and Russian areas in the spring, in combination with observing the trajectories and the online NRT (near-real-time) in-situ CO data from the Zeppelin Observatory. Information on the number of fires in our pre-defined area is provided as an e-mail alert system from FIRMS (Fire Information for Resource Management System) <http://earthdata.nasa.gov/data/near-real-time-data/firms>. This SatMonAir monitoring tool is relevant for detecting episodes of long-range transport of aerosols to Norway and Scandinavia. The system was not running for the full year of 2012, but for a first test period in spring 2012 no major episodes of long-range transport of aerosols to our target regions were detected. The system has been in operation in 2013 and is planned operational also for 2014.

New in the 2013 contract *SatMonAir II* is that we also introduce comparison with the directly overpass (swat) data from MOPITT.

Figure 34 gives examples of plots/products included in the SatMonAir transport monitoring tool.

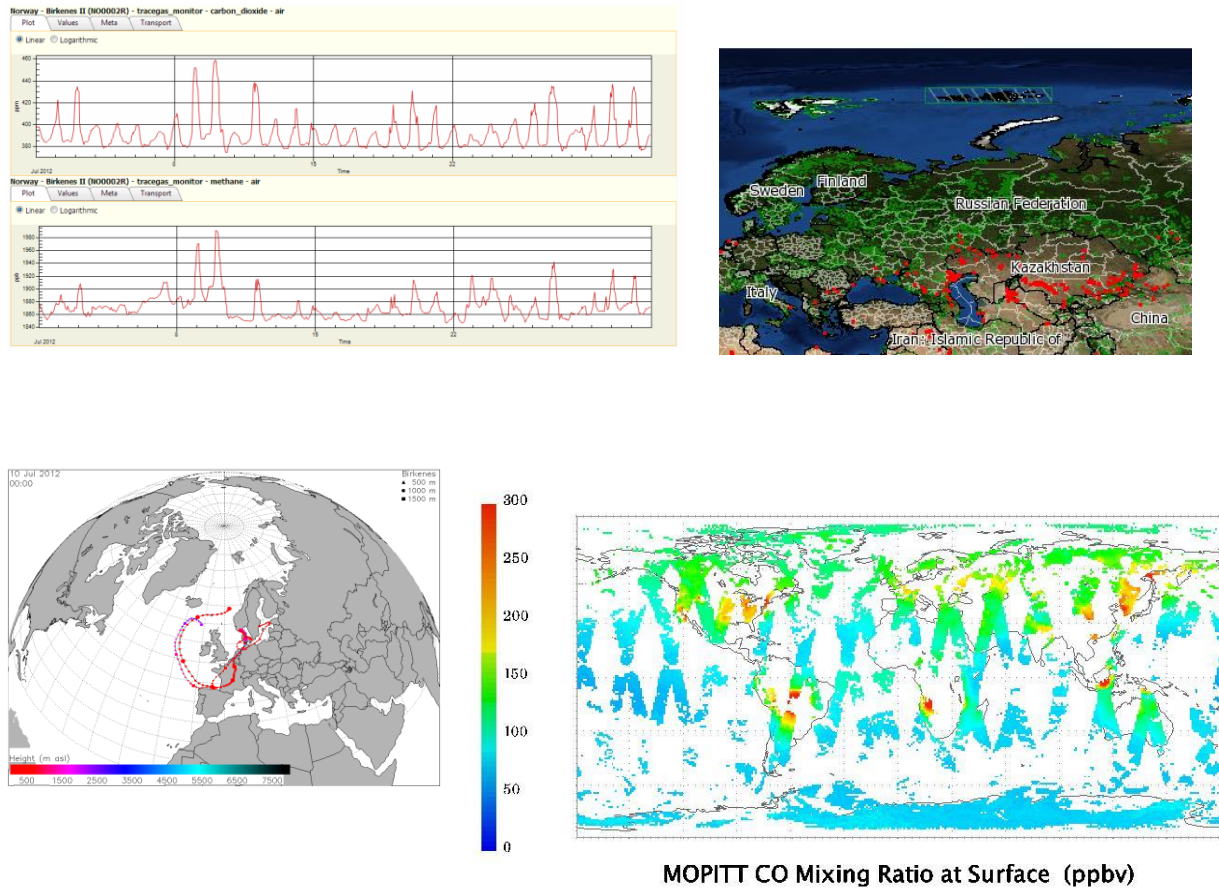


Figure 34: Examples of plots and products used in the SatMonAir monitoring tool for detecting long range transport; NRT in-situ data from Birkenes (top left), FIRMS fire product (top right), FLEXTRA trajectories (bottom left) and MOPITT swat data (bottom right).

7. Aerosols and climate: Observations from Zeppelin and Birkenes Observatories

Atmospheric aerosol influences climate by scattering incoming visible solar radiation back into space before it can reach the ground, be absorbed there and warm the earth surface. This so called direct aerosol climate forcing is mostly cooling, but can be moderated if the aerosol itself absorbs solar radiation, e.g. if it consists partly of light absorbing carbon or light absorbing minerals. In this case, the aerosol warms the surrounding atmosphere, the so-called semi-direct effect. Atmospheric aerosol particles also affect the reflectivity and lifetime of clouds, which is termed the indirect aerosol climate effect. Here as well, the effect can be cooling as well as warming for climate, but in most cases, the cloud reflectivity and lifetime are increased, leading again to a cooling effect.

This reporting period has been characterised by the publication of the 5th assessment report of the UN Intergovernmental Panel on Climate Change (IPCC 2013). Only the summary for policy makers (SPM) is available at this point, and the most important conclusions here is put into the context of the Norwegian climate monitoring programme and the results obtained here:

- The radiative forcing due to aerosol-radiation interactions (including adjustments of cloud reflectivity and lifetime) is quantified to -0.9 W/m^2 , with an uncertainty range of $-1.9 - -0.1 \text{ W/m}^2$ (IPCC, 2013, SPM). This also includes the direct interaction of aerosol particles and radiation, which has a mostly cooling effect, but may also be warming, e.g. for black carbon.
- IPCC AR5 has high confidence in stating that atmospheric aerosol has in the past offset a significant fraction of greenhouse gas radiative warming, although the magnitude is connected with uncertainty. Due to the decline of aerosol concentrations as reported in Tørseth et al (2012), Collaud Coen et al., (2013), and Asmi et al., (2013), the total anthropogenic radiative forcing will be even larger in the future. Uncertainties in assessing aerosol climate forcing hamper the attribution of changes in the climate system.
- IPCC AR5 mentions progress since AR4 concerning observations of climate relevant aerosol properties such as particle size distribution, particle hygroscopicity, chemical composition, mixing state, optical and cloud nucleation properties. This includes the parameters covered by the Norwegian climate monitoring programme, and underlines the importance of these observations. IPCC AR5 also mentions a lack of long time series on these parameters and stresses that existing time series need to be continued for maximising their informative value.
- IPCC AR5 stresses that the aerosol radiative forcing estimate is less negative than the one given in IPCC AR4 due to a re-evaluation of aerosol absorption. This conclusion is largely based on an assessment of black carbon (BC) ¹⁵ radiative forcing (Bond et al., 2013) (for a terminology of BC, see Petzold et al., 2013). The Bond et al., (2013) study is very comprehensive, including uncertainty range of BC radiative forcing, concerns have been raised orally on several occasions in scientific forums on the best estimate of BC radiative forcing given in this study. Bond et al., (2013), contains one BC radiative forcing assessment of $+0.24 \text{ W/m}^2$ based on ground-station measurements of aerosol absorption which have a known accuracy, and one assessment of $+0.71 \text{ W/m}^2$ based on data retrieved from ground-based remote sensing of the whole atmospheric column, which have an unknown accuracy. Yet, the latter number is given as best estimate. If the lower number for the BC radiative forcing was true, the potential for mitigating climate change by regulating BC emissions would be greatly reduced. This highlights the importance of ground-based in situ measurements of aerosol absorption of known accuracy, which are included in the Norwegian climate monitoring programme but lacking in many regions around the globe.
- In the chapter on key uncertainties in drivers of climate change, IPCC AR5 states: “Uncertainties in aerosol-cloud interactions and the associated radiative forcing remain large. As a result, uncertainties in aerosol forcing remain the dominant contributor to the overall uncertainty in net anthropogenic forcing, despite a better understanding of some of the relevant atmospheric processes and the availability of global satellite monitoring”. The respective ground-station observations, measurements of the concentration of cloud condensation nuclei or their size distribution, are now in place in Norway, but not covered by Norwegian climate monitoring.

¹⁵ The term “black carbon” (BC) is used here following a terminology paper drafted by the WMO Global Atmosphere Watch Scientific Advisory Group for aerosol. Black carbon is defined by 5 simultaneous properties: 1) high fraction of sp^2 -bonded carbon; 2) aggregate of carbon spherules; 3) thermally refractory up to 4000 K; 4) hydrophobic; 5) strong broadband absorption of visible light. There exists no measurement principle that is sensitive to all these properties at once, therefore no instrument that is sensitive to BC and only to BC. Only BC properties can be measured unambiguously, such as the absorption coefficient (using the broadband light absorptivity) or the elemental carbon (EC) concentration (using thermal refractiveness and carbonic composition).

7.1 Observations of climate relevant aerosol properties: recent developments in Norway and internationally

Due to hosting both, the data centre of the European Monitoring and Evaluation Programme (EMEP) and the WMO Global Atmosphere Watch (GAW) World Data Centre for Aerosol (WDCA), NILU has a position connecting the community for measuring air quality and climate relevant atmospheric aerosol properties with the community using this data to constrain models for assessing and predicting the aerosol climate effects. This community is represented by the AeroCom project, an initiative for comparing these models among each other and with various data sources, which is now conveniently hosted by the Norwegian Meteorological Institute. While the year 2012 was governed by contributions to publications feeding into the 5th IPCC assessment report, 2013 was characterised by more ordinary research activities in understanding the atmospheric aerosol life cycle. It is important to highlight and mention that NILU's work in hosting the WMO GAW World Data Centre for Aerosol, among many other synergy effects, ensures a rather efficient dissemination of the data on atmospheric aerosol properties collected within the Norwegian climate monitoring programme, and increases its visibility. The already close collaboration between the EMEP and GAW WDCA data centres at NILU and the AeroCom aerosol climate model initiative at the Norwegian Meteorological Institute will be intensified further by a common project newly approved by the Norwegian Research Council. This collaboration will strengthen Norway's already good position in climate research and advance the understanding of the aerosol's role in the climate system.

Table 3: Aerosol observations at Zeppelin, Birkenes and Troll Observatory following the GAW recommendations. Parameters in green are funded by the Norwegian Environment Agency and included in this report.

	Zeppelin/Ny-Ålesund	Birkenes	Troll
Particle Number Size Distribution (fundamental to all aerosol processes)	fine mode ($0.01 \mu\text{m} < D_p < 0.8 \mu\text{m}$) in collaboration with Stockholm University	fine and coarse mode ($0.01 \mu\text{m} < D_p < 10 \mu\text{m}$)	fine mode ($0.03 \mu\text{m} < D_p < 0.8 \mu\text{m}$)
Aerosol Scattering Coefficient (addressing direct climate effect)	spectral at 450, 550, 700 nm, in collaboration with Stockholm University	spectral at 450, 550, 700 nm	spectral at 450, 550, 700 nm
Aerosol Absorption Coefficient (addressing direct climate effect)	single wavelength at 525 nm, in collaboration with Stockholm University	single wavelength (525 nm) and spectral	single wavelength at 525 nm
Aerosol Optical Depth (addressing direct climate effect)	spectral at 368, 412, 500, 862 nm in collaboration with WORCC	spectral at 340, 380, 440, 500, 675, 870, 1020, 1640 nm, in collaboration with Univ. Valladolid	spectral at 368, 412, 500, 862 nm
Aerosol Chemical Composition (addressing direct + indirect climate effect)	main components (ion chromatography), heavy metals (inductively-coupled-plasma mass-spectrometry)	main components (ion chromatography), heavy metals (inductively-coupled-plasma mass-spectrometry)	main components (ion chromatography), discontinued from 2011 due to local contamination.
Particle Mass Concentration	---	PM _{2.5} , PM ₁₀	PM ₁₀ , discontinued from 2011 due to local contamination
Cloud Condensation Nuclei (addressing indirect climate effect)	size integrated number concentration at variable supersaturation in collaboration with Korean Polar Research Institute	number concentration at variable supersaturation, installed in 2012	---

NILU continues to operate 3 observatories measuring aerosol properties relevant for quantifying the aerosol climate effects, both the direct and the indirect effects: 1) Zeppelin Mountain / Ny Ålesund (in collaboration with the Norwegian Polar Institute and Stockholm University); 2) Birkenes Atmospheric Observatory, Aust-Agder, Southern Norway; 3) Troll Atmospheric Observatory, Antarctica (observatory operated by NILU, main station operated by Norwegian Polar Institute). The station locations represent the focal areas of the polar regions,

which are more vulnerable to climate change, as well as the regions where the largest fraction of the Norwegian population lives. Recent developments at these stations include:

1. **Zeppelin Mountain:** After modernising the aerosol instrumentation in the past year, the measurement of aerosol microphysical and optical aerosol properties at Zeppelin resumed normal operation within the WMO GAW programme. Despite performing good quality assurance on the measurement programme, the collaboration partner Stockholm University who operates the respective instruments had some delay in delivering the quality assured data due to funding restrictions on the Swedish side. The process to remedy these problems is ongoing.
2. **Birkenes Atmospheric Observatory:** Apart from resuming the operation of the extended aerosol instrument set at Birkenes according to the quality standards of WMO GAW and the European infrastructure project ACTRIS (see section 3.1), this year's focus has been placed on workshop intercomparisons of selected instruments. Despite strictly following the operating procedures agreed within the networks, certain instrument malfunctions can pass unnoticed if the instruments within a network are not intercompared directly on the same sample. To this end, ACTRIS has organised intercomparison workshops for absorption photometers (measuring the aerosol absorption coefficient) and Differential or Scanning Mobility Particle Sizers (DMPS / SMPS, measuring the fine-mode particle number size distribution) in which the respective instruments from Birkenes participated. For the Birkenes absorption photometer in service since 2006, it was discovered that it overestimates aerosol absorption by a factor of 1.77 due to a design problem despite being operated correctly. This highlights the importance of such intercomparison workshops and facilitates the correction of the Birkenes aerosol absorption time series also in hindcast (the correction has already been applied for this report). For the Birkenes DMPS, it was found that its operation status is in full compliance with network quality objectives (sizing uncertainty <3%, counting uncertainty < 10%). The mode of operation could be optimised to extend the upper end of the measured particle size distribution from 550 nm to 800 nm.
3. **Troll Atmospheric Observatory:** Funded by a base funding project controlled by the Norwegian Research Council (Strategisk Institutttsatsing, SIS), an article on the annual cycle of the baseline aerosol at Troll was finished and submitted the past year (Fiebig et al., 2013). The article investigates the named annual cycle as observed in the particle number size distribution and aerosol scattering coefficient data collected at Troll. It is shown that the baseline aerosol annual cycles in both parameters have the same physical origin. A comparison with data collected at the Antarctic stations South pole and Dome C, yields that the baseline air annual cycle observed at Troll is common to the whole Central Antarctic plateau. Following the Troll baseline air masses backwards with the Lagrangian transport model FLEXPART, the article demonstrates that these air masses descend over Antarctica after being transported in the free troposphere and lower stratosphere from mid-latitudes (there uplifted in fronts) or from the inter tropical convergence zone (uplifted by convection). The article shows further that the aerosol particles contained in Antarctic baseline air are formed in situ by photochemical oxidation of precursor substances. The article draws a comprehensive picture of this natural aerosol process that will help climate models to distinguish better between natural and anthropogenic aerosol processes, and therefore between natural and anthropogenic aerosol climate effects. On the fieldwork side, it needs to be mentioned that the atmospheric observatory will finally be moved in the upcoming 2013/14 Antarctic summer season to a location virtually undisturbed by local contamination, after the necessary budget has been allocated. The current location is only 200 m apart from the Troll station main building, which is in reach of turbulent diffusion. This has led to typically 80% or more of the data collected at the current atmospheric observatory to be locally contaminated and unsuitable for scientific use, which implies severe limitations on the kind of scientific questions possible to investigate.

An overview of all aerosol parameters currently measured at the 3 observatories can be found in Table 3. Parameters where observations are funded by KLIF (and which are covered in this report) are written in green type.

7.2 Optical aerosol properties measured at Birkenes: estimating the local, instantaneous direct aerosol radiative forcing

Figure 35 shows a time series of the daily averaged optical properties for the dry-state PM10 aerosol measured at Birkenes, not only for 2012, but for the whole period since January 2010 when the upgraded station has been in full operation. Following the measurement protocol, the particle fraction with aerodynamic diameters smaller than 10 μm is selected, and the particles are brought to or close to the dry-state, which is defined as a relative humidity smaller than 40%, which in turn is considered sufficient for hygroscopic particle growth to be negligible. This protocol follows the recommendations of the WMO GAW aerosol network, and is identical with the recommendations of the relevant European networks (EUSAAR8, ACTRIS). The rationale behind these recommendations is that any measurement protocol will alter the aerosol thermodynamic state from the ambient state before measurement by bringing the sample into the station building. By conditioning the sample in the described way and following the same quality assurance procedures, the observations are nevertheless comparable across stations within the network.

The top panel of Figure 35 shows the time series of the aerosol scattering coefficient σ_{sp} at three wavelengths across the visible spectrum. The aerosol scattering coefficient is quantifying the fraction of light redirected from its original direction due to scattering by particles. An instrument called integrating nephelometer measures it. Together with the aerosol absorption coefficient σ_{ap} , quantifying particle absorption of incident light in the aerosol volume depicted in the second panel of Figure 35, these parameters give the information necessary to quantify the local, ground-level direct aerosol climate effect. The absorption coefficient is measured by a filter absorption photometer that operates at 525 nm wavelength. The correction factor found for the Birkenes instrument during the recent intercomparison workshop has been included in this graph and all the forthcoming analysis. For comparison with the nephelometer, the data has been transferred to a wavelength of 550 nm assuming an absorption Ångström coefficient α_{ap} of -1, adding 2% systematic uncertainty to the data. Whereas σ_{sp} and σ_{ap} shown in the 2 top panels of Figure 35 scale with the particle concentration, the parameters shown in the bottom 2 panels don't, and rather represent properties of an average individual particle in the aerosol. The scattering Ångström coefficient \tilde{a}_{sp} plotted in the third panel parameterises the wavelength dependence of σ_{sp} . It is largely determined by the concentration ratio of particles in the fine size range ($D_p < 1 \mu\text{m}$) and coarse size range ($D_p > 1 \mu\text{m}$), and becomes higher the more fine range particles are present in the aerosol as compared to the coarse range. The single scattering albedo ω_0 depicted in the fourth panel quantifies the fraction of incident light interacting with the particles in an aerosol volume by scattering, rather than being absorbed by the particles. For a purely scattering aerosol, ω_0 is 1, and decreases with increasing fraction of light absorbing components in the aerosol particle phase. Since ω_0 is derived from σ_{sp} and σ_{ap} , the ω_0 wavelength plotted matches one of the wavelength of the integrating nephelometer, and is close to the wavelength of the filter absorption photometer. All panels include not only the time series of the daily averages, but also the 8 week running median centred around the data point, plotted as heavy line, to facilitate detection of possible seasonal variations.

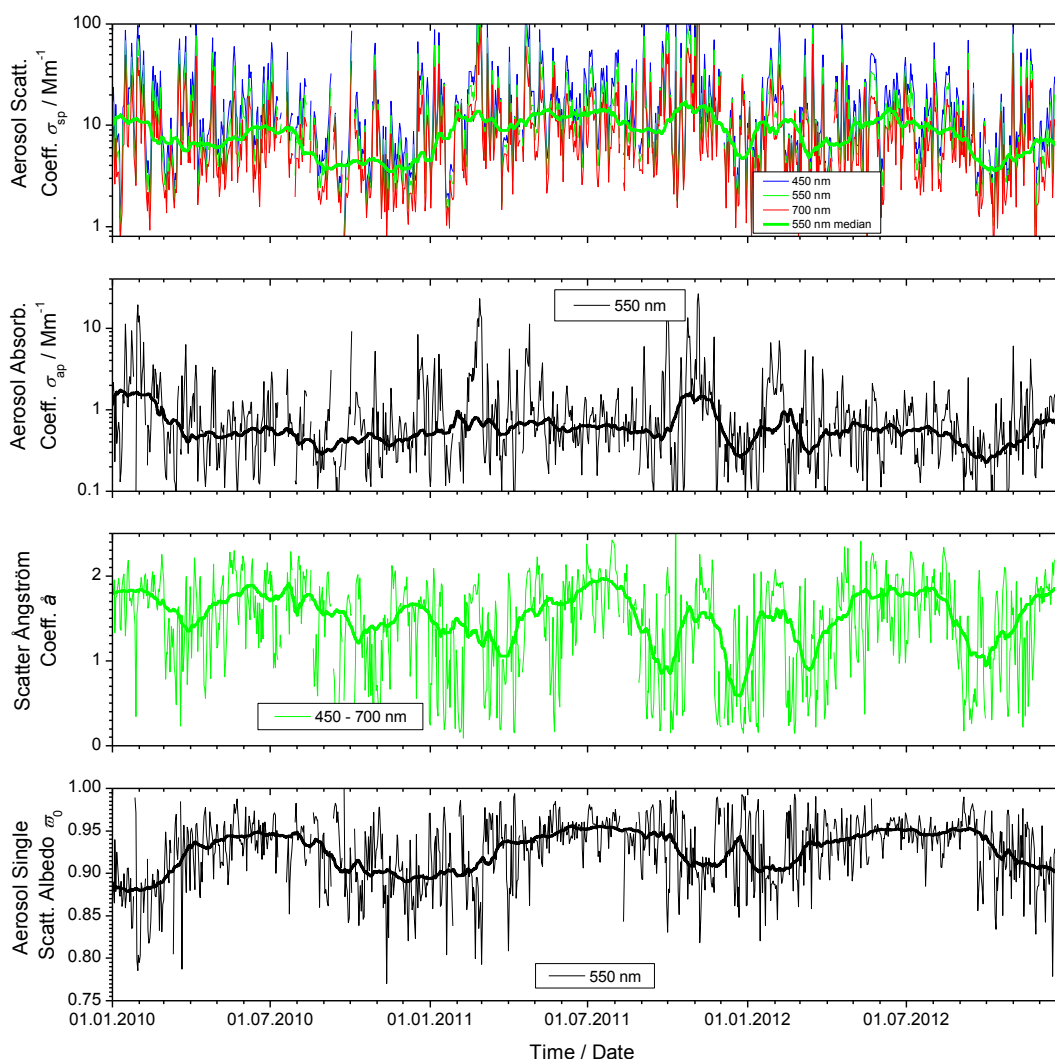


Figure 35: Time series of aerosol optical properties daily means measured for 2010 - 2012 at Birkenes. The top panel shows the aerosol scattering coefficient σ_{sp} at 450, 550, and 700 nm wavelength measured by integrating nephelometer. The second panel depicts the aerosol absorption coefficient σ_{ap} at 550 nm wavelength measured by filter absorption photometer, shifted from the instrument wavelength at 525 nm to 550 nm for consistent comparison assuming an absorption Ångström coefficient of -1. The third and fourth panels show the scattering Ångström coefficient \tilde{a}_{sp} and the single scattering albedo ω_0 as derived properties, respectively.

With now 3 full years of data available, it is possible to draw a more reliable and comprehensive picture of the aerosol encountered at Birkenes. The σ_{sp} values measured at Birkenes range between 3 - 20 1/Mm, where about 8 1/Mm are typical for remote locations, and 40 1/Mm typical for continental background (Delene & Ogren, 2002). The range encountered at Birkenes thus reflects the air mass types arriving at Birkenes by long-range transport. There is also a slight annual cycle detectable in the σ_{sp} time series, with values at the upper end of the encountered range occurring more often in summer than in winter. This feature is likely due to air masses with higher σ_{sp} being transported more often to Birkenes in summer than in winter, but without being completely absent in winter. This phenomenon will be discussed more closely in the next section.

For the aerosol absorption coefficient σ_{ap} , the literature values range between 0.1 1/Mm in remote locations and 8 1/Mm in continental background air (Delene & Ogren, 2002). Just as with σ_{sp} , the σ_{ap} values fit nicely into this range due to the mixed nature of air masses encountered at Birkenes. A seasonal cycle cannot be detected for σ_{ap} . The same conclusion applies to the scattering Ångström coefficient \tilde{a}_{sp} , which describes the wavelength dependence of σ_{sp} . Here, the values range from 2 for remote locations, where coarse range particles are almost absent, to around 0 for marine aerosol with a significant coarse range particle concentration from sea spray. Negative values of \tilde{a}_{sp} are also possible for extreme coarse range particle concentrations as encountered in desert dust aerosol. As expected, the values measured at Birkenes are close to those for remote locations, with occasional transport events from the continent.

In contrast to the other aerosol optical parameters measured at Birkenes, the single scattering albedo ω_0 exhibits a clear annual cycle. The literature values range from close to 1 for polar locations most almost no absorbing components, values around 0.92 for continental background locations to values even lower than 0.8 closer to source regions of absorbing aerosol components, e.g. sources of fossil fuel or biomass combustion. For Birkenes, a range from 0.88 in winter to 0.95 in summer is observed. These values are significantly higher, i.e. less absorbing, as reported for the previous years due to the mentioned correction of the σ_{ap} values, leading to a decrease of the measured aerosol absorption. The annual cycle however, which was connected with biomass burning emissions in previous reports, is robust against this correction.

The effect of a climate forcer is usually quantified by its radiative forcing ΔF , i.e. the deviation of the atmospheric radiation budget at the top of the troposphere with and without the forcer present and undisturbed otherwise. For radiative forcing of the direct climate effect of atmospheric aerosol ΔF_{ae} , a full scale radiative transfer model is required for an exact calculation. However, by making a number of assumptions, it is possible to estimate the radiative forcing efficiency $\Delta F_{ae}/\delta$ of the direct aerosol climate effect, i.e. the radiative forcing normalised by the aerosol optical depth, a measure of the total amount of aerosol particles in the atmospheric column. Using the approach of Haywood & Shine (1995, eq. 3) as quoted in Sheridan & Ogren (1999), $\Delta F_{ae}/\delta$ can be calculated from the aerosol optical parameters measured at Birkenes by using the following assumptions:

- a constant fractional day length of 0.5
- a constant atmospheric transmissivity of 0.76 above the aerosol layer assumed to be located in the boundary layer.
- a constant fractional cloud cover of 0.6
- a constant surface albedo of 0.15 (forest), alternatively one of 0.85 when considering a snow covered surface.
- an integration of ΔF_{ae} across the solar spectrum by using the aerosol optical property values at 550 nm wavelength where the spectral intensity of the solar radiation reaching the earth surface is highest.
- neglecting the fact that all ground-based instruments measure the aerosol optical properties for the dry-state aerosol (relative humidity < 40%), whereas the AOD is measured for ambient conditions of relative humidity.

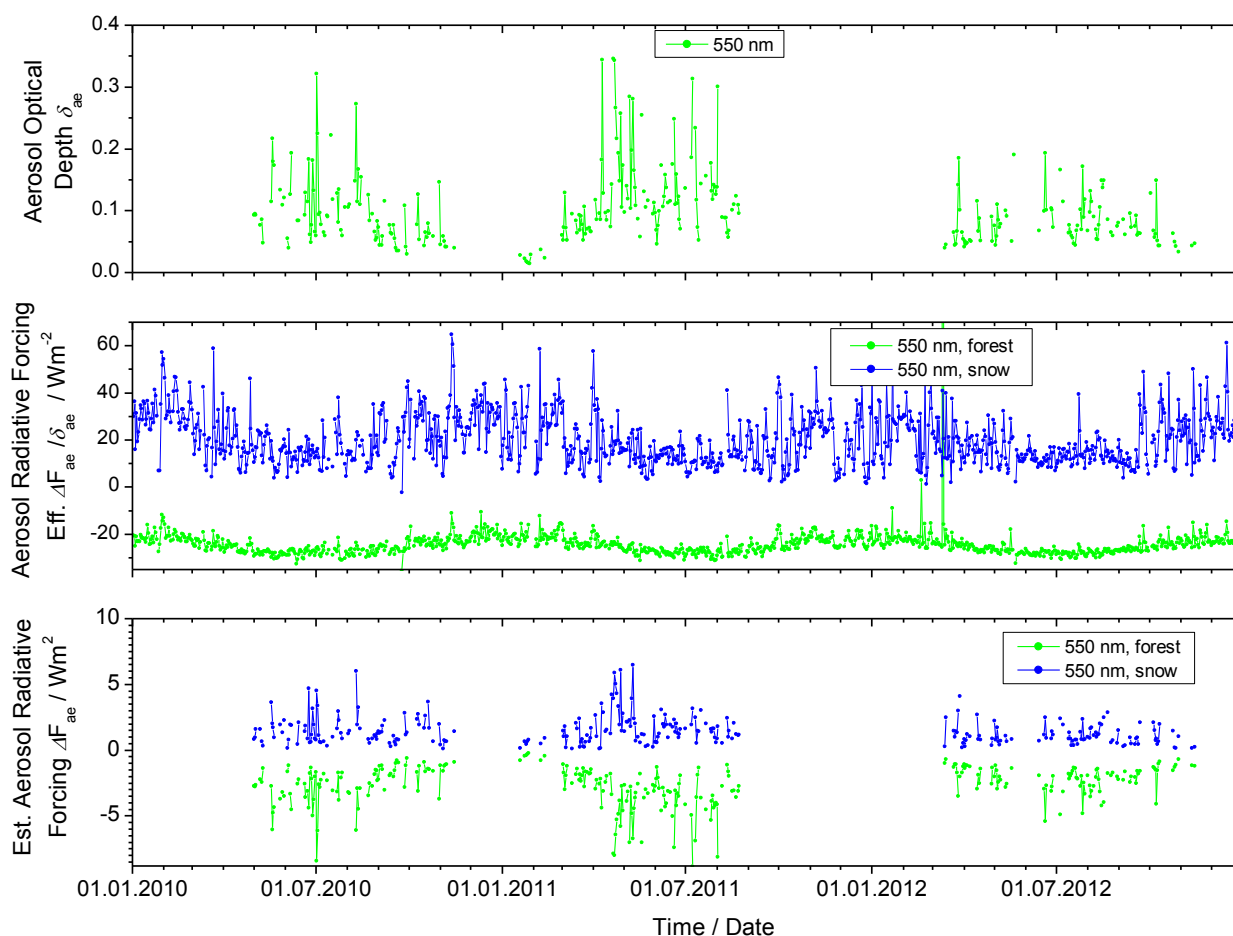


Figure 36: 2010 - 2012 time series of the cloud-screened aerosol optical depth (AOD) at 550 nm wavelength in the atmospheric column above Birkenes (upper panel), as well as the radiative forcing efficiency $\Delta F_{ae}/\delta$ (middle panel) and the estimated local, instantaneous, solar aerosol radiative forcing ΔF_{ae} , the latter two both for surface albedos for forest and snow.

Thus, the approach may not allow to calculate the true aerosol direct radiative forcing directly, but allows to study the relative dependence of $\Delta F_{ae}/\delta$ on changes in the various aerosol properties. Since the aerosol optical depth is also measured at Birkenes, ΔF_{ae} may be calculated from $\Delta F_{ae}/\delta$ when the aerosol optical depth δ is available, which happens more often in summer since this measurement requires a direct and cloud-free view of the sun.

Figure 36 summarises the obtained Birkenes 2010 - 2012 time series of the aerosol optical depth $\delta_{550\text{ nm}}$ (top panel), the radiative forcing efficiency $\Delta F_{ae}/\delta$ (middle panel), and the estimated direct, local, instantaneous radiative forcing ΔF_{ae} (bottom panel), all at 550 nm wavelength, and the latter two for both, the standard surface albedo used in the approach (representative of forest) and the albedo of snow covered landscape. In the $\delta_{550\text{ nm}}$ time series, the slight annual cycle found in the previous years is reconfirmed despite the data coverage being significantly better in summer than in winter, which reflects the requirement of a cloud-free view of the sun for this measurement. Typical values range from 0.12 in summer to 0.4 in winter. The radiative forcing efficiency $\Delta F_{ae}/\delta$ however exhibits a clear annual cycle, which reflects the annual cycle of the scattering albedo ω_0 observed at Birkenes. In winter when the aerosol at Birkenes is more light-absorbing, $\Delta F_{ae}/\delta$ is less negative, i.e. less cooling, as compared to summer over an assumed forest surface. This trend is independent of the surface albedo assumed for the calculation. Over a snow-covered surface, $\Delta F_{ae}/\delta$ even becomes positive (warming), more so in winter than in summer. When taking the aerosol optical depth into account and looking at the estimated radiative forcing ΔF_{ae} , the tendency of the Birkenes aerosol to have a warming effect in winter becomes less pronounced due to the low winter aerosol optical depth at Birkenes. Despite all assumptions, the estimate reconfirms that the Birkenes winter aerosol may have a net warming effect due to its content of absorbing components.

To summarise this section, we can conclude that the 3 year time series of aerosol optical properties available for Birkenes now reconfirms the tendencies found in the previous reports. The observed warming winter aerosol

forcing over a snow-covered surface at Birkenes may lead to a locally slightly shortened snow cover season, but since atmospheric aerosol is a SLCF, this effect is fully reversible.

7.3 Physical aerosol properties measured at Birkenes in 2010-2012

The physical aerosol properties covered here include the particle number size distribution in the particle diameter range $30 \text{ nm} < D_p < 550 \text{ nm}$ measured by a Differential Mobility Size Spectrometer (DMPS). The data collected in 2012 by the DMPS are displayed in Figure 37 as colour contour plot. In this type of plot, the x-axis holds the time of the observation, whereas the y-axis holds the particle diameter D_p on a logarithmic scale. This is common practice since D_p usually spans several orders of magnitude. The colour scale holds the particle concentration, normalised to the logarithmic size interval, $dN / d\log D_p$, also on a logarithmic (colour) scale.

Even though a particle size distribution isn't uniquely connected to a specific air mass type, it is normally fairly characteristic, and can serve as valuable indication of air mass origin, which at Birkenes shifts with the synoptic weather situation. In describing particle number size distributions, it is often referred to log-normal modes the size distribution consists of, which are commonly referred to as "Aitken-mode" for the one peaking at $10 \text{ nm} < D_p < 100 \text{ nm}$, and accumulation -mode for the one peaking between $100 \text{ nm} < D_p < 500 \text{ nm}$. Reconfirming findings of previous years' reports, the most common types of air masses occurring at Birkenes and their particle size distribution include (omitting special cases of long-range transport):

- **Clean Arctic background aerosol**, characterised by a distinct accumulation mode peaking at 150 nm particle diameter, with peak particle concentrations of 200 cm^{-3} .
- **Continental aerosol**, characterised by an accumulation mode peaking between 150 - 240 nm particle diameter, depending on how long the aerosol had time to self-process, and peak particle concentrations between $1000 - 1500 \text{ cm}^{-3}$, in addition to the presence of an Aitken-mode.
- **Arctic haze**, characterised by the absence of an Aitken-mode, and an accumulation mode peaking at 200 nm particle diameter, with peak particle concentrations of 1500 cm^{-3} .

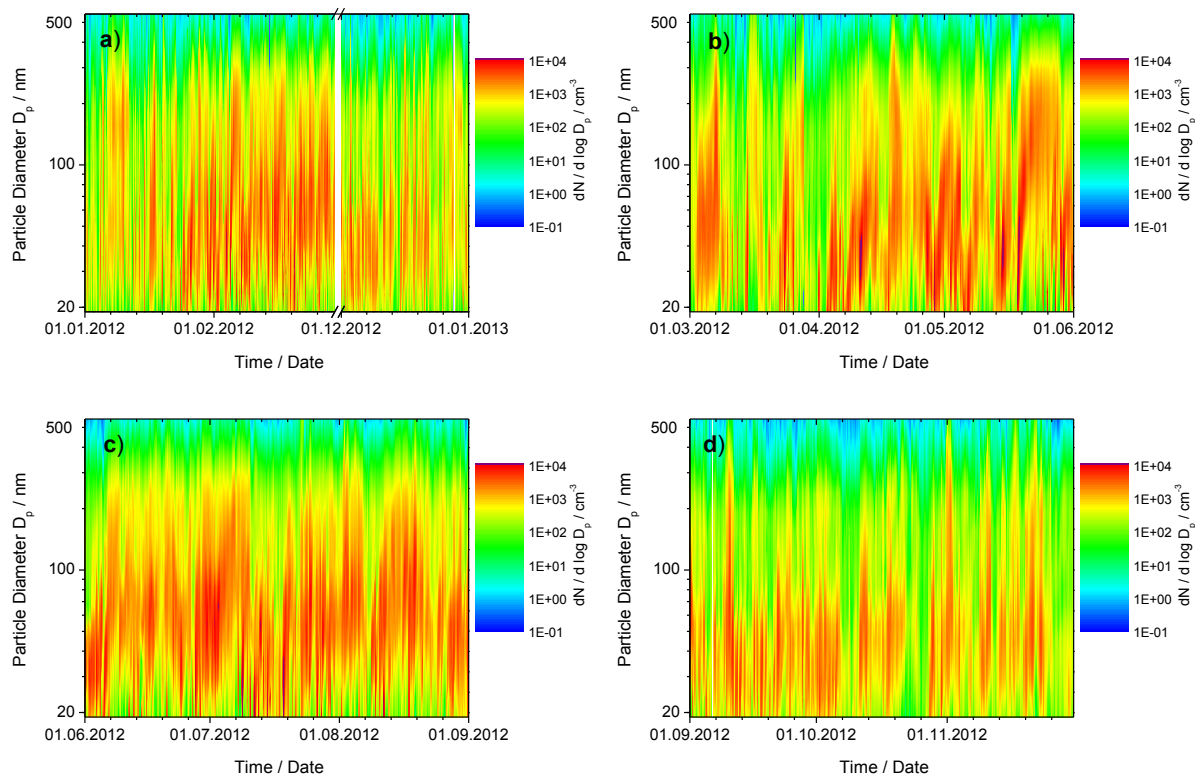


Figure 37: 2012 time series of particle number size distribution at Birkenes, panel a) winter, panel b) spring, panel c) summer, panel d) autumn.

At Birkenes, these aerosol types can appear combined with an additional mode in the Aitken size range ($10 \text{ nm} < D_p < 100 \text{ nm}$). These have an atmospheric lifetime of a couple of hours to a day (Jaenicke, 1980) before they either grow larger by mass uptake from the gas-phase, or coagulate with particles in the accumulation mode size range ($100 \text{ nm} < D_p < 500 \text{ nm}$). Particles in the Aitken-size range are therefore relatively young and newly formed, and have to be of local or regional origin, where a locally generated Aitken-mode peaks around 30 nm particle diameter, a regionally generated around 70 nm particle diameter. As mentioned in previous reports, at least two possible sources for such particles are known for continental background locations like Birkenes:

- **Biogenic aerosol**, generated from condensing oxidised precursor gases, e.g. terpenes, emitted by vegetation. Events of strong biogenic aerosol formation are characterised by the formation of new particles. These events show by the appearance of a new mode in the particle size distribution that first quickly grows from particle diameters below 10 nm, then with decelerating velocity to particle diameters of about 60 nm.
- **Wood combustion aerosol**, generated usually by domestic heating with wood burning stoves. The particle formation is here located in the combustion chamber and exhaust pipe.

However, wood combustion aerosol is distinguished by another characteristic. It contains significant amounts of light absorbing carbon. For fresh pine wood combustion aerosol, the single scattering albedo ω_0 has typical values of as low as 0.85 (Lewis et al., 2008).

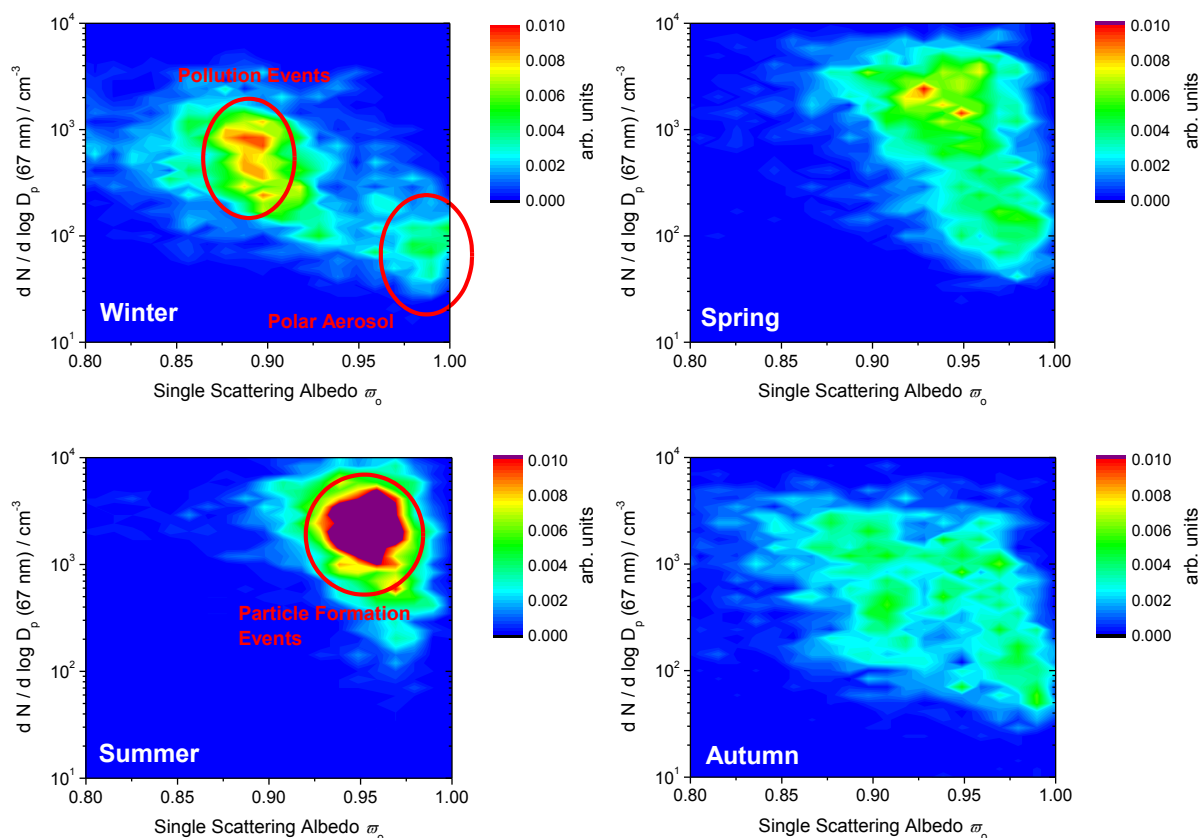


Figure 38: The probability of occurrence of Birkenes aerosols of a given single scattering albedo ω_0 and Aitken-mode peak particle concentration. The x-axis holds ω_0 , the y-axis the particle number size distribution concentration at 67 nm, which is close to the peak of the Aitken-mode. The colour code states the probability of occurrence of this combination of values in dimensionless units. The data are discriminated by season, with one panel collecting the data for each season. The analysis is based on the whole accessible time series from 2010 to 2012.

In order to quantify the occurrence of the two Birkenes aerosol types of regional origin (biogenic and wood combustion) on top of the aerosol types from long range transport, find more objective criteria for their occurrence, and create a connection between the annual cycle observed in the single scattering albedo ω_0 and regional sources, the statistical analysis presented in last years' report was updated using the datasets of 2010 - 2012 in order to present a consolidated analysis and to include recent data corrections. The analysis, displayed in Figure 38, discriminates the data by season. The panels, one for each season, show ω_0 on the abscissa and one point of the particle size distribution $dN / d \log D_p$, the one at $D_p = 67$ nm particle diameter, on the ordinate. This particle diameter is usually close to the peak of the Aitken-particle mode, the mode containing regionally formed particles. The colour code in the plots quantifies the probability of occurrence of the respective combination of values in arbitrary units.

The analysis is easiest to interpret when focussing in first on the panels for winter and summer. In winter, 2 peaks of aerosols with high likelihood of occurrence are obvious:

- One peak of aerosols with single scattering albedo $\omega_0 < 0.91$ and Aitken-mode peak concentrations $dN / d \log D_p (67 \text{ nm}) > 300 \text{ cm}^{-3}$, values which are common for biomass burning aerosol and marked in Figure 6.4 as pollution events. Since these aerosols are dominated by Aitken-mode particles with small lifetime, they need to be of regional origin, which indicates domestic heating by wood burning as source.
- One peak of aerosols with single scattering albedo $\omega_0 > 0.97$ and Aitken-mode peak concentrations $dN / d \log D_p (67 \text{ nm}) < 200 \text{ cm}^{-3}$, values which are common for Arctic aerosol.

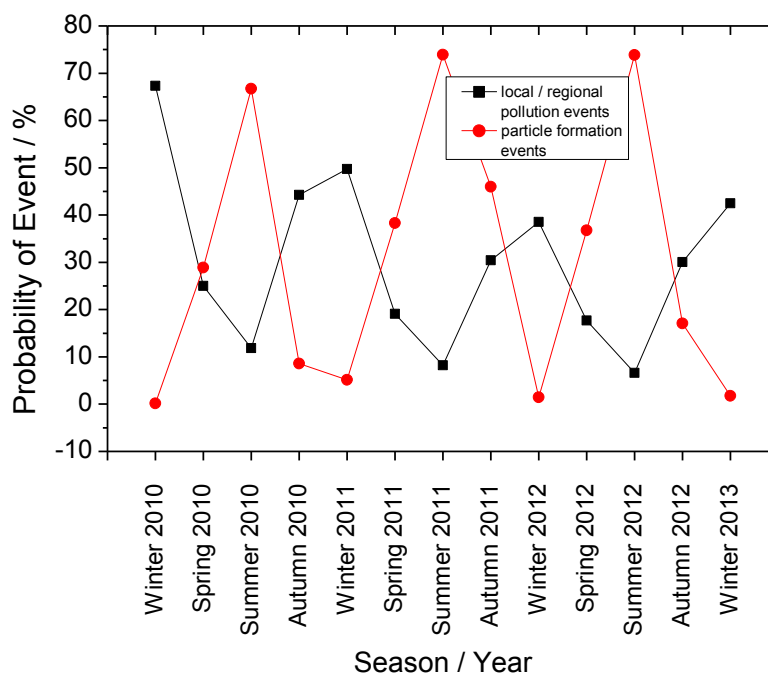


Figure 39: Frequency of occurrence by season of local or regional combustion events, as well as occurrence of particle formation events in Birkenes for the 2010-2012 period as determined by combined analysis of particle number size distribution and single scattering albedo.

The summer panel in contrast shows only one peak of aerosols with high likelihood to occur:

- a peak of aerosols with single scattering albedo $\omega_0 > 0.92$ and Aitken-mode peak concentrations $dN / d \log D_p$ (67 nm) $> 750 \text{ cm}^{-3}$, values typical for events of particle formation from biogenic precursors. These aerosols are also dominated by Aitken-mode particles, this young and of regional origin. However, particles from oxidation of biogenic precursor substance, e.g. terpenes, show little absorption, which explains the high single scattering albedo.

The panels for spring and autumn show intermediate states between summer and winter.

With this knowledge, it is possible to define updated objective criteria for the presence of regional pollution (“wood combustion”) aerosol ($\omega_0 < 0.91$, $dN / d \log D_p$ (67 nm) $> 300 \text{ cm}^{-3}$) and for regional biogenic particle formation aerosol ($\omega_0 > 0.92$, $dN / d \log D_p$ (67 nm) $> 750 \text{ cm}^{-3}$). Figure 39 contains a graph depicting the seasonal probability of occurrence of these two aerosol types for the years 2010 - 2012. For both types of events, clear annual cycles are readily detectable. Regional biogenic particle formation events occur most frequently in summer and least frequently in winter, which correlates nicely with the atmospheric oxidation capacity for oxidising biogenic precursor gases into condensable particle mass. The oxidation capacity in turn is controlled by solar insolation, which obviously peaks in summer. Regional pollution (“wood combustion”) events show the exact opposite annual cycle, with occurrence frequency peaking in winter and being lowest in summer.

Strictly speaking, the criteria found for regional pollution aerosol at Birkenes (low single scattering albedo/high absorption, high concentration of recently formed Aitken-mode particles/regional origin) aren’t sufficient to attribute these events to biomass burning. However, the analysis benefits from the results of the project “Strategic Aerosol Observation and Modelling Capacities for Northern and Polar Climate and Pollution” (SACC), a base-funding project channelled through the Norwegian Research Council (Strategisk Instituttssatsing, SIS). One of the SACC work packages is dedicated to finding an updated source attribution for the air masses arriving at Birkenes. This is to be achieved by adding a time series of the particle levoglucosan concentration to the data available for Birkenes by analysing archived aerosol filter samples back to 2008. Levoglucosan is a tracer substance, which is highly specific for biomass burning. The first results of this work have recently become available. Even though the final quality assurance, and therefore a graph of the data, are still lacking, it is safe to state at this point that the particle-bound levoglucosan concentrations at Birkenes show the same annual cycle as the occurrence of regional pollution aerosol. It is thus safe to conclude that the winter regional pollution events at Birkenes are due to biomass burning.

The SACC project plan for the upcoming year includes further work on the Birkenes aerosol source attribution. This will be achieved by using all data on aerosol properties available for Birkenes (microphysical, optical, chemical) in a cluster analysis to the dominating source types and assign occurrence frequencies to them, which is in fact an extended and mathematically strict version of the statistical analysis presented in this section. Together with the Lagrangian transport model FLEXPART, it will also be possible to determine where the dominating source types originate, which will likely confirm the regional origin of the winter pollution events at Birkenes.

7.4 Observations of the total aerosol load above Ny-Ålesund and Birkenes

The aerosol optical depth (AOD) is a quantitative measure of the extinction of solar radiation by aerosol scattering and absorption between the point of observation and the top of the atmosphere. It is determined by the total concentration of particulates in the atmosphere. The wavelength dependence of AOD, described by the Ångström exponent (AE) is a qualitative indicator of the particle size and contains information about the aerosol type. The larger the Ångström exponent, the smaller the size of the particles measured.

During the last years the number of stations measuring AOD has increased significantly. Figure 40 shows the networks of sun-photometer operated in Scandinavia (from *Toledano et al.*, 2012). Photos of the standard instruments used for monitoring of spectral resolved AOD in Ny-Ålesund and Birkenes and their characteristics are described in Appendix I.

In 2002, PMOD/WRC in collaboration with NILU, started AOD observations in Ny-Ålesund, as part of the global network of AOD observations on behalf of the WMO GAW program. A **Precision Filter Radiometer (PFR, [Wehrl, 2000, 2005])** is utilized to measure extinction in four narrow spectral bands, by the WMO recommended wavelengths: at 368 nm, 415 nm, 500 nm and 862 nm. Direct sun measurements are performed with the instrument located on the roof of the Sverdrup. **Samples are recorded with one minute time resolution.** Data quality control includes instrumental control like detector temperature and solar pointing control as well as objective cloud screening. SCIAMACHY TOMSOMI ozone columns and meteorological data from Ny-Ålesund were used in the retrieval. Ångström coefficients are derived for each set of measurements using all four PFR channels. **Calibration is performed annually** at PMOD/WRC. Near Real Time data are displayed at www.pmodwrc.ch/worcc. Quality assured data (1 hour averages) are available via the World Data Center of Aerosols, WDACS, hosted at NILU (see <https://ebas.nilu.no>). Ny-Ålesund is one of the initial 12 site starting to operate PFRs, and a study showing trend-analysis of AOD from the baseline GAW-PFR station from 2000-2012 is presently prepared by *Nyeki et al.* [2013].

At the Birkenes observatory a sun-photometer is operated since spring 2009. The instrument is a CIMEL type CE-318 sun-photometer (#513). While the PFR measures direct sun light only, the Cimel instrument is an automatic sun and sky radiometer, equipped with spectral interference filters centered at selected wavelengths: 340, 380, 440, 500, 675, 870, 1020, and 1640 nm. It is a standard instrument of the Aerosol Robotic Network AERONET network [*Holben et al.*, 1998; *NASA*, 2011]. The measurements at Birkenes are performed in collaboration with the University of Valladolid (Spain), who perform the annual calibration (RIMA-AERONET sub-network, in 2012 funded via ACTRIS). Cimel sun photometer data can be found at <http://aeronet.gsfc.nasa.gov>. The values are recorded every 15 minutes. They centrally processed and cloud screened by AERONET [*Smirnov et al.*, 2000]. Derived estimates of spectral AOT are expected to be accurate within ± 0.01 for wavelengths larger than 440 nm [e.g., *Holben et al.*, 1998].

Due to low aerosol loading in the polar region, accuracy requirements for AOT measurements are more stringent than those usually encountered in established sun photometer networks. Measurements at Ny-Ålesund are part of the POLAR-AOD network, which was founded to organize polar sun-photometer measurements within the

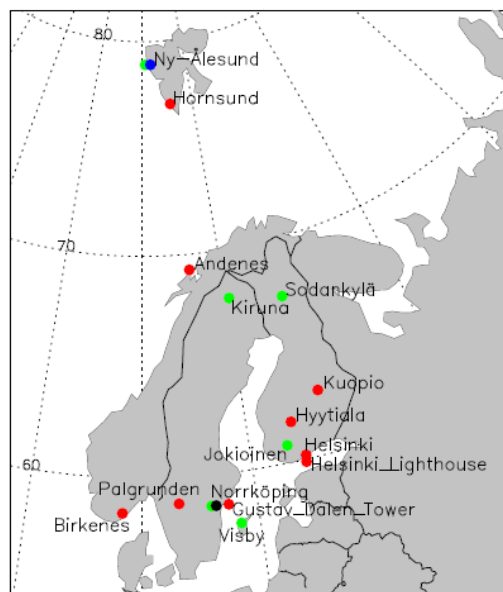


Figure 40: Location of sun photometer sites in the European Arctic sector and Scandinavia. Colour symbols denote networks: AERONET sites (red), GAW-PFR (green), Polar-AOD (blue) [this Figure is equal to Figure 1 from *Toledano et al.*, 2012].

framework of the International Polar Year [see *Mazzola et al., 2012; Tomasi et al., 2007, 2012*]. *Mazzola et al. [2012]* reported results from an inter-comparison campaign held in spring 2006 in Ny-Ålesund and a validation campaign, which took place in 2008 in Izaña/Tenerife, bringing together several groups and various instruments used for Polar-AOD observations. They found that spectral values of AOD derived from measurements taken with different instruments agree very well, presenting at both 500 nm and 870 nm wavelengths average values of root mean square difference and standard deviation of the difference equal to 0.003. These results confirmed that sun photometry is a valid technique for aerosol monitoring in the pristine atmospheric turbidity conditions usually observed at high latitudes.

7.4.1 Measurements of the total aerosol load above Ny-Ålesund

NILU's measurements of the aerosol optical depth in Ny-Ålesund (N 78°55', E 11°51', Alt 46 m) started in May 2002, in collaboration with PMOD/WRC. In Ny-Ålesund the sun is below 5° between 10 October and 4 March, limiting the period with suitable sun-photometer observations to the spring-summer seasons (NILU contributes to an initiative to fill the gap in the winter-time AOD climatology by using a novel lunar photometry, which may undergo first tests in 2014).

In 2012 sun-photometer observations were made between March 11 and September, 30, and for 99 days AOD values are available. The monthly mean and sunlight-season average values of AOD at 500 nm and Ångström coefficients measured between 2002 and 2012 are summarized in Table 4a: a/b and visualized in Figure 41. Monthly AOD averages are calculated from hourly averaged values with more than 10% of valid observations included.

The data reveal the expected pattern, high aerosol load with larger AOD (about 0.12 at 500 nm wavelength) during the Arctic haze period in spring, and low summer values (about 0.06). 2012 was a year with only comparable low aerosol loadings during spring (around 0.1 during March-May), after that typical summer values of 0.06 and slightly higher autumn values around 0.07 were measured. The Ångström exponent in Svalbard does not show such a clear seasonal pattern as the AOD. Apparently, there is a minimum in May at the end of the haze season, and then the AE increases slightly during the summer. The multi-annual monthly means is around 1.5, thus indicating dominance of fine particle. In 2012 90% of all hourly averaged Ångström exponents were above 1.05, thus showing the high fraction of smaller particles (see Figure 41).

Table 4a: Monthly mean and sunlight-season average values of AOD at 500 nm measured in Ny-Ålesund between 2002 and 2012. The values given are mean and standard deviation.

Month	March	April	May	June	July	August	September
	AOD						
2002		0.06 ± 0.01	0.08 ± 0.03	0.06 ± 0.02	0.07 ± 0.12	0.07 ± 0.08	0.06 ± 0.05
2003	0.15 ± 0.12	0.11 ± 0.05	0.15 ± 0.06	0.10 ± 0.03	0.04 ± 0.01	0.05 ± 0.02	0.06 ± 0.03
2004	0.06 ± 0.00	0.12 ± 0.08	0.13 ± 0.09	0.06 ± 0.01	0.10 ± 0.07	0.05 ± 0.02	0.04 ± 0.02
2005	0.08 ± 0.03	0.12 ± 0.07	0.10 ± 0.03	0.05 ± 0.02	0.05 ± 0.02	0.04 ± 0.03	0.03 ± 0.01
2006	0.12 ± 0.03	0.16 ± 0.07		0.04 ± 0.00	0.05 ± 0.02	0.05 ± 0.04	0.04 ± 0.03
2007		0.10 ± 0.05	0.10 ± 0.12	0.07 ± 0.03	0.05 ± 0.01	0.05 ± 0.02	0.04 ± 0.03
2008	0.13 ± 0.05	0.14 ± 0.06	0.14 ± 0.04	0.06 ± 0.02	0.06 ± 0.02	0.09 ± 0.03	0.16 ± 0.03
2009			0.11 ± 0.03	0.08 ± 0.02	0.11 ± 0.04	0.10 ± 0.02	0.09 ± 0.01
2010	0.11 ± 0.03	0.08 ± 0.03	0.08 ± 0.01	0.06 ± 0.01	0.05 ± 0.01	0.05 ± 0.01	
2011			0.08 ± 0.02	0.08 ± 0.01	0.05 ± 0.01	0.06 ± 0.02	0.05 ± 0.01
2012	0.10 ± 0.03	0.10 ± 0.02	0.10 ± 0.03	0.06 ± 0.02	0.06 ± 0.02	0.07 ± 0.03	0.07 ± 0.03

Table 4b: Monthly mean and sunlight-season average values of Ångström coefficient measured in Ny-Ålesund between 2002 and 20012. The values given are mean and standard deviation.

Month	March	April	May	June	July	August	September
	AE						
2002		0.9 ± 0.1	1.4 ± 0.1	1.2 ± 0.3	1.2 ± 0.2	1.3 ± 0.4	1.2 ± 0.5
2003	0.9 ± 0.5	1.3 ± 0.3	1.3 ± 0.2	1.5 ± 0.1	1.5 ± 0.3	1.4 ± 0.5	1.4 ± 0.3
2004	1.3 ± 0.1	1.2 ± 0.3	1.4 ± 0.5	1.7 ± 0.2	1.6 ± 0.4	1.5 ± 0.3	1.3 ± 0.3
2005	1.1 ± 0.3	1.4 ± 0.4	1.0 ± 0.2	1.6 ± 0.3	1.7 ± 0.2	1.4 ± 0.7	1.5 ± 0.4
2006	0.9 ± 0.1	0.9 ± 0.3		1.7 ± 0.2	1.4 ± 0.3	1.3 ± 0.6	1.4 ± 0.3
2007		1.4 ± 0.4	1.4 ± 0.6	1.7 ± 0.2	1.6 ± 0.2	1.7 ± 0.3	1.5 ± 0.4
2008	1.4 ± 0.2	1.3 ± 0.2	1.4 ± 0.2	1.4 ± 0.4	1.2 ± 0.2	1.3 ± 0.3	1.4 ± 0.3
2009			1.3 ± 0.4	1.4 ± 0.2	1.3 ± 0.3	1.2 ± 0.1	1.1 ± 0.1
2010	1.0 ± 0.03	1.4 ± 0.02	1.3 ± 0.02	1.3 ± 0.03	1.4 ± 0.02	1.0 ± 0.01	
2011			1.7 ± 0.03	1.8 ± 0.1	1.5 ± 0.1	1.4 ± 0.3	1.6 ± 0.2
2012	1.1 ± 0.2	1.3 ± 0.2	1.2 ± 0.2	1.1 ± 0.1	1.3 ± 0.2	1.4 ± 0.2	1.5 ± 0.2

Individual episodes have a large impact on observed monthly averages. Huge emissions from boreal forest fires in North America are likely to explain the elevated AOD levels end of July 2004 [Stohl *et al.* 2006]. Agricultural fires in Eastern Europe resulted in elevated pollution levels in Arctic in spring 2006 [Stohl *et al.*, 2007; Myhre *et al.*, 2007]. The increase in AOD in August and September 2008 was caused by the plume from the Kasatochi volcano (52.17°N, 175.51°W), erupting on 7 to 8 August 2008, reaching Ny-Ålesund (see e.g. Hoffman *et al.*, 2010; Kristiansen *et al.*, 2010). The column AOD over the Svalbard region was influenced by stratospheric volcanic aerosol from 3 July 2009 and 22 June 2011 onward. This which was caused by the eruptions of Sarychev volcano (48° 06'0" N, 153° 12'0" E, Russia's Kuril Islands, erupted of June 12, 2009), and Nabro (13.37°N, 41.70°E, Eritrea, erupted on 13 June 2011 [see Glantz *et al.*, 2013, O'Neill *et al.*, 2012]. While the stratospheric contribution is low, less than 0.02, compared to the total AOD, the influence can be clearly spotted when occurring the summer/autumn periods [for details see Glantz *et al.*, 2013].

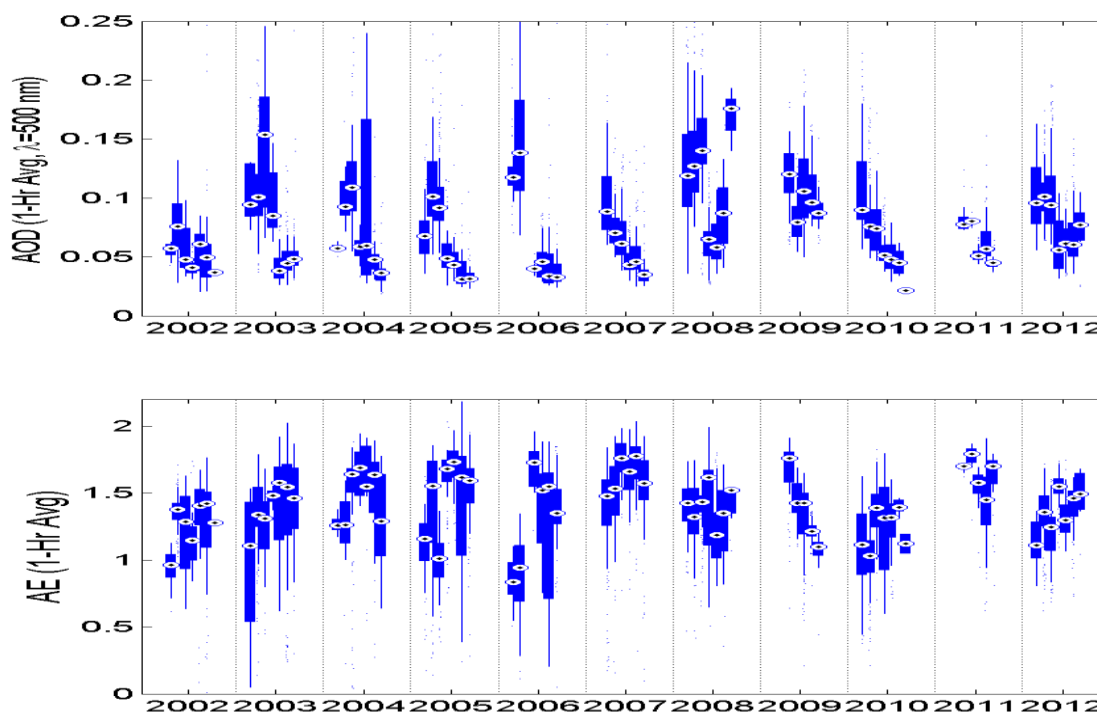


Figure 41: Monthly average aerosol optical depth (AOD at 500 nm) (upper panel) and Ångström exponent (lower panel) measured in Ny-Ålesund during the sunlit periods in 2002 - 2012. On each box, the central mark is the median, the edges of the box are the 25th and 75th percentiles, the whiskers extend to the most extreme data points not considered outliers, and outliers (in terms of monthly averages, although not considered outlier in terms of pollutions events with high aerosol loads) are shown as very small dots.

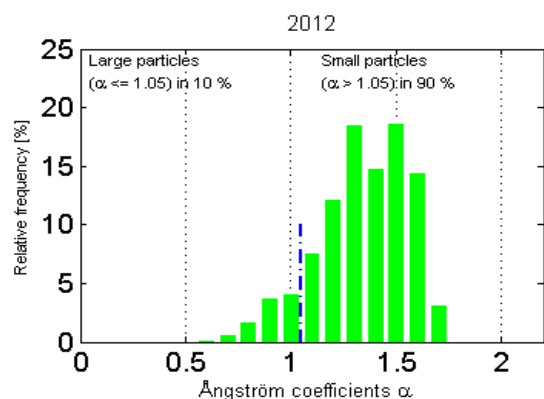
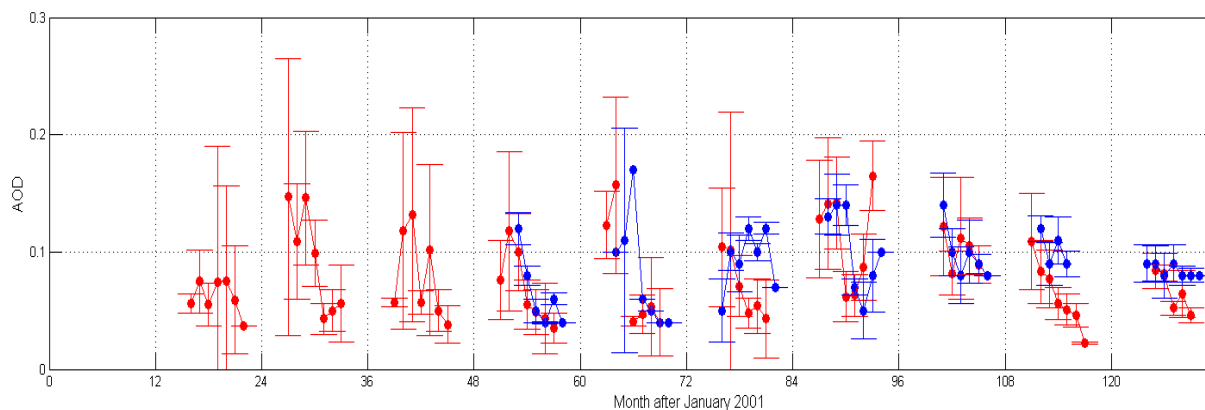


Figure 42: Relative frequency of hourly averaged Ångström a exponent (= AE) measured in 2012. If a threshold for fine particle is set at around $a = 1.05$, in 2012 the fine mode fraction has dominated the particle composition in Ny-Ålesund (in 90% a as larger than 1.05).

A supplementary data-set recorded in the Svalbard area was considered for comparison with the PFR sun-photometer data, consisting of the daily spectral series of AOD measured at from Hornsund (77.0°N, 15.6°E), which is an AERONET site ca. 230 km south of Ny-Ålesund (from the Polish Academy of Sciences), on Polar Bear Bay (Spitsbergen). Level 2.0 data were downloaded from the AERONET (Holben et al., 1998) website (<http://aeronet.gsfc.nasa.gov/>), derived from measurements made using a Cimel CE-318 sun-photometer. Figure 41 shows the total aerosol column measurements (AOD) between 2002 and 2012 made at Ny-Ålesund and Hornsund. While during other years AOD seems slightly higher at Hornsund, in 2012 the monthly averaged values were - except in May - slightly lower than in Ny-Ålesund. Further research is needed to better understand the cause of the spatial-temporal variations.

For trend-analysis we would like to refer to the recent publication made by Tomasi et al. (2012), who analysed long-term trends using the data from AWI starting in 1991 (co-located with the PFR). Contrary to the larger negative trend described by Tomasi et al. (2007), for the 30-year data record the authors only found a very weak negative trend (0.021 % / year). Slowly increasing stratospheric AOD over the last decade as result of minor volcanic eruptions (Solomon, 2011). Results obtained here, are consistent with these findings.



2012	March	April	May	June	July	August	September	October
Ny-Ålesund	0.10 ±	0.11 ±	0.10 ±	0.06 ±	0.06 ±	0.07 ±	0.07 ±	
Hornsund		0.09 ±	0.10 ±	0.09 ±	0.06 ±	0.05 ±	0.05 ±	0.04 ±

Figure 43: Time series of and sunlight-season average values of AOD at 500 nm from observations made at Ny-Ålesund (N 78°55', E 11°51', Alt 46 m) (red symbols) and Hornsund (N 77°00', E 15°33', Alt 10 m) (blue panel). The values given are mean and standard deviation.

7.4.2 Measurements of the total aerosol load above the Birkenes observatory

Aerosol optical depth measurements started at the Birkenes observatory (N 58°23, E 08°15, Alt 230 m), in spring 2009, utilizing an automatic sun and sky radiometer (CIMEL type CE-318). The retrieval method is that of the AERONET version 2 direct sun algorithm (for details: <http://aeronet.gsfc.nasa.gov>). Quality assured (Level 2) data are available for the first four years of operation, 2009-2012. In 2012 measurements were made between March and November. The necessary post-calibration was made in May 2013.

Monthly mean averages of AOD at 500 nm and the Ångström exponent (440-870 nm), together with their associated standard deviations (sigma) and the number of days (N) for 2009 to 2012 are given in Table 5.

Table 5: Monthly mean and sunlight-season average values of AOD at 500 nm and Ångström coefficient AE measured at the Birkenes observatory in the time period between 2009 and 2012. The values given are mean, standard deviation and number of days with observations (#).

Year	2009		2010		2011		2012	
Month	AOD/#	AE	AOD/#	AE	AOD/#	AE	AOD/#	AE
January					0.02 ± 0.01	0.96 ±		
February					0.03 ± 0.01	1.04 ±		
March					0.07 ± 0.02	0.98 ±	0.07 ± 0.05	1.08 ±
April	0.29 ± 0.00 / 01	1.52 ± 0.00			0.21 ± 0.19	1.17 ±	0.05 ± 0.02	1.57 ±
May	0.09 ± 0.05 / 22	1.16 ± 0.31	0.10 ± 0.04 / 13	1.34 ±	0.13 ± 0.07	1.30 ±	0.08 ± 0.04	1.41 ±
June	0.09 ± 0.05 / 25	1.42 ± 0.27	0.09 ± 0.04 / 16	1.38 ±	0.10 ± 0.04	1.46 ±	0.09 ± 0.04	1.70 ±
July	0.18 ± 0.06 / 11	1.43 ± 0.44	0.10 ± 0.07 / 18	1.44 ±	0.13 ± 0.06	1.58 ±	0.07 ± 0.03	1.59 ±
August	0.17 ± 0.07 / 13	1.14 ± 0.20	0.10 ± 0.05 / 15	1.49 ±	0.09 ± 0.05	1.59 ±	0.08 ± 0.03	1.54 ±
September	0.10 ± 0.04 / 15	0.96 ± 0.24	0.05 ± 0.02 / 16	1.30 ±			0.07 ± 0.01	1.12 ±
October	0.08 ± 0.03 / 12	1.05 ± 0.18	0.07 ± 0.03 / 10	1.30 ±			0.06 ± 0.03	1.38 ±
November			0.04 ± 0.01 / 06	1.30 ±			0.04 ± 0	0.76 ±

As already seen in measurements made in Ny-Ålesund, also the observations from Birkenes show comparable low values (below 0.09 ± 0.04 - maximum in June) during 2012. This is very evident in Figure 41, which shows monthly mean AOD measured during the last four years. The AOD observations from 2012 are located at the lower edge of the natural spread seen since the start of the observations in 2009. The monthly mean AOD values obtained during 2012 were compared with the seasonal variation of AOD for Scandinavian AERONET sites. Quality assured and cloud screened data (Level 2) were available for Gustav Dalen Tower, Helsinki Lighthouse, Hyytiala, and Palgrunden Gustav Dalen Tower (N 58°35, E 17°28, Alt 25 m), Helsinki Lighthouse (N 59°56, E 24°55, Alt 20 m), Hyytiala (N 61°50, E 24°17, Alt 191 m), and Palgrunden (N 58°45, E 13°09, Alt 49 m) (see Table 5 and Figure 45 right panel)

The monthly averaged data show a maximum aerosol load (high AOD) during summer period, which is consistent with what was observed in the rest of Southern Scandinavia. In 2012 at Birkenes were slightly lower during summer, but somewhat higher during autumn, compared with the Swedish/Finish sites. Longer time series are needed to see whether this was a peculiarity of 2012 or a more general tendency within Southern Scandinavia. The clear larger Ångström exponent between June and August indicate a predominance of finer particulates in Southern Norway during summer. The Ångström exponent decreased towards winter-time, indicating larger particles. The annual cycle can be linked to long-range transport patterns from e.g. the European continent. For further results and a general overview of sun photometer measurements in Scandinavia, see Toledano *et al.* (2012).

Table 6: Aerosol optical depth (500 nm) at Birkenes (N 58°23, E 08°15, Alt 230 m), compared to AOD measured at AERONET sites in Scandinavia: Gustav Dalen Tower (N 58°35, E 17°28, Alt 25 m), Helsinki Lighthouse (N 59°56, E 24°55, Alt 20 m), Hyttiala (N 61°50, E 24°17, Alt 191 m), and Palgrunden (N 58°45, E 13°09, Alt 49 m).

Month [2012]	Birkenes	Gustav Dalen Tower	Helsinki Lighthouse	Hyttiala	Palgrunden
March	0.07 ± 0.05				
April	0.05 ± 0.02	0.10 ± 0.06			
May	0.08 ± 0.04	0.11 ± 0.01	0.08 ± 0.01	0.09 ± 0.04	0.11 ± 0.03
June	0.09 ± 0.04	0.08 ± 0.02	0.07 ± 0.03	0.08 ± 0.02	0.10 ± 0.03
July	0.07 ± 0.03	0.13 ± 0.10	0.10 ± 0.06	0.14 ± 0.11	0.10 ± 0.05
August	0.08 ± 0.03	0.11 ± 0.05	0.08 ± 0.03	0.10 ± 0.04	0.08 ± 0.04
September	0.07 ± 0.01	0.06 ± 0.04	0.04 ± 0.01	0.05 ± 0.01	0.05 ± 0.07
October	0.06 ± 0.03	0.03 ± 0.01		0.03 ± 0.00	0.03 ± 0.02
November	0.04 ± 0.00				

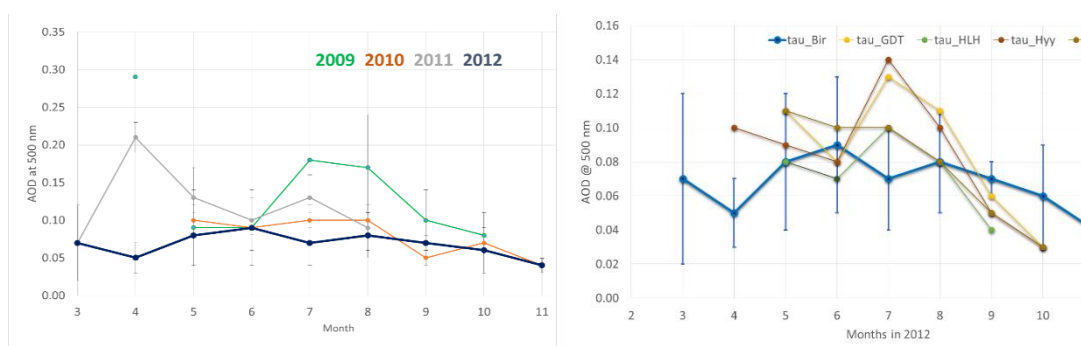


Figure 44: Monthly mean AOD (\pm standard deviation) measured between 2009 and 2012 (left panel) For comparison, in the right panel the seasonal variation of AOD for Scandinavian AERONET sites (with available Level 2 data) for 2012 is given (Gustav Dalen Tower, Helsinki Lighthouse, Hyttiala, and Palgrunden; see Table 6 for location).

7.4.3 Use of aerosol data retrieved from satellites as complementary information

For a long time there have been relative few systematic observations of Arctic aerosols based on Earth Observation data alone, but many global and European studies cover the area of Southern Scandinavia [e.g. Myhre *et al.*, 2005, Schaap *et al.*, 2008, Glantz *et al.*, 2009]. More recently, retrievals have been developed for spectral AOD over snow, in the Arctic regions, using AATSR data in the visible [Istomina *et al.*, 2009] and infrared regions [Istomina *et al.*, 2011], as well as MODIS [Mei *et al.*, 2013]. Although very promising results were obtained from these studies, the data investigated cover limited periods and high biases in the retrievals of AOT were found. This means that investigations of the polar aerosols over bright surfaces based on space-borne data can not be performed at a quantitative level yet. A comparison of AOD in the Arctic with model, satellite and ground-based data has been published by von Hardenberg *et al.* [2012]. This study includes a comparison to Scandinavian sun-photometer sites (Ny-Ålesund, ALOMAR, and Sodankylä), but only a very incomplete ground-based dataset was used for comparison (a couple of seasons), despite the existence of much longer time series. In 2013, Di Pierro *et al.* [2013] and Winker *et al.* [2013] reported the 3-D distribution of tropospheric aerosols as characterized by CALIOP onboard of the CALIPSO satellite. CALIOP aerosol records mainly cover the occurrence of enhanced aerosol loadings; typical background aerosol loadings in the Arctic are below the detection limit of the space-borne LIDAR.

Glantz *et al.* (2013) compared 9-years of MODIS retrievals of aerosol optical properties with sun-photometer AOD observations from Ny-Ålesund and Hornsund/Longyearbyen. The authors found reasonable good agreement, especially during summer time (82% of the satellite values are within the predicted uncertainties of the MODIS retrievals), while there was more variation in spring (62% values were within the uncertainty), most likely due to more heterogeneous aerosol conditions in spring. A review on “aerosol remote sensing in polar regions”, including comparisons to satellite data from MISR, MODIS and AATSR sensors is presently prepared by Tomasi *et al.* (2013).

8. Transport of air to the Zeppelin Observatory

We have performed an analysis and assessment of the source regions of the air masses arriving at Zeppelin in the period 2001-2012. Analyses of the air mass origin are important for the understanding of the observed levels of the gases and aerosols. We have analysed the origin of the air arriving at Zeppelin in 2012 and compared to previous years. Air mass trajectories are calculated using the FLEXTRA trajectory model (<http://www.nilu.no/trajectories/>) and using meteorological data provided from European Centre for Medium Range Weather Forecasts (ECMWF). 7 days backward trajectories from ECMWF have been used to investigate the major transport pathways to Svalbard and Zeppelin.¹⁶ The origin of the air arriving at Zeppelin is categorised in following 6 sectors:

1. **Arctic region:** Clean Arctic air: Air mass trajectories with all trajectory points north of 65° N
2. **Atlantic sector:** Clean marine air: Air mass trajectories with all trajectory points between 10° W and 70° W and from south of 65° N.
3. **North American sector:** Polluted air: If at least 50% of the trajectory points are between 70° W and 180° W, and from south of 65° N.
4. **European sector:** Polluted air: If at least 50% of the trajectory points were between 10° W and 30° E, and from south of 65° N.
5. **Russian sector:** Polluted air: If air mass trajectories with all points between 30° E and 180° E and from south of 65° N.
6. **Undefined sector:** 20% the trajectories do not come from a distinct sector.

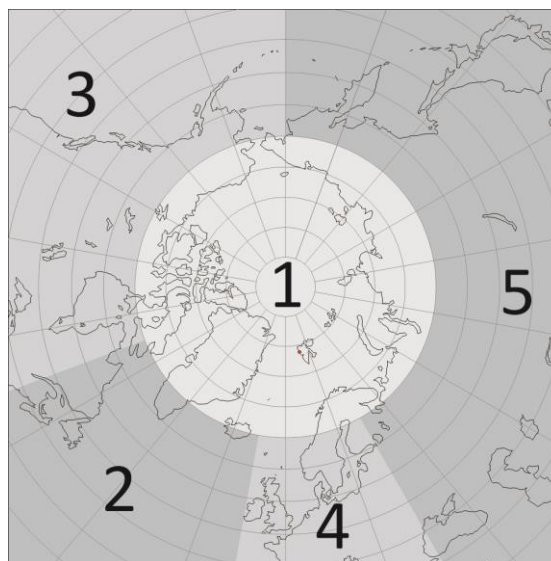


Figure 45: The sectors used to classify the air arriving at the Zeppelin Observatory. 1 is Arctic sector, 2 is Atlantic sector, 3 is North American sector, 4 is European sector and 5 is Russian sector.

Air from the Arctic and Atlantic sector are assumed to contain minimal influence of pollution, as there are almost no industrial sources in these areas, and one can say that the air is 'clean' (although there are increasing industrial activity in the northern part of Russia).

Background values of the greenhouse gases components are defined from those 'clean air' areas with 6 out of 8 trajectories (sampling day +/- 12 hours) within the sector, as described above.

Figure 46 shows the share of polluted and clean air arriving at the Zeppelin observatory for the years 2001-2012. The most striking result of this analysis is that in particularly 2007 and

¹⁶ The spatial resolution is T106, which correspond to a latitude/longitude resolution of 1x1 degrees, the temporal resolution is 6 hours, and 91 levels (60 levels before February 2006) are available in the vertical direction. The data sets used are so-called analysis, which is a combination of observations and numerical calculations. This includes measurements from satellites, radio sondes, buoys, weather stations, etc. which are assimilated into a meteorological model that produce an estimate of the state of the atmosphere at a given time.

2008 the fraction of air arriving at Zeppelin categorized as clean marine and Arctic air was clearly higher than the previous years. As described in section 4.1. the CH₄ concentration has increased since 2005. This can point in the direction of a possible Arctic source or accumulation of methane in the Arctic, particularly during late summer and autumn. Also the year 2003 with high methane concentration had a large fraction of clean air arriving at Zeppelin. 2009 is a somewhat different. In 2009 there were many episodes with polluted air transported to Zeppelin but no episodes as extreme as the record one observed in spring 2006 (Stohl et al., 2007; Myhre et al 2007). In contrast to the last years the site experienced higher influence of polluted air masses from central Europe and from the Russian sector in 2009. Clean arctic marine air dominated only on 59% of the days which is considerable lower than previous years. At the same time the category with mixed air from various sectors has increased slightly, thus the results are connected with uncertainty. 2012 was a quite typical year, with relatively high influence of air from the Russian sector .

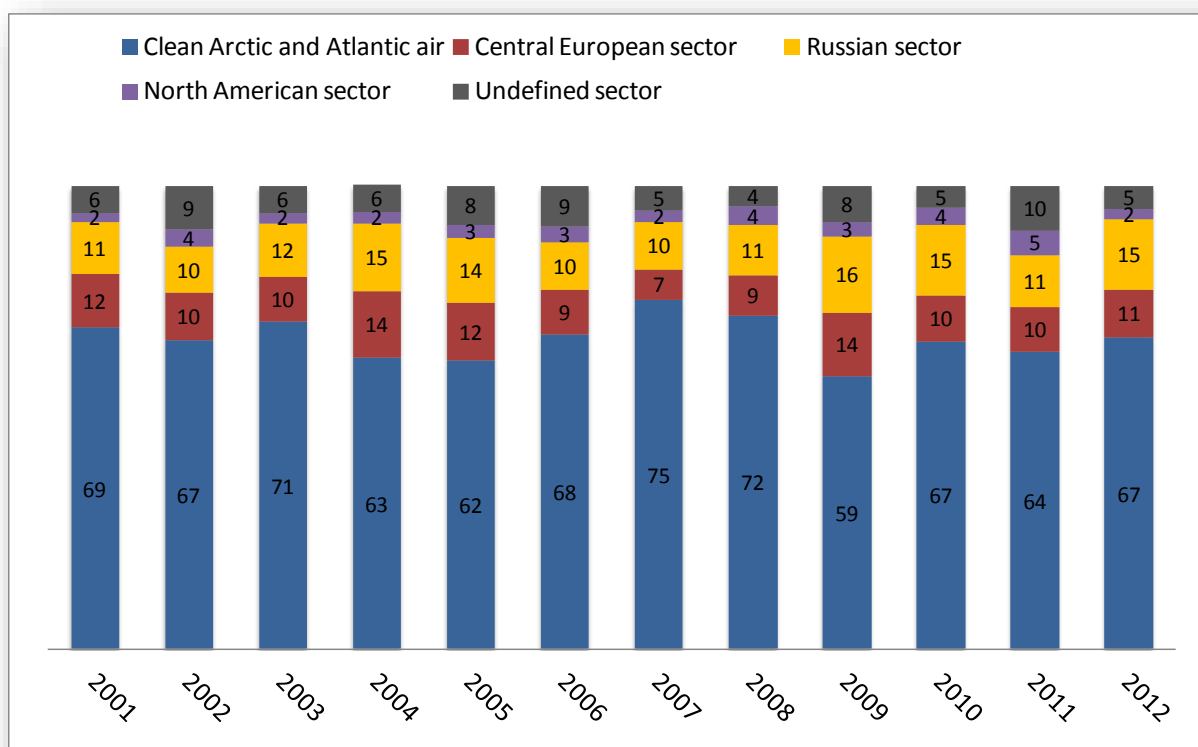


Figure 46: The percentage of polluted and clean air arriving at Zeppelin in the period 2001-2012 from the various sectors.

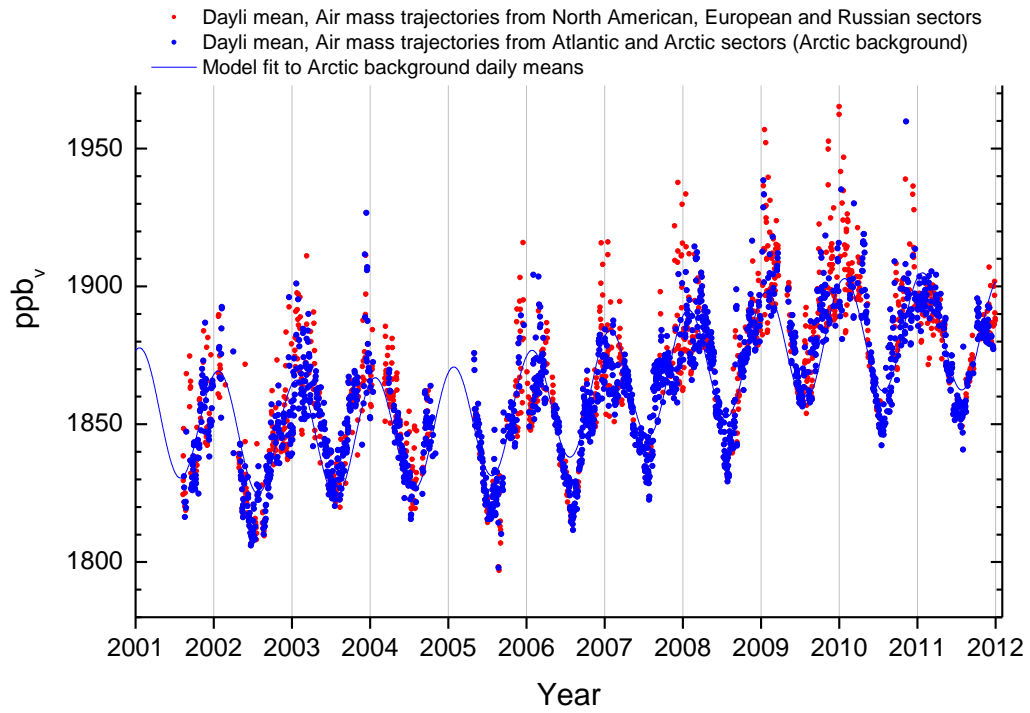


Figure 47: The daily mean methane observations when clean air is arriving (blue dots), compared to daily mean influenced by air from the polluted sections (reds dots).

9. References

- Aas, W., Solberg, S., Manø, S., Yttri, K.E. (2013) Monitoring of long-range transboundary air pollution. Annual report 2012. [In Norwegian]. Kjeller, NILU (Statlig program for forurensningsovervåking. Rapport 1148/2013. M 3/2013) (NILU OR 14/2013).
- Andreae, M.O., Jones, C.D., Cox, P.M. (2005) Strong present-day aerosol cooling implies a hot future. *Nature*, 435, 1187-1190.
- Asmi, A., Collaud Coen, M., Ogren, J.A., Andrews, E., Sheridan, P., Jefferson, A., Weingartner, E., Baltensperger, U., Bukowiecki, N., Lihavainen, H., Kivekäs, N., Asmi, E., Aalto, P.P., Kulmala, M., Wiedensohler, A., Birmili, W., Hamed, A., O'Dowd, C., Jennings, S.G., Weller, R., Flentje, H., Fjaeraa, A.M., Fiebig, M., Lund Myhre, C., Hallar, A.G., Laj, P. (2012) Aerosol decadal trends - Part 2: In-situ aerosol particle number concentrations at GAW and ACTRIS stations. *Atmos. Chem. Phys. Discuss.*, 12, 20849-20899.
- Bergamaschi, P., Frankenberg, C., Meirink, J.F., Krol, M., Dentener, F., Wagner, T., Platt, U., Kaplan, J. O., Körner, S., Heimann, M., Dlugokencky, E.J., Goede, A. (2007) Satellite cartography of atmospheric methane from SCIAMACHY onboard ENVISAT 2. Evaluation based on inverse model simulations. *J. Geophys. Res.*, 112, D02304, doi:10.1029/2006JD007268.
- Bond, T.C., Doherty, S.J., Fahey, D.W., Forster, P.M., Berntsen, T., DeAngelo, B.J., Flanner, M.G., Ghan, S., Kärcher, B., Koch, D., Kinne, S., Kondo, Y., Quinn, P.K., Sarofim, M.C., Schultz, M.G., Schulz, M., Venkataraman, C., Zhang, H., Zhang, S., Bellouin, N., Guttikunda, S.K., Hopke, P.K., Jacobson, M.Z., Kaiser, J.W., Klimont, Z., Lohmann, U., Schwarz, J.P., Shindell, D., Storelvmo, T., Warren, S.G., Zender, C.S. (2013) Bounding the role of black carbon in the climate system: A scientific assessment. *J. Geophys. Res.*, 118, 5380-5552.
- Bousquet, P., Ringeval, B., Pison, I., Dlugokencky, E. J., Brunke, E.-G., Carouge, C., Chevallier, F., Fortems-Cheiney, A., Frankenberg, C., Hauglustaine, D. A., Krummel, P. B., Langenfelds, R. L., Ramonet, M., Schmidt, M., Steele, L. P., Szopa, S., Yver, C., Viovy, N., Ciais, P. (2011) Source attribution of the changes in atmospheric methane for 2006-2008. *Atmos. Chem. Phys.*, 11, 3689-3700, doi:10.5194/acp-11-3689-2011.
- Cohen, A.J., Anderson, H.R., Ostro, B., Pandey, K.D., Krzyzanowski, M., Künzli, N., Gutschmidt, K., Pope, A., Romieu, I., Samet, J.M., Smith, K. (2005) The global burden of disease due to outdoor air pollution. *J. Toxicol. Environ. Health A*, 68, 1301-1307.
- Collaud Coen, M., Andrews, E., Asmi, A., Baltensperger, U., Bukowiecki, N., Day, D., Fiebig, M., Fjaeraa, A.M., Flentje, H., Hyvärinen, A., Jefferson, A., Jennings, S.G., Kouvarakis, G., Lihavainen, H., Lund Myhre, C., Malm, W.C., Mihapopoulos, N., Molenaar, J.V., O'Dowd, C., Ogren, J.A., Schichtel, B.A., Sheridan, P., Virkkula, A., Weingartner, E., Weller, R., Laj, P. (2012) Aerosol decadal trends - Part 1: In-situ optical measurements at GAW and IMPROVE stations. *Atmos. Chem. Phys. Discuss.*, 12, 20785-20848.
- Delene, D.J., Ogren, J.A. (2002) Variability of aerosol optical properties at four North American surface monitoring sites. *J. Atmos. Sci.*, 59, 1135-1150.
- Di Pierro, M., Jaeglé, L., Eloranta, E. W., Sharma, S. (2013) Spatial and seasonal distribution of Arctic aerosols observed by the CALIOP satellite instrument (2006-2012). *Atmos. Chem. Phys.*, 13, 7075-7095, doi: 10.5194/acp-13-7075-2013.
- Dubovik, O., Holben, B.N., Eck, T.F., Smirnov, A., Kaufman, Y.J., King, M.D., Tanre, D., Slutsker, I. (2002) Variability of absorption and optical properties of key aerosol types observed in worldwide locations. *J. Atmos. Sci.*, 59, 590-608.
- Dubovik, O., Smirnov, A., Holben, B.N., King, M.D., Kaufman, Y.J., Eck, T.F., Slutsker, I. (2000) Accuracy assessments of aerosol optical properties retrieved from Aerosol Robotic Network (AERONET) Sun and sky radiance measurements. *J. Geophys. Res.*, 105, 9791-9806.
- Dusek, U., Frank, G.P., Hildebrandt, L., Curtius, J., Schneider, J., Walter, S., Chand, D., Drewnick, F., Hings, S., Jung, D., Borrmann, S., Andreae, M.O. (2006) Size matters more than chemistry for cloud-nucleating ability of aerosol particles. *Science*, 312, 1375-1378.
- Fiebig, M., Hirdman, D., Lunder, C.R., Ogren, J.A., Solberg, S., Stohl, A. (2013) Annual cycle of Antarctic baseline aerosol: controlled by photooxidation-limited aerosol formation. *Atmos. Chem. Phys. Discuss.*, 13, 23057-23088.
- Fisher, R.E., Sriskantharajah, S., Lowry, D., Lanoisellé, M., Fowler, C.M.R., James, R.H., Hermansen, O., Lund Myhre, C. Stohl, A., Greinert, J., Nisbet-Jones, P.B.R., Mienert, J., Nisbet, E.G. (2011) Arctic methane sources: Isotopic evidence for atmospheric inputs. *Geophys. Res. Lett.*, 38, L21803, doi:10.1029/2011GL049319.

- Forster, P., Ramaswamy, V., Artaxo, P., Berntsen, T., Betts, R., Fahey, D.W., Haywood, J., Lean, J., Lowe, D.C., Myhre, G., Nganga, J., Prinn, R., Raga, G., Schulz, M., Van Dorland, R. (2007) Changes in atmospheric constituents and in radiative forcing. In: *Climate Change 2007: The physical science basis. Contribution of Working Group I to the fourth assessment report of the Intergovernmental Panel on Climate Change*. Ed. by Solomon, S., Qin, D., Manning, M., Chen, Z., Marquis, M., Averyt, K.B., Tignor, M., Miller, H.L. Cambridge, Cambridge University Press.
- Glantz, P., Johansson, C., Kokhanovsky, A., von Hoyningen-Huene, W. (2009) Estimating PM_{2.5} over southern Sweden using space-borne optical measurements. *Atmos. Environ.*, **43**, 5838-5846.
- Glantz, P., Tesche, M., Struthers, H., Stebel, K. (2012) Satellite and ground-based observations of aerosol optical properties in the Arctic for the period 2003-2011. Poster presented at the CRAICC meeting, Oslo, 26th - 28th August, 2012.
- Haywood, J.M., Shine, K.P. (1995) The effect of anthropogenic sulfate and soot aerosol on the clear sky planetary radiation budget. *Geophys. Res. Lett.*, **22**, 603-606.
- Heintzenberg, J. (1980) Particle size distribution and optical properties of arctic haze. *Tellus*, **32**, 251-260.
- Herber, A., Thomason, L.W., Gernandt, H., Leiterer, U., Nagel, D., Schulz, K., Kaptur, J., Albrecht, T., Notholt, J. (2002) Continuous day and night aerosol optical depth observations in the Arctic between 1991 and 1999. *J. Geophys. Res.*, **107**, 4097, doi:10.1029/2001JD000536.
- Hoffmann, A., Ritter, C., Stock, M., Maturilli, M., Eckhardt, S., Herber, A., Neuber, R. (2010) Lidar measurements of the Kasatochi aerosol plume in August and September 2008 in Ny-Alesund, Spitsbergen, J. *Geophys. Res.*, **115**, D00L12, doi:10.1029/2009JD013039.
- Holben, B., Eck, T., Slutsker, I., Tanré, D., Buis, J., Setzer, A., Vermote, E., Reagan, J., Kaufman, Y. (1998) AERONET- a federated instrument network and data archive for aerosol characterization. *Remote Sens. Environ.*, **66**, 1-16.
- IPCC (2007) Summary for Policymakers. In: *Climate Change 2007: The Physical Science Basis. Contribution of Working Group I to the Fourth Assessment Report of the Intergovernmental Panel on Climate Change*. Ed. by: Solomon, S., Qin, D., Manning, M., Chen, Z., Marquis, M., Averyt, K.B., Tignor, M., Miller, H.L. Cambridge, Cambridge University Press.
- IPCC (2013) SPM: Summary for Policymakers. In: *Climate Change 2013: The Physical Science Basis. Contribution of Working Group I to the Fifth Assessment Report of the Intergovernmental Panel on Climate Change*. Ed. by: Stocker, T.F., Qin, D., Plattner, G.-K., Tignor, M., Allen, S.K., Boschung, J., Nauels, A., Xia, Y., Bex, V. and Midgley, P.M. Cambridge, United Kingdom and New York, NY, USA, Cambridge University Press.
- IPCC (2013) Climate Change 2013: The Physical Science Basis. Contribution of Working Group I to the Fifth Assessment Report of the Intergovernmental Panel on Climate Change. Ed. by: Stocker, T.F., Qin, D., Plattner, G.-K., Tignor, M., Allen, S.K., Boschung, J., Nauels, A., Xia, Y., Bex, V. and Midgley, P.M. Cambridge, United Kingdom and New York, NY, USA, Cambridge University Press.
- Isaksen, I.S.A., Hov, Ø. (1987) Calculation of trends in the tropospheric concentration of O₃, OH, CO, CH₄ and NO_x. *Tellus*, **39B**, 271-285.
- Isaksen, I.S.A., Gauss, M., Myhre, G., Walter Anthony, K.M., Ruppel, C. (2010) Strong atmospheric chemistry feedback to climate warming from Arctic methane emissions. *Global Biogeochem. Cycles*, **25**, GB2002, doi:10.1029/2010GB003845.
- Istomina, L.G., von Hoyningen-Huene, W., Kokhanovsky, A.A., Burrows, J.P. (2009) Retrieval of aerosol optical thickness in arctic region using dual-view AATSR observations, *Proceedings of ESA Atmospheric Science Conference*, Barcelona, 07.-11. Sept. 2009. ESA SP-676.
- Istomina, L.G., von Hoyningen-Huene, W., Kokhanovsky, A.A., Schultz, E., Burrows, J.P. (2011) Remote sensing of aerosols over snow using infrared AATSR observations. *Atmos. Meas. Tech.*, **4**, 1133-1145, doi:10.5194/amt-4-1133-2011.
- Jaenicke, R. (1980) Natural aerosols. *Ann. New York Acad. Sci.*, **338**, 317-329.
- Kiehl, J.T. (2007) Twentieth century climate model response and climate sensitivity. *Geophys. Res. Lett.*, **34**, L22710, doi:10.1029/2007GL31383.
- Kreidenweis, S.M., Petters, M.D., Chuang, P.Y. (2009) Cloud particle precursors. In: *Clouds in the perturbed climate system : Their relationship to energy, balance, atmospheric dynamics, and precipitation*. Ed. by: Heintzenberg, J., Charlson, R.J. Cambridge, MA, MIT Press (Strüngmann Forum Reports). pp. 291-318.
- Kristiansen, N.I., Stohl, A., Prata, A.J., Richter, A., Eckhardt, S., Seibert, P., Hoffmann, A., Ritter, C., Bitar, L., Duck, T.J., Stebel, K. (2010) Remote sensing and inverse transport modeling of the Kasatochi eruption sulfur dioxide cloud. *J. Geophys. Res.*, **115**, D00L16, doi:10.1029/2009JD013286.

- Kulmala, M., Vehkamäki, H., Petäjä, T., DalMaso, M., Lauri, A., Kerminen, V.-M., Birmili, W., McMurry, P.H. (2004) Formation and growth rates of ultrafine atmospheric particles: a review of observations. *J. Aerosol Sci.*, 35, 143-176.
- Law, K., Stohl, A. (2007) Arctic air pollution: Origins and impacts. *Science*, 315, 1537-1540.
- Lewis, K., Arnott, W.P., Moosmüller, H., Wold, C.E. (2008) Strong spectral variation of biomass smoke light absorption and single scattering albedo observed with a novel dual-wavelength photoacoustic instrument. *J. Geophys. Res.*, 113, D16203, doi: 10.1029/2007JD009699.
- Löhndahl, J., Swietlicki, E., Lindgren, E., Loft, S. (2010) Aerosol exposure versus aerosol cooling of climate: what is the optimal emission reduction strategy for human health? *Atmos. Chem. Phys.*, 10, 9441-9449.
- Mazzola, M., Stone, R.S., Herber, A., Tomasi, C., Lupi, A., Vitale, V., Lanconelli, C., Toledano, C., Cachorro, V.E., O'Neill, N.T., Shiobara, M., Aaltonen, V., Stebel, K., Zielinski, T., Petelski, T., Ortiz de Galisteo, J.P., Torres, B., Berjon, A., Goloub, P., Li, Z., Blarel, L., Abboud, I., Cuevas, E., Stock, M., Schulz, K.-H., Virkkula, A. (2011) Evaluation of sun photometer capabilities for retrievals of aerosol optical depth at high latitudes: The POLAR-AOD intercomparison campaigns. *Atmos. Environ.*, 52, 4-17, doi:10.1016/j.atmosenv.2011.07.042.
- McFiggans, G., Artaxo, P., Baltensperger, U., Coe, H., Facchini, M.C., Feingold, G., Fuzzi, S., Gysel, M., Laaksonen, A., Lohmann, U., Mentel, T.F., Murphy, D.M., O'Dowd, C.D., Snider, J.R., Weingartner, E. (2006) The effect of physical and chemical aerosol properties on warm cloud droplet activation. *Atmos. Chem. Phys.*, 6, 2593-2649, doi:10.5194/acp-6-2593-2006.
- Mei, L., Xue, Y., de Leeuw, G., von Hoyningen-Huene, W., Kokhanovsky, A.A., Istomina, L., Guang, J., Burrows, J.P. (2013) Aerosol optical depth retrieval in the Arctic region using MODIS data over snow. *Rem. Sens. Environ.*, 128, 234-245, doi: 10.1016/j.rse.2012.10.009.
- Myhre, C.L., Hermansen, O., Fjæraa, A.M., Lunder, C., Schmidbauer, N., Stebel, K., Prata, F. (2010) Greenhouse monitoring at the Zeppelin station - annual report 2008. Kjeller, NILU (Statlig program for forurensningsovervåking. Rapport 1071/2010) (TA 2633/2010) (NILU OR 24/2010).
- Myhre, C.L., Toledano, C., Myhre, G., Stebel, K., Yttri, K.E., Aaltonen, V., Johnsrud, M., Frioud, M., Cachorro, V., de Frutos, A., Lihavainen, H., Campbell, J.R., Chaikovsky, A.P., Shiobara, M., Welton, E.J., Tørseth, K. (2007) Regional aerosol optical properties and radiative impact of the extreme smoke event in the European Arctic in spring 2006. *Atmos. Chem. Phys.*, 7, 5899-5915.
- Myhre, G., Fuglestad, J.S., Berntsen, T.K., Lund, M.T. (2011) Mitigation of short-lived heating components may lead to unwanted long-term consequences. *Atmos. Environ.*, 45, 6103-6106.
- Myhre, G., Stordal, F., Johnsrud, M., Diner, D.J., Geogdzhayev, I.V., Haywood, J.M., Holben, B.N., Holzer-Popp, T., Ignatov, A., Kahn, R.A., Kaufman, Y.J., Loeb, N., Martonchik, J.V., Mishchenko, M.I., Nalli, N.R., Remer, L.A., Schroedter-Homscheidt, M., Tanré, D., Torres, O., Wang, M. (2005) Intercomparison of satellite retrieved aerosol optical depth over ocean during the period September 1997 to December 2000. *Atmos. Chem. Phys.*, 5, 1697-1719, doi: 10.5194/acp-5-1697-2005.
- NASA Goddard Space Flight Center (2011) AERONET Aerosol Robotic Network. URL: <http://aeronet.gsfc.nasa.gov/> [2011-06-09].
- Nyeki et al. (2013) Ground-based aerosol optical depth trends at baseline GAW-PFR stations from 2000 - 2012. Manuscript in preparation for *J. Geophys. Res.*
- O'Neill, N., Eck, T., Smirnov, A., Holben, B. (2008) Spectral Deconvolution Algorithm (SDA), Technical memo, version 4.1. AERONET, NASA. URL: http://aeronet.gsfc.nasa.gov/new_web/PDF/tauf_tauc_technical_memo.pdf
- O'Neill, N.T., Perro, C., Saha, A., Lesins, G., Duck, T.J., Eloranta, E.W., Nott, G.J., Hoffman, A., Karumudi, M.L., Ritter, C., Bourassa, A., Abboud, I., Carn, S.A., Savastiouk, V. (2012), Properties of Sarychev sulphate aerosols over the Arctic. *J. Geophys. Res.*, 117, D04203, doi:10.1029/2011JD016838.
- Prather, M., Ehhalt, D., Dentener, F., Derwent, R.G., Dlugokencky, E., Holland, E., Isaksen, I.S.A., Katima, J., Kirchhoff, V., Matson, P., Midgley, P.M., Wang, M. (2001) Atmospheric chemistry and greenhouse gases. In: *Climate Change 2001: The Scientific Basis, Contribution of Working Group I to the Third Assessment Report of the Intergovernmental Panel on Climate Change*. Ed. by: Houghton, J.T., Ding, Y., Griggs, D.J., Noguer, M., van der Linden, P.J., Dai, X., Maskell, K. and Johnson, C.A. Cambridge, Cambridge University Press. pp. 239-287.
- Petzold, A., Ogren, J.A., Fiebig, M., Laj, P., Li, S.-M., Baltensperger, U., Holzer-Popp, T., Kinne, S., Pappalardo, G., Sugimoto, N., Wehrli, C., Wiedensohler, A., Zhang, X.-Y. (2013) Recommendations for reporting "black carbon" measurements. *Atmos. Phys. Chem.*, 13, 8365-8379.
- Raes, F., Van Dingenen, R., Vignati, E., Wilson, J., Putaud, J.-P., Seinfeld, J. H., Adams, P. (2000) Formation and cycling of aerosols in the global troposphere. *Atmos. Environ.*, 34, 4215-4240.

- Repo, M.E., Susiluoto, S., Lind, S.E., Jokinen, S., Elsakov, V., Biasi, C., Virtanen, T., Pertti, J., Martikainen, P.J. (2009) Large N₂O emissions from cryoturbated peat soil in tundra. *Nature Geosci.*, 2, 189-192.
- Rigby, M., Prinn, R.G., Fraser, P.J., Simmonds, P.G., Langenfelds, R.L., Huang, J., Cunnold, D.M., Steele, L.P., Krummel, P.B., Weiss, R.F., O'Doherty, S., Salameh, P.K., Wang, H.J., Harth, C.M., Mühle, J., Porter, L.W. (2008) Renewed growth of atmospheric methane. *Geophys. Res. Lett.*, 35, L22805, doi:10.1029/2008GL036037.
- Rodríguez, E., Toledano, C., Cachorro, V.E., Ortiz, P., Stebel, K., Berjón, A., Blindheim, S., Gausa, M., de Frutos, A.M. (2012) Aerosol characterization at the sub-Arctic site Andenes (69°N, 16°E), by the analysis of columnar optical properties. *Quart. J. Roy. Meteorol. Soc.*, 138, 471-482, doi:10.1002/qj.921.
- Schaap, M., Timmermans, R.M.A., Koelemeijer, R.B.A., de Leeuw, G., Bultjes, P.J.H. (2008) Evaluation of MODIS aerosol optical thickness over Europe using sun photometer observations. *Atmos. Environ.*, 42, 2187-2197, doi:10.1016/j.atmosenv.2007.11.044.
- Schuur, E., Abbot, B. (2011) High risk of permafrost thaw. *Nature*, 480, 32-33.
- Seinfeld, J., Pandis, S. (1998) Atmospheric chemistry and physics: From air pollution to climate change. New York, John Wiley & Sons.
- Sheridan, P.J., Ogren, J.A. (1999) Observations of the vertical and regional variability of aerosol optical properties over central and eastern North America. *J. Geophys. Res.*, 104, 16793-16805.
- Shindell, D., Faluvegi, G. (2009) Climate response to regional radiative forcing during the twentieth century. *Nature Geosci.*, 2, 294-300.
- Simmonds, P.G., Manning, A.J., Cunnold, D.M., Fraser, P.J., McCulloch, A., O'Doherty, S., Krummel, P.B., Wang, R.H.J., Porter, L.W., Derwent, R.G., Gready, B., Salameh, P., Miller, B.R., Prinn, R.G., Weiss, R.F. (2006) Observations of dichloromethane, trichloroethene and tetrachloroethene from the AGAGE stations at Cape Grim, Tasmania, and Mace Head, Ireland. *J. Geophys. Res.*, 111, D18304, doi:10.1029/2006JD007082.
- Smirnov, A., Holben, B.N., Eck, T.F., Dubovik, O., Slutsker, I. (2000) Cloud-screening and quality control algorithms for the AERONET database. *Remote Sens. Environ.*, 73, 337-349.
- Sodemann, H., Pommier, M., Arnold, S.R., Monks, S.A., Stebel, K., Burkhardt, J.F., Hair, J.W., Diskin, G.S., Clerbaux, C., Coheur, P.-F., Hurtmans, D., Schlager, H., Blechschmidt, A.-M., Kristjánsson, J.E., Stohl, A. (2011) Episodes of cross-polar transport in the Arctic troposphere during July 2008 as seen from models, satellite, and aircraft observations. *Atmos. Chem. Phys.*, 11, 3631-3651, doi:10.5194/acp-11-3631-2011.
- Solomon, S., Daniel, J.S., Neely III, R.R., Vernier, J.-P., Dutton, E.G., Thomason, L.W. (2011) The persistently variable "background" stratospheric aerosol layer and global climate change. *Science*, 333, 866-870. doi:10.1126/science.1206027.
- Stohl, A., Seibert, P. (1998) Accuracy of trajectories as determined from the conservation of meteorological tracers. *Quart. J. Roy. Meteorol. Soc.*, 124, 1465-1484.
- Stohl, A., Andrews, E., Burkhardt, J.F., Forster, C., Herber, A., Hoch, S.W., Kowal, D., Lunder, C., Mefford, T., Ogren, J.A., Sharma, S., Spichtinger, N., Stebel, K., Stone, R., Strom, J., Tørseth, K., Wehrl, C., Yttri, K.E. (2006) Pan-Arctic enhancements of light absorbing aerosol concentrations due to North American boreal forest fires during summer 2004. *J. Geophys. Res.*, 111, D22214, doi:10.1029/2006JD007216.
- Stohl, A., Berg, T., Burkhardt, J.F., Fjæraa, A.M., Forster, C., Herber, A., Hov, Ø., Lunder, C., McMillan, W.W., Oltmans, S., Shiobara, M., Simpson, D., Solberg, S., Stebel, K., Ström, J., Tørseth, K., Treffeisen, R., Virkkunen, K., Yttri, K.E. (2007) Arctic smoke - record high air pollution levels in the European Arctic due to agricultural fires in Eastern Europe in spring 2006. *Atmos. Chem. Phys.*, 7, 511-534.
- Stohl, A., Forster, C., Frank, A., Seibert, P., Wotawa, G. (2005) Technical note: The lagrangian particle dispersion model flexpart version 6.2. *Atmos. Chem. Phys.*, 5, 2461-2474.
- Stohl, A., Hittenberger, M., Wotawa, G. (1998) Validation of the lagrangian particle dispersion model FLEXPART against large scale tracer experiment data. *Atmos. Environ.*, 32, 4245-4264.
- Stohl, A., Wotawa, G., Seibert, P., Kromp-Kolb, H. (1995) Interpolation errors in wind fields as a function of spatial and temporal resolution and their impact on different types of kinematic trajectories. *J. Appl. Meteor.*, 34, 2149-2165.
- Toledano, C., Cachorro, V., Gausa, M., Stebel, K., Aaltonen, V., Berjón, A., Ortiz de Galisteo, J.P., de Frutos, A.M., Bennouna, Y., Blindheim, S., Myhre, C.L., Zibordi, G., Wehrl, C., Kratzer, S., Hakansson, B., Carlund, T., de Leeuw, G., Herber, A., Torres, B. (2011) Overview of sun photometer measurements of aerosol properties in Scandinavia and Svalbard. *Atmos. Environ.*, 52, 18-28, doi:10.1016/j.atmosenv.2011.10.022.

- Tomasi, C., Vitale, V., Lupi, A., Di Carmine, C., Campanelli, M., Herber, A., Treffeisen, R., Stone, R.S., Andrews, E., Sharma, S., Radionov, V., von Hoyningen-Huene, W., Stebel, K., Hansen, G.H., Myhre, C.L., Wehrli, C., Aaltonen, V., Lihavainen, H., Virkkula, A., Hillamo, R., Ström, J., Toledano, C., Cachorro, V.E., Ortiz, P., de Frutos, A.M., Blindheim, S., Frioud, M., Gausa, M., Zielinski, T., Petelski, T., Yamanouchi, T. (2007) Aerosols in polar regions: A historical overview based on optical depth and in situ observations. *J. Geophys. Res.*, 112, D16205, doi:10.1029/2007JD008432.
- Tomasi, C., Lupi, A., Mazzola, M., Stone, R., Dutton, E., Herber, A., Radionov, V., Holben, B., Sorokin, M.G., Sakerin, M.S., Terpigova, S.A., Sobolewski, P.S., Lanconelli, C., Petkov, B.H., Busetto, M., Vitale, V. (2012) An update on Polar aerosol optical properties using POLAR-AOD and other measurements performed during the International Polar Year. *Atmos. Environ.*, 52, 29-47, doi: 10.1016/j.atmosenv.2012.02.055.
- Tomasi, C., Kokhanovsky, A.A., Lupi, A., Ritter, C., Mazzola, M., Lanconelli, C., Vitale, V., Herber, A., Altonen, V., Wehrli, C., Nyeki, S., Stebel, K., Zielinski, T., Petelski, T., Radionov, V.F., Sakerin, S.M., Kabanov, D.M., Polkin, V.V., Stone, R.S. (2013) Aerosol remote sensing in polar regions. Manuscript in preparation for *Earth Sci. Rev.*
- Von Hardenberg, J., Vozella, L., Tomasi, C., Vitale, V., Lupi, A., Mazzola, M., van Noije, T.P.C., Strunk, A., Provenzale, A. (2012) Aerosol optical depth over the Arctic: a comparison of ECHAM-HAM and TM5 with ground-based, satellite and reanalysis data. *Atmos. Chem. Phys.*, 12, 6953-6967, doi:10.5194/acp-12-6953-2012.
- Walter, K.M., Edwards, M.E., Grosse, G., Zimov, S.A., Chapin III, F.S. (2007) Thermokarst lakes as a source of atmospheric CH₄ during the last deglaciation. *Science*, 318, 633-636.
- Wehrli, C. (2000) Calibrations of filter radiometers for determination of atmospheric optical depth. *Metrologia*, 37, 419-422.
- Wehrli, C. (2005) GAWPFR: A network of aerosol optical depth observations with precision filter radiometers. In: *WMO/GAW Experts workshop on a global surface based network for long term observations of column aerosol optical properties*. Geneva, World Meteorological Organization (GAW Report No. 162, WMO TD No. 1287).
- Winker, D.M., Tackett, J.L., Getzewich, B.J., Liu, Z., Vaughan, M.A., Rogers, R. R. (2012) The global 3-D distribution of tropospheric aerosols as characterized by CALIOP. *Atmos. Chem. Phys. Discuss.*, 12, 24847-24893.
- WMO (2013) Greenhouse Gas Bulletin. The state of greenhouse gases in the atmosphere using global observations through 2012. Geneva, World Meteorological Organization (Bulletin No. 9, 6 November 2013). URL: http://www.wmo.int/pages/prog/arep/gaw/ghg/documents/GHG_Bulletin_No.9_en.pdf
- WMO (2012) Greenhouse Gas Bulletin. The state of greenhouse gases in the atmosphere using global observations through 2011. Geneva, World Meteorological Organization (Bulletin No. 8, 19 November 2012). URL: http://www.wmo.int/pages/prog/arep/gaw/ghg/documents/GHG_Bulletin_No.8_en.pdf
- WMO (2011) Scientific assessment of ozone depletion: 2010. Geneva, World Meteorological Organization (Global ozone research and monitoring project, Report No. 52).
- WMO (2009) Greenhouse Gas Bulletin. The state of greenhouse gases in the atmosphere using global observations through 2008. Geneva, World Meteorological Organization (Bulletin No. 5, 23 November 2009). URL: http://www.wmo.int/pages/prog/arep/gaw/ghg/documents/ghg-bulletin2008_en.pdf
- Zaelke, D.J., Ramanathan, V. (2012) Going beyond carbon dioxide. *The New York Times*, Dec 6, 2012. URL: https://www.nytimes.com/2012/12/07/opinion/going-beyond-carbon-dioxide.html?_r=1&

APPENDIX 1

Description of instruments, methods and trend analysis

In this appendix are the instrumental methods used for the measurements of the various greenhouse gases presented. Additionally we explain the theoretical methods used in the calculation of the trends. In the end of the section we show how the annual mean values presented in Table 2 are calculated.

Details about greenhouse gas measurements and recent improvement and extensions

Halogenated compounds

NILU performs measurements of halogenated greenhouse gases as well as methane and carbon monoxide using automated gas chromatographs with high sampling frequencies at Zeppelin. A mass spectrometric detector is used to determine more than 20 halogenated compounds, automatically sampled 12 times per day. Methane and CO are sampled 3 times per hour. This high sampling frequency gives valuable data for the examination of episodes caused by long-range transport of pollutants as well as a good basis for the study of trends and global atmospheric change. Close cooperation with AGAGE-partners on the halocarbon instrument and audits on the methane and CO-instruments results in data of high quality. (Audits performed by EMPA on the behalf of GAW/WMO)

At the Birkenes Observatory a very different approach is used. At this site Picarro Cavity Ring-Down Spectroscopy (CRDS) is employed. This is a state of the art infrared spectrometer for field measurements with very high time resolution and precision. The CRDS technology allows monitoring of CO₂ and CH₄ in moist air. During post-processing concentrations are re-calculated for dry air. This is required to remove the variability of moisture in the atmosphere, and to make the monitoring results comparable with traditional FTIR monitoring methods.

Table 7: Instrumental details for greenhouse gas measurements at Zeppelin and Birkenes.

Component		Instrument and method	Time res.	Calibration procedures	Comment
Methane (Birkenes)	CH ₄	Picarro CRDS G1301 CO ₂ /CH ₄ /H ₂ O	5 s	Working std. calibrated against GAW stds at EMPA	Measurements started 19. May 2009. Data coverage in 2012 was 100%, no days were lacking daily mean.
Methane (Zeppelin)	CH ₄	GC-FID/Picarro CRDS from 20.4.2012	5 sec	NOAA reference standards	Data coverage 2012: 93%
Nitrous oxide (Zeppelin)	N ₂ O	GC-FID	30 min	Data coverage 2012: 68%	Hourly, working std. calibrated vs. NOAA stds
Carbon monoxide	CO	GC-HgO/UV	20 min	Every 20 min, working std. calibrated vs. GAW std.	Data coverage 2012: 90%
Carbon dioxide (Zeppelin)	CO ₂	Picarro CRDS from 20.4.2013	1 h/5 sec	NOAA reference standards	CO ₂ measurements in cooperation with ITM Stockholm University (SU). Data coverage 2012: 93%
Carbon dioxide (Birkenes)	CO ₂	Picarro CRDS G1301 CO ₂ /CH ₄ /H ₂ O	5 s	Working std. calibrated against GAW stds at EMPA	Measurements started 19 May 2009.
CFC-11 CFC-12 CFC-113 CFC-115 HFC-125 HFC-134a HFC-152a HFC-365mfc HCFC-22 HCFC-141b HCFC-142b H-1301 H-1211	CFCl ₃ CF ₂ Cl ₂ CF ₂ ClCFCl ₂ CF ₃ CF ₂ Cl CHF ₂ CF ₃ CH ₂ FCF ₃ CH ₃ CHF ₂ CF ₃ CH ₂ CHF ₂ CH ₃ CHF ₂ Cl CH ₃ CFCl ₂ CH ₃ CF ₂ Cl CF ₃ Br CF ₂ ClBr	ADS-GCMS	4 h	Every 4 hours, working std. calibrated vs. AGAGE std.	This instrument was not in operation in 2012 (see next row). Data coverage 2011: no data reported from this instrument after 31.12.2010 The measurements of the CFCs have higher uncertainty and are not within the required precision of AGAGE. See next section for details.

Table 7, cont.:

Component		Instrument and method	Time res.	Calibration procedures	Comment
Methyl Chloride	CH ₃ Cl				
Methyl Bromide	CH ₃ Br				
Methylendichloride	CH ₂ Cl ₂				
Chloroform	CHCl ₃				
Methylchloroform	CH ₃ CCl ₃				
TriChloroethylene	CHClCCl ₂				
Perchloroethylene	CCl ₂ CCl ₂				
Sulphurhexafluoride	SF ₆				
Tetrafluormethane	CF ₄	Medusa-GCMS	2 h	Every 2	Data coverage 2012:
PFC-116	C ₂ F ₆	No. 19		hours,	70%
PFC-218	C ₃ F ₈			working std.	
PFC-318	c-C ₄ F ₈			calibrated vs.	
Sulphurhexafluoride	SF ₆			AGAGE std	
Sulfuryl fluoride	SO ₂ F ₂				
HFC-23	CHF ₃				
HFC-32	CH ₂ F ₂				
HFC-125	CHF ₂ CF ₃				
HFC-134a	CH ₂ FCF ₃				
HFC-143a	CH ₃ CF ₃				
HFC-152a	CH ₃ CHF ₂				
HFC-227ea	CF ₃ CHFCF ₃				
HFC-236fa	CF ₃ CH ₂ CF ₃				
HFC-245fa	CF ₃ CH ₂ CHF ₂				
HFC-365mfc	CF ₃ CH ₂ CHF ₂ CH ₃				
HCFC-22	CHF ₂ Cl				
HCFC-124	CHClFCF ₃				
HCFC-141b	CH ₃ CFCl ₂				
HCFC-142b	CH ₃ CF ₂ Cl				
CFC-11	CFCl ₃				
CFC-12	CF ₂ Cl ₂				
CFC-113	CF ₂ ClCFCl ₂				
CFC-114	CF ₂ ClCF ₂ Cl				
CFC-115	CF ₃ CF ₂ Cl				
H-1211	CF ₃ Br				
H-1301	CF ₂ ClBr				
H-2402	CF ₂ BrCF ₂ Br				
Methyl Chloride	CH ₃ Cl				
Methyl Bromide	CH ₃ Br				
Methyl Iodide	CH ₃ I				
Methylendichloride	CH ₂ Cl ₂				
Chloroform	CHCl ₃				
Methylchloroform	CH ₃ CCl ₃				
Dibromomethane	CH ₂ Br ₂				
Bromoform	CHBr ₃				
TriChloroethylene	TCE				
Perchloroethylene	PCE				
Ethane	C ₂ H ₆				
Benzene	C ₆ H ₆				
Carbonyl Sulfide	COS				
Ozone	O ₃		5 min		

Data quality and uncertainties; In 2001 - 2010 measurements of a wide range of hydrochlorofluorocarbons, hydrofluorocarbons (HCFC-141b, HCFC-142b, HFC-134a etc.), methyl halides (CH₃Cl, CH₃Br, CH₃I) and the halons (e.g. H-1211, H-1301) were measured with good scientific quality by using ADS-GCMS. The system also measured other compounds like the chlorofluorocarbons, but the quality and the precision of these measurements was not at the same level. Table 8 shows a list over those species measured with the ADS-GCMS at Zeppelin Observatory. The species that are in blue are of acceptable scientific quality and in accordance with recommendations and criteria of the AGAGE network for measurements of halogenated greenhouse gases. Those listed in red have higher uncertainty and are not within the required precision of AGAGE. There are various reasons for this increased uncertainty; unsolved instrumental problems e.g. possible electron overload in detector (for the CFC's), influence from other species, detection limits (CH₃I, CHClCl₂) and unsolved calibration problems (CHBr₃).

Table 8: ADS-GCMS measured species. Good scientific quality data in Blue; Data with reduced quality data in Red. The data are available through <http://ebas.nilu.no>. Please read and follow the stated data policy upon use.

Compound	Typical precision (%)	Compound	Typical precision (%)
SF ₆	1.5	H1301	1.5
HFC134a	0.4	H1211	0.4
HFC152a	0.6	CH ₃ Cl	0.6
HFC125	0.8	CH ₃ Br	0.8
HFC365mfc	1.7	CH ₃ I	5.1
HCFC22	0.2	CH ₂ Cl ₂	0.4
HCFC141b	0.5	CHCl ₃	0.3
HCFC142b	0.5	CHBr ₃	15
HCFC124	2.3	CCl ₄	0.5
CFC11	0.3	CH ₃ CCl ₃	0.6
CFC12	0.3	CHClCCl ₂	1.2
CFC113	0.2	CCl ₂ CCl ₂	0.7
CFC115	0.8		

Table 9 gives an overview over the species measured with the Medusa-GCMS and GC-MD systems at the AGAGE stations and the typical precision with the different instruments. The Medusa-GCMS instrument at the Zeppelin Observatory is considered as an AGAGE station and the measurements performed meet the same criteria as shown in Table 9.

Table 9: AGAGE measured species.

Compound	Typical precision (%)	Compound	Typical precision (%)
CF ₄	0.15	H1301	1.5
C ₂ F ₆	0.9	H1211	0.5
C ₃ F ₈	3	H2402	2
SF ₆	0.4	CH ₃ Cl	0.2
SO ₂ F ₂	1.6	CH ₃ Br	0.5
HFC23	0.7	CH ₃ I	2
HFC32	5	CH ₂ Cl ₂	0.8
HFC134a	0.4	CHCl ₃	0.6
HFC152a	1.2	CHBr ₃	0.6
HFC125	1	CCl ₄	1
HFC143a	1.2	CH ₃ CCl ₃	0.7
HFC365mfc	10	CHClCCl ₂	2.5
HCFC22	0.3	CCl ₂ CCl ₂	0.5
HCFC141b	0.4	C ₂ H ₂	0.5
HCFC142b	0.6	C ₂ H ₄	2
HCFC124	2	C ₂ H ₆	0.3
CFC11	0.15	C ₆ H ₆	0.3
CFC12	0.05	C ₇ H ₈	0.6
CFC13	2		
CFC113	0.2		
CFC114	0.3		
CFC115	0.8		

Methane

Revision of the methane data series in 2012 and 2013

The methane data series from Zeppelin has been revised as part of the EU project INGOS, WP2 - *Correction and harmonisation of historic concentration measurements* (<http://www.ingos-infrastructure.eu/>) during 2012. All original measurement signals have been processed with new improved software to recalculate every single measurement over the last 12 years. This new software facilitates systems for QA/QC and detection of measurement errors. The data series has got a clean-up and the precision of existing measurements has improved.

Over the last 12 years period a selected number of working standards have been stored and was last year analysed against new reference standards using new improved instrumentation. All other working standards are linked to these through comparative measurements. Hence, all calibrations over the 12 year period have been recalculated and the whole time series adjusted accordingly.

There were two instruments, the GC-FID and a new Picarro (Cavity Ring-Down Spectrometer) run in parallel in 2012. The Picarro also participated in a GAW audit during autumn 2012 with good results. Comparisons of the data from the two instruments are shown below.

N₂O measurements

N₂O is measured using a gas chromatograph with an electron capture detector. The instrument has performed well during the period, but have a gap in measurements late fall 2012 due to problems with delivery of carrier gas. The instrument needs a special gas mixture to perform well. This special gas has long delivery times from

the producer. When the gas purchased turned out to be the wrong mixture it took two months to get a new batch delivered, resulting in a data coverage of only 68% for the year 2012.

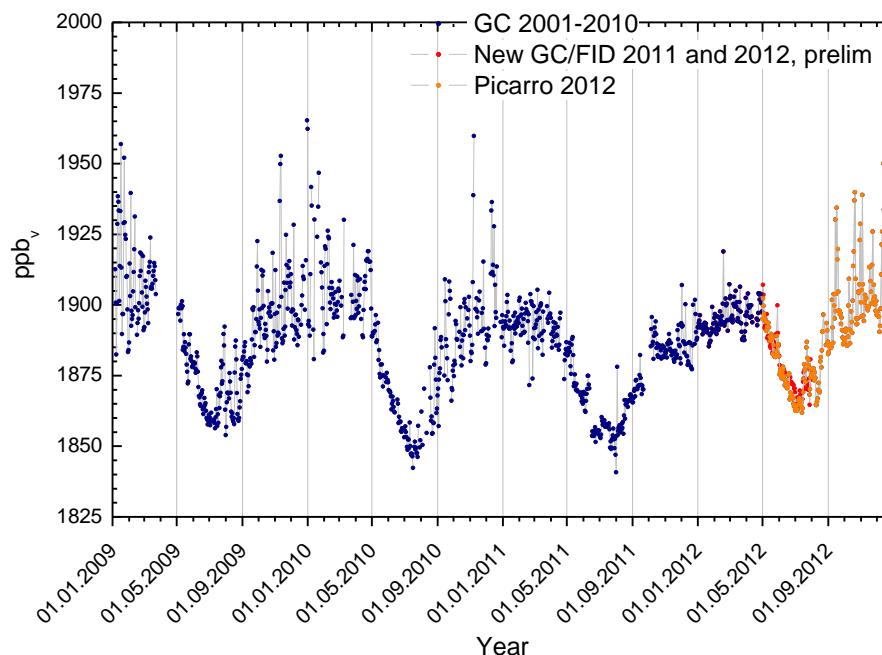


Figure 48: Daily mean of methane measured with the old GC (2001-2010), new GC-FID in 2011 -> and a new Picarro (Cavity Ring-Down Spectrometer) run in parallel in 2012.

CO₂ measurements

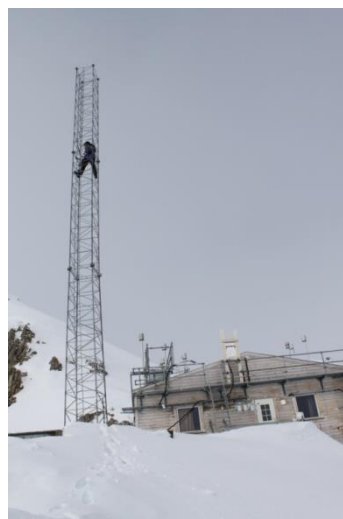
At the Zeppelin station carbon dioxide (CO₂) is monitored in cooperation with Stockholm University (Institute of Applied Environmental Research, ITM). SU maintained a continuous infrared CO₂ instrument, which has been monitoring from 1989 to summer 2013. This instrument was run in parallel with NILU's new cavity ring down instrument for one year before it was stopped. Measurements are since then monitored by NILU's instrument and calibrated against SU-ITM's set of NOAA reference standards as a cooperation between the two institutes. Both methods were included in the GAW audit in September 2012, showing good results for both methods and good consistency between instruments.

The continuous data are enhanced by the weekly flask sampling programme in co-operation with NOAA CMDL. Analysis of the flask samples provides CH₄, CO, H₂, N₂O and SF₆ data for the Zeppelin station.

Air inlet at Zeppelin

There has also been improved air inlet for the GHG measurements at Zeppelin to reduce possible influence from the station and visitors at the stations. The inlet is now moved away from the station and taken from a tower nearby for the following components:

- N₂O/CH₄
- CO
- Halogenated compounds
- NOAA flask sampling program



NILU engineer Are Bäcklund about to install a new air inlet for the Medusa instrument. Photo: Ove Hermansen, NILU

Details about aerosol optical depth measurements

The amount of particles in the air during sunlit conditions is continuous monitored by means of a Precision-Filter-Radiometer (PFR) sun photometer, located at the Sverdrup station in Ny-Ålesund and a Cimel instrument at Birkenes. The observations in Ny-Ålesund are performed in collaboration with PMOD/WRC (C. Wehrli), Davos, Switzerland. The main instrument characteristics are given below.



AERONET - Cimel C-318

- Sun (9 channels) and sky radiances
- Wavelength range: 340-1640 nm
- 15 min sampling
- No temperature stabilized
- AOD uncertainty: 0.01-0.02

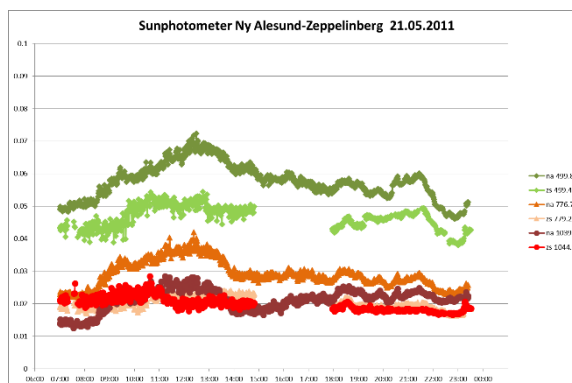


PFR-GAW - Precision Filter Radiometer

- Direct sun measurements (4 channels)
- Wavelength range: 368-862 nm
- Continuous sampling (1 min)
- Temperature stabilized
- AOD uncertainty: 0.01

Figure 49: Photos and typical features of the standard instrument of the AERONET (left panel) and GAW PFR network instruments (right panel)

In addition, 2011 NILU and the Alfred Wegener Institute (AWI) started tests with an instrument to monitor AOD on top of the Zeppelin Mountain, which is a unique opportunity to separate the boundary layer contribution from the total column, and thereby get new insights into the contribution of local versus long-range transport of aerosols. After successful tests, NILU ordered a solar-tracker in 2012, but due to long delivery times, only in spring 2013, measurements on a more routine basis started (quality assured measurements made at Zeppelin mountain are available from March-June 2013, and will be reported in 2014). The Figure below shows a photo of the system mounted at Zeppelin Mountain and an example of measurements performed at two altitudes during a particular day in 2011. It can be seen that the boundary layer contribution accounts for roughly 10 - 30% of the total aerosol columns.



Photos of the sun-photometer mounted at Zeppelin mountain (left panel) and example of AOD observations from Zeppelin and the main village (right panel)

Aerosol optical depth measurements started at the new Birkenes observatory in spring 2009, utilizing an automatic sun and sky radiometer (CIMEL type CE-318), with spectral interference filters centered at selected wavelengths: 340, 380, 440, 500, 675, 870, 1020, and 1640 nm. The measurement frequency is approximately 15 minutes (this depends on the air-mass and time of day). Calibration was performed in Izaña in the period 13 May to 24 of July 2008 (RIMA-AERONET sub-network). Between 11 December 2009 and 26 January 2010 and between 16 September and November 2011, at Autilla del Pino (Palencia, Spain), the operational calibration platform managed by GOA for RIMA-AERONET sun photometers. In the context of ACTRIS (Aerosols, Clouds, and Trace gases Research Infra Structure Network, an EU (FP7) project) Transnational Access instrument calibration has been completed 14 May 2013 at the GOA-UVA (Spain) installation of the AERONET-EUROPE Calibration Service Centre. Raw data are processed and quality assured centrally by AERONET. All data reported here are quality assured data (AERONET level 2.0).

The sun-photometer measurements in Ny-Ålesund are part of the global network of aerosol optical depth (AOD) observations, which started in 1999 on behalf of the WMO GAW program. The instrument is located on the roof of the Sverdrup station, Ny-Ålesund, close to the EMEP station on the Zeppelin Mountain (78.9°N, 11.9°E, 474 m a.s.l.). The Precision Filter Radiometer (PFR) has been in operation since May 2002. In Ny-Ålesund the sun is below 5° of elevation from 10 October to 4 March, limiting the period with sufficient sunlight to the spring-early autumn season. However, during the summer months it is then possible to measure day and night if the weather conditions are satisfactory. The instrument measures direct solar radiation in four narrow spectral bands centered at 862, 501, 411, and 368 nm. Data quality control includes instrumental control like detector temperature and solar pointing control as well as objective cloud screening. Measurements are made at full minutes are averages of 10 samples for each channel made over a total duration of 1.25 seconds. SCIAMACHY TOMSOMI ozone columns and meteorological data from Ny-Ålesund are used for the retrieval of aerosol optical depth (AOD).

Outlook on observations of aerosol properties in Ny-Ålesund beyond 2013/14

Currently, a major obstacle to obtaining a complete year around AOD climatology in the Arctic arises from the long polar night. To fill gaps in the aerosol climatology plans are ongoing to deploy and test a lunar photometer to Ny-Ålesund in spring 2014. This is a collaborative initiative between PMOD/WRC, ISAC-CNR, NILU and others.

On the observations of aerosol properties at Birkenes

Up to 2009, the instrumentation for observing properties of atmospheric aerosol particles at Birkenes consisted of a Differential Mobility Particle Sizer (DMPS), a single-wavelength Particle Soot Absorption Photometer (PSAP), and PM_{2.5} and PM₁₀ filter samplers for collecting samples for chemical analysis. A DMPS measures the particles number size distribution, usually in the range of about 0.02 - 0.8 µm particle diameter. After putting the aerosol particle phase into a defined state of charge by exposing them to an ionised atmosphere in thermal equilibrium, the DMPS uses a cylindrical capacitor to select a narrow size fraction of the particle phase. The particle size in the selected size fraction is determined by the voltage applied to the capacitor. The particle number concentration in the selected size fraction is then counted by a Condensation Particle Counter (CPC). A mathematical inversion that considers charge probability, diffusional losses of particles in the system, transfer function of the capacitor, and counting efficiency of the CPC is then used to calculate the particle number size distribution. A PSAP measures the aerosol absorption coefficient by measuring the decrease in optical transmissivity of a filter while the filter is loaded with the aerosol sample. The transmissivity time series is subsequently translated into a absorption coefficient time series by using Lambert-Beer's law, the same law also

used in optical spectroscopy. The PM_{2.5} and PM₁₀ filter samples of the aerosol particle phase are analysed by ion chromatography to reveal the chemical speciation.

From 2010, all instruments measuring aerosol properties in Birkenes listed in section 7.1 were in full operation. This now also includes a 3-wavelength integrating nephelometer and an Optical Particle Counter (OPC). The integrating nephelometer measures the aerosol scattering coefficient at three wavelengths across the visible spectrum by illuminating an aerosol-filled confined volume with a Lambertian light source, and collecting the light scattered by the particles in the volume. This observation is complementary to the measurements of the aerosol absorption coefficient by PSAP, and is used to increase the accuracy of the PSAP measurements. Nephelometer and PSAP together yield the aerosol optical properties, which are essential for quantifying the direct aerosol climate effect. The OPC measures the particle number size distribution in the size range of 0.25 - 10 µm particle diameter, and is thus complementary to the DMPS measurements. Together, DMPS and OPC cover the full particle size range commonly considered by atmospheric aerosol observations. In the OPC, the particles in the sample pass through a laser beam. By correlating the amplitude of the peak of scattered light generated while passing the laser beam with particle size, the particle size distribution is measured.

In 2012, the measurement programme at Birkenes has been extended with a cloud condensation nucleus counter (CCNC) and a multi-wavelength absorption photometer. The absorption photometer will measure the aerosol absorption coefficient at three wavelength across the visible spectrum, and will, after an intercomparison period, replace the old single wavelength instrument used so far. It isn't included in this report since the intercomparison period isn't concluded, and since this intercomparison is a part of our activity in the EU-project ACTRIS and performed at the World Calibration Centre for Aerosol Physics in Leipzig (Germany) is still under analysis. The information on spectral particle absorption will allow conclusion about the nature of the absorber, and its distribution with particle size. The CCNC will measure the number of particles available for acting as cloud condensation nuclei as a function of particle size and water vapour supersaturation. The instrument achieves this by exposing the sample to an "artificial cloud" of defined user-selectable supersaturation. This will ultimately allow statements not only on the direct, but also the indirect aerosol climate effect.

All in situ observations of aerosol properties representing the ground-level are conducted for the aerosol at dry-state (RH < 40%) for obtaining inter-comparability across the network.

This full picture will not only allow a better source apportionment of the aerosol observed. The full set of optical properties will also facilitate an estimate of local, instantaneous direct aerosol radiative forcing, and a comparison with the radiative forcing of greenhouse gases at the site.

Model studies: calculation of trends

To calculate the annual trends the observations have been fitted as described in Simmonds et al. (2006) by an empirical equation of Legendre polynomials and harmonic functions with linear, quadratic, and annual and semi-annual harmonic terms:

$$f(t) = a + b \left(\frac{N}{12} \right) \cdot P_1 \left(\frac{t}{N} - 1 \right) + \frac{1}{3} \cdot d \left(\frac{N}{12} \right)^2 \cdot P_2 \left(\frac{t}{N} - 1 \right) + c_1 \cdot \cos(2\pi t) + s_1 \sin(2\pi t) + c_2 \cos(4\pi t) + s_2 \sin(4\pi t)$$

The observed f can be expressed as functions of time measures from the 2N-months interval of interest. The coefficient a defines the average mole fraction, b defines the trend in the mole fraction and d defines the acceleration in the trend. The c and s define the annual and inter-annual cycles in mole fraction. N is the mid-point of the period of investigation. P_i are the Legendre polynomials of order i .

Determination of background data

Based on the daily mean concentrations an algorithm is selected to find the values assumed as clean background air. If at least 75% of the trajectories within +/- 12 hours of the sampling day are arriving from a so-called clean sector, defined below, one can assume the air for that specific day to be non-polluted. The remaining 25% of the trajectories from European, Russian or North-American sector are removed before calculating the background.

APPENDIX 2

Acknowledgements

We thank the AERONET and RIMA staff for their support calibrating the Cimel instrument, located at the Birkenes observatory. We also acknowledge the European Union Seventh Framework Programme (FP7/2007-2013) under grant agreement Nr. 262254 [ACTRIS] for support for developing the measurements of trace gases and aerosol particles at Birkenes and Zeppelin.

We thank the Dr. Susanne Kratzer, from Stockholm University, Sweden, and for establishing and maintaining the Palgrunden (58.8°N, 13.2°E) AERONET sites used in this investigation. The CALIOP L3 data were obtained from the NASA Langley Research Center Atmospheric Science Data Center. Access to the data is greatly appreciated.

We gratefully acknowledge the work of the station personnel from the Norwegian Polar Institute for taking care of the observations in Ny-Ålesund. The authors acknowledge the NOAA Air Resources Laboratory (ARL) for the provision of the HYSPLIT transport and dispersion model and/or READY website (arl.noaa.gov/ready.php). Analyses and visualization used in this report were produced with the Giovanni online data system, developed and maintained by the NASA GES DISC. We also acknowledge the MODIS mission scientists and associated NASA personnel for the production of the data used here. SCIAMACHY TOSOMI ozone overpass data were obtained from the TEMIS website (temis.nl/protocols/o3field/overpass_scia.html), Meteorological data for Ny-Ålesund were received via eKlima (www.eklima.no), the web portal from the Norwegian Meteorological Institute. We greatly acknowledge the personnel for obtaining the data and making them publicly available.

Christoph Wehrli and Carlos Toledano are acknowledged due to their contributions with the aerosol observations, quality assurance and interpretations.

Christoph Wehrli
WORCC, PMOD/WRC, Dorfstrasse 33, Davos Dorf
CH-7260, Switzerland

Carlos Toledano
Grupo de Óptica Atmosférica
Universidad de Valladolid
Prado de la Magdalena s/n
47071 Valladolid, Spain

Utførende institusjon NILU - Norsk institutt for luftforskning P.O. Box 100, 2027 Kjeller	ISBN-nummer 978-82-425-2675-5 (trykt) 978-82-425-2676-2 (elektronisk)
---	--

Oppdragstakers prosjektansvarlig Cathrine Lund Myhre	Kontaktperson Miljødirektoratet Harold Leffertstra	M-nummer M-142 2014

	År 2014	Sidetall 85	Miljødirektoratets (tidl. Klif) kontraktnummer 3012029
--	------------	----------------	--

Utgiver NILU - Norsk institutt for luftforskning NILU OR 21/2014 NILU project no. O-99093/O-105020	Prosjektet er finansiert av Miljødirektoratet og NILU - Norsk institutt for luftforskning
---	--

Forfatter(e) C.L. Myhre, O. Hermansen, A.M. Fjæraa, C. Lunder, M. Fiebig, N. Schmidbauer, T. Krognæs, K. Stebel
--

Tittel - norsk og engelsk
Overvåking av klimagasser og partikler på Svalbard og Birkenes i 2012: Årsrapport
Monitoring of greenhouse gases and aerosols at Svalbard and Birkenes in 2012 - Annual report

Sammendrag - summary

Rapporten presenterer aktiviteter og måleresultater fra klimagassovertvåkingen ved Zeppelin observatoriet på Svalbard for årene 2001-2012 og klimagassmålinger og klimarelevant partikkelmålinger fra Birkenes for 2009-2012.

Overvåkingsprogrammet utføres av NILU - Norsk institutt for luftforskning og er finansiert av Miljødirektoratet og NILU - Norsk institutt for luftforskning.

The report summaries the activities and results of the greenhouse gas monitoring at the Zeppelin and observatory situated on Svalbard in Arctic Norway during the period 2001-2012 and the greenhouse gas monitoring and aerosol observations from Birkenes for 2012.

The monitoring programme is performed by the NILU - Norwegian Institute for Air Research and funded by the Norwegian Environment Agency and NILU - Norwegian Institute for Air Research.

4 emneord
Drivhusgasser, partikler, Arktis, halokarboner

4 subject words
Greenhouse gases, aerosols, Arctic, halocarbons

Miljødirektoratet

Telefon: 03400/73 58 05 00 | Faks: 73 58 05 01

E-post: post@miljodir.no

Nett: www.miljodirektoratet.no

Post: Postboks 5672 Sluppen, 7485 Trondheim

Besøksadresse Trondheim: Brattørkaia 15, 7010 Trondheim

Besøksadresse Oslo: Strømsveien 96, 0602 Oslo

Om Statlig program for forurensningsovervåking

Statlig program for forurensningsovervåking omfatter overvåking av forurensningsforholdene i luft og nedbør, skog, vassdrag, fjorder og havområder. Overvåkingsprogrammet dekker langsiktige undersøkelser av:

- overgjødning
- forsuring (sur nedbør)
- ozon (ved bakken og i stratosfæren)
- klimagasser
- miljøgifter

Overvåkingsprogrammet skal gi informasjon om tilstanden og utviklingen av forurensningssituasjonen, og påvise eventuell uheldig utvikling på et tidlig tidspunkt. Programmet skal dekke myndighetenes informasjonsbehov om forurensningsforholdene, registrere virkningen av iverksatte tiltak for å redusere forurensningen, og danne grunnlag for vurdering av nye tiltak. Miljødirektoratet er ansvarlig for gjennomføringen av overvåkingsprogrammet.

M-142 2014

ISBN 978-82-425-2675-5 (trykt)

ISBN 978-82-425-2676-2 (elektronisk)